CONJUGATE EFFECTS OF HEAT AND MASS TRANSFER ON NATURAL CONVECTION FLOW ALONG A VERTICAL FLAT PLATE WITH CHEMICAL REACTION

by

MAHMUDA BINTE MOSTOFA RUMA
Student No. 100509005P
Registration No. 100509005, Session: October-2005

MASTER OF PHILOSOPHY
IN
MATHEMATICS

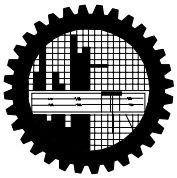

Department of Mathematics
BANGLADESH UNIVERSITY OF ENGINEERING AND TECHNOLOGY, DHAKA-1000
February- 2011

The thesis titled

CONJUGATE EFFECTS OF HEAT AND MASS TRANSFER ON NATURAL CONVECTION FLOW ALONG A VERTICAL FLAT PLATE WITH CHEMICAL REACTION

Submitted by

MAHMUDA BINTE MOSTOFA RUMA
Student No. 100509005 P, Registration No. 100509005, Session: October-2005, a part time student of M. Phil. (Mathematics) has been accepted as satisfactory in partial fulfillment for the degree of

Master of Philosophy in Mathematics

on 19, February- 2011

BOARD OF EXAMINERS

1. _____
   Dr. Md. Abdul Alim (Supervisor)
   Associate Professor (Chairman)
   Dept. of Mathematics, BUET, Dhaka-1000

2. _____
   Dr. Md. Abdul Hakim Khan Member
   Professor and Head (Ex-Officio)
   Dept. of Mathematics, BUET, Dhaka-1000

3. _____
   Dr. Md. Mustafa Kamal Chowdhury Member
   Professor
   Dept. of Mathematics, BUET, Dhaka-1000

4. _____
   Dr. Amulya Chandra Mandal Member
   Professor (External)
   Dept. of Mathematics
   Dhaka University, Dhaka-1000

Abstract

In this thesis, the conjugate effects of heat and mass transfer on natural convection flow along a vertical flat plate in absence of heat generation with chemical reaction and the conjugate effects of heat and mass transfer on natural convection flow along a vertical flat plate in presence of heat generation with chemical reaction have been investigated. The physical problems are represented mathematically by different sets of governing equations along with the corresponding boundary conditions. Using the appropriate transformation, the governing equations i.e. the equations of continuity, momentum, energy and concentration are transformed into a set of non-dimensional boundary layer equations along with the corresponding boundary conditions, which are then solved numerically using finite-difference method together with the Keller box scheme. Here, the attention is focused on the evaluation of the surface shear stress in terms of local skin friction, rate of heat transfer in terms of local Nusselt number and rate of species concentration in terms of local Sherwood number, velocity profiles as well as temperature profiles. The software FORTRAN 90 is used to perform computational job and the post processing software TECHPLOT has been used to display the numerical results graphically. A selection of parameters set is also considered for computation consisting of heat generation parameter Q, Prandtl number Pr, Schmidt number Sc, Chemical reaction parameter and buoyancy ratio parameter N. The results in terms of local skin friction, local Nusselt number, Local Sherwood number are shown in tabular forms. Velocity profiles, temperature profiles, skin friction coefficient, rate of heat transfer and rate of species concentration heat transfer have been displayed graphically and analyzed for various values of heat generation parameter, chemical reaction parameter, buoyancy ratio parameter, the Schmidt number and the Prandtl number as well.

Author's Declaration

I am hereby declaring that the work in this dissertation entitled "CONJUGATE EFFECTS OF HEAT AND MASS TRANSFER ON NATURAL CONVECTION FLOW ALONG A VERTICAL FLAT PLATE WITH CHEMICAL REACTION" has been carried out in accordance with the regulations of Bangladesh University of Engineering and Technology (BUET), Dhaka, Bangladesh. The work is also original except where indicated by and attached with special reference in the context. Also this dissertation has not been submitted to any other University for any degree either in home or abroad or no part of it has been submitted for any attempt to get other degrees or diplomas.

All views expressed in the dissertation are those of the author and in no way or by no means represent those of Bangladesh University of Engineering and Technology (BUET), Dhaka.

(MAHMUDA BINTE MOSTOFA RUMA)

Date: 19 February, 2011

Acknowledgements

At the outset I am pronouncing my thankfulness to the Almighty who give me the ability to carry out such a research work.

My gratitude will always be for my supervisor Dr. Md. Abdul Alim, Associate Professor, Department of Mathematics, BUET, who continuously guided me from all directions. It is my great gratification for having the opportunity to work under his supervision. I would like to express my heart-rending admiration to my supervisor who has encouraged and rightly initiated me to step into the wide area of mathematics and its application in the engineering fields. I am not less grateful and thankful to the efforts, perseverance, sincerity, enormous will-force, clarity, accuracy, completeness, monumental patience, generous co-operation and fellow-feeling he showed for me to venture this research and bring this painstaking task to a successful end.

I am also deeply indebted to Ms. Nazma Parvin, Assistant Professor of the Department of Mathematics, BUET, for her wise and liberal co-operation providing for me during my course of M.Phil. degree.

I would also like to show my deep gratitude to all my teachers of the Department of Mathematics, BUET, for their intelligent and open-minded support. I would also like to thank the staff of the Department of Mathematics, BUET, in providing me all necessary help from the department during my course of M. Phil. degree.

Last but not the least, I would like to express my heart-greet thanks to my parents and my husband without whose encouragement and support this work would not be what it has been today.

Finally, I would like to thank my colleagues at Eastern University for their co-operation.

Contents

Nomenclature

l	Length of the flat plate
C_f	Local skin friction coefficient
C_p	Specific heat at constant pressure
f'	Derivative of f with respect to y
Gr	Grashof number
g	Acceleration due to gravity
k	Thermal conductivity
N	Buoyancy ratio parameter
Nu	Nusselt number
Pr	Prandtl number
Sc	Schmidt number
Sh	Sherwood number
Q	Heat generation parameter
q_w	Heat flux at the surface
J_w	Concentration flux.
T	Temperature of the fluid in the boundary layer
T_∞	Temperature of the ambient fluid
T_f	Temperature at the surface
$(\bar{u}, \bar{v})$	Dimensionless velocity components along the $(\bar{x}, \bar{y})$axes
(u, v)	Dimensionless velocity components along the (x, y)axes
x, y	Axis in the direction along and normal to the surface respectively
D	Molececular diffusivity of the species concentration

Greek symbols

β_T	Coefficient of thermal expansion
B_c	Coefficient of concentration expansion
θ	Dimensionless temperature function
θ_w	Surface temperature parameter
μ	Viscosity of the fluid
ν	Kinematic viscosity
ρ	Density of the fluid
γ	Chemical reaction parameter
τ_w	Shearing stress
ψ	Non-dimensional stream function
ϕ	Dimensionless concentration temperature
η	Quasi- similarity variable

List of Tables

List of Figures

Chapter 1

1.1 Introduction

The study of heat transfer is of great importance to the scientist and engineers because of its almost universal occurrence in many branches of science and engineering. Although heat transfer analysis is the most important for the proper sizing of fuel elements in the nuclear reactors cores to prevent burnout. The performance of aircraft also depends upon the case with which the structure and engines can be cooled. The design of chemical plants is usually done on the basis of heat transfer analysis and the analogous mass transfer processes. The amount of energy transfer as heat can be determined from energy-conservation consideration (first law of thermodynamics). Energy transfer as heat will take place from the assembly (body) with the higher temperature, if these two are permitted to interact through a diathermal wall (second law of thermodynamics). The transfer and conversion of energy from one form to another is the basis to all heat transfer process and hence, they are governed by the first as well as the second law of thermodynamics. Heat transfer is commonly associated with fluid dynamics. The knowledge of temperature distribution is essential in heat transfer studies because of the fact that the heat flow takes place only wherever there is a temperature gradient in a system. The heat flux which is defined as the amount of heat transfer per unit area in unit time can be calculated from the physical laws relating to the temperature gradient and the heat flux.

When a body is introduced into a fluid at different temperatures forms a source of equilibrium disturbance due to the thermal interaction between the body and the fluid. The fluid elements near the body surface assume the temperature of the body and then begin the transmission of heat into the fluid and the variation of temperature is accompanied by density variations. In particular, if the density variation is caused by the non-uniformity of the temperature is called convection. The convective mode of heat transfer is generally divided into two basic processes. If the motion of the fluid arises from an external agent then the process is termed forced convection. This type of fluid flow is caused in general by a fan,

blower, the bursting of a tire etc. Such problems are very frequently encountered in technology where the heat transfers to or from a body is often due to imposed flow of a fluid of different temperature from that of the body. On the other hand, if no such externally induced flow is provided and the flow arises from the effect of a density difference resulting from temperature or concentration difference, in a body forced field such as the gravitational field, then the process is termed natural convection. Generally, the density difference gives rise to buoyancy forces, which drive the flow. Buoyancy induced convective flow is of great importance in many heat removal processes in engineering technology and has attracted the attention of many researchers in the last few decades due to the fact that both science and technology are being interested in passive energy storage systems, such as the cooling of spent fuel rods in nuclear power applications and the design of solar collectors. In particular, it has been ascertained that free convection induced the thermal stress, which leads to critical structural damage in the piping systems of nuclear reactors. The buoyant flow arising from heat rejection to the atmosphere, heating of rooms, fires, and many other heat transfer processes, both natural and artificial, are other examples of natural convection flows. Nazar et al. (2002a, 2002b) considered the free convection boundary layer flow on an isothermal horizontal circular cylinder and on an isothermal sphere. Yao (1983) has studied the problem of natural convection flow along a vertical wavy surface. Also the problem of free convection boundary layer on a vertical plate with prescribed surface heat flux was investigated by Merkin and Mahmood (1990).

The application of boundary layer techniques to mass transfer has been considerable assistance in developing the theory of separation processes and chemical kinetics. Some of the interesting problems that have been studied are mass transfer from droplets, free convection on electrolysis in non-isothermal boundary layer. Heat, mass and momentum transfer on a continuously moving or a stretching sheet has several applications in electrochemistry and polymer processing.

Gebhart and Pera (1971) investigated the nature of vertical natural convection flow resulting from the combined buoyancy effects of thermal and mass diffusion. Diffusion and chemical reaction in an isothermal laminar flow along a soluble flat plate was studied and an appropriate mass-transfer analogue to the flow along a flat plate that contains a species say, A slightly soluble in the fluid say, B has been discussed by Fairbanks and Wick (1950).

Hossain and Rees (1999) have investigated the combined effect of thermal and mass diffusion in natural convection flow along a vertical wavy surface. The effects of chemical reaction, heat and mass transfer on laminar flow along a semi-infinite horizontal plate have been studied by Anjalidevi and Kandasamy.

By taking advantage of the mathematical equivalence of the thermal boundary layer problem with the concentration analogue, results obtained for heat transfer characteristics can be carried directly over to the case of mass transfer by replacing the Prandtl number Pr by the Schmidt number Sc. However, the presence of a chemical reaction term in the mass diffusion equation generally destroys the formal equivalence with the thermal energy problem and moreover, generally prohibits from constructing the otherwise attractive similarity solutions.

The application of the boundary layer theory with chemical reaction has been applied to some problems of free and mixed convection flow from the surface of simple geometry by the above authors. Chang (2006) investigated the Numerical simulation of micropolar fluid flow along a flat plate with wall conduction and buoyancy effects. Sparrow and Lee (1982) looked at the problem of vertical stream over a heated horizontal circular cylinder. They have obtained a solution by expanding velocity and temperature profiles in powers of x, the co-ordinate measuring distance from the lowest point on the cylinder. The exact solution is still out of reach due to the non-linearity in the Navier-Stokes equations. It appears that Merkin (1982) was the first who presented a complete solution of this problem using Blasius and Görtler series expansion method along with an integral method and a finite-difference scheme. Ingham investigated the free convection boundary layer flow on an isothermal horizontal cylinder. Recently, Nazar et al. (2002a) have considered the problem of natural convection flow from lower stagnation point to upper stagnation point of a horizontal circular cylinder immersed in a micropolar fluid

The interaction between the conduction inside and the buoyancy forced flow of fluid along a solid surface is termed as conjugate heat transfer (CHT) process. In practical systems, such as heat exchangers, the convection in the surrounding fluid significantly influences the conduction in a tube wall. Accordingly, the conduction in the solid body and the convection in the fluid should be determined simultaneously.

The CHT problems have been studied by several research groups with the help of mathematical models for simple heat exchanger geometries. Miyamoto et al. (2004) reviewed the early theoretical and experimental works of the CHT problems for a viscous fluid. Miyamoto observed that a mixed-problem study of the natural convection has to be performed for an accurate analysis of the thermo-fluid-dynamic (TFD) field if the convective heat transfer depends strongly on the thermal boundary conditions. Pozzi et al. (1988) investigated the entire TFD field resulting from the coupling of natural convection along and conduction inside a heated flat plate by means of two expansions, regular series and asymptotic expansions.

The CHT problems associated with the heat generating plate washed by laminar forced convection flow were studied by Karvinen , Sparrow et al. and Garg et al. using an approximate method. Moreover, analytical and numerical solutions were performed by Vynnycky et al. (1982) for the CHT problem associated with the forced convection flow over a conducting slab sited in an aligned uniform stream.

The effect of conjugate natural convection flow on or from various heated shapes has been studied by Merkin and Pop (1982), Vynnycky and Kimura (1982), Kimura et al (1998) and Yu and Lin (1982). Also the problem of the conjugate conduction natural convection heat transfer along a thin vertical plate with non uniform heat generation have been studied by Mendez and Trevino (2000), Cheng (1982) studied the mixed convection along a horizontal cylinder and along a sphere in a saturated porous medium. Taher and Molla (2005) studied natural convection boundary layer flow on a sphere in presence of heat generation and then Molla et al. (2005) have studied magnetohydrodynamic natural convection flow on a sphere in presence of heat generation.

In the present study the focus is given on the conjugate effects of heat and mass transfer on natural convection flow along a vertical flat plate with chemical reaction. The developed equations representing the effects are converted into the dimensionless equations by using suitable transformations with a goal to attain similarity solutions. The non-dimensional equations are then transformed into non-linear equations by introducing a non-similarity transformation. The resulting non-linear equations, together with their corresponding boundary conditions based on conduction and convection, are solved numerically with the

help of the finite difference scheme together with the Keller-box method. Consideration is given to the situation where the buoyancy forces assist the natural convection flow for various combinations of the chemical reaction parameter γ, buoyancy ratio parameter N, Prandtl number Pr and Schmidt number Sc. The results help us to predict the different kinds of behavior that can be observed when the relevant parameters are made to vary.

Chapter 2

Conjugate Effects of Heat and Mass Transfer on Natural Convection Flow along a Vertical Flat Plate with Chemical Reaction

2.1 Introduction

This chapter describes the conjugate effects of heat and mass transfer for a natural convection flow along a vertical flat plate with chemical reaction. The natural convection laminar flow from a vertical flat plate immersed in a viscous incompressible optically thin fluid in the presence of chemical reaction effects has been investigated. The governing boundary layer equations are first transformed into a non-dimensional form and the resulting nonlinear system of partial differential equations are then solved numerically using a very efficient finite-difference method known as the Keller-box scheme. Here we have focused our attention on the evaluation of the shear stress in terms of local skin friction, the rate of heat transfer in terms of local Nusselt number and the rate of species concentration in terms of local Sherwood number, Streamline profiles as well as Isotherm profiles for some selected values of parameter sets consisting of the Prandlt number *Pr*, Schmidt number S_c, Chemical reaction parameter γ and Buoyancy ratio parameter N.

2.2 Formulation of the problem

A time independent natural convection boundary layer flow of a steady two dimensional viscous incompressible fluid along a vertical flat plate in presence of heat and mass transfer has been investigated. It is assumed that the surface temperature of the sphere, T_f, is constant, where $T_f > T_\infty$. Here T_∞ is the ambient temperature of the fluid, T is the temperature of the fluid in the boundary layer, g is the acceleration due to gravity and $\left(\bar{u}, \bar{v}\right)$ are velocity components along the $\left(\bar{x}, \bar{y}\right)$ axes. The physical configuration considered is as shown in Fig.2.1:

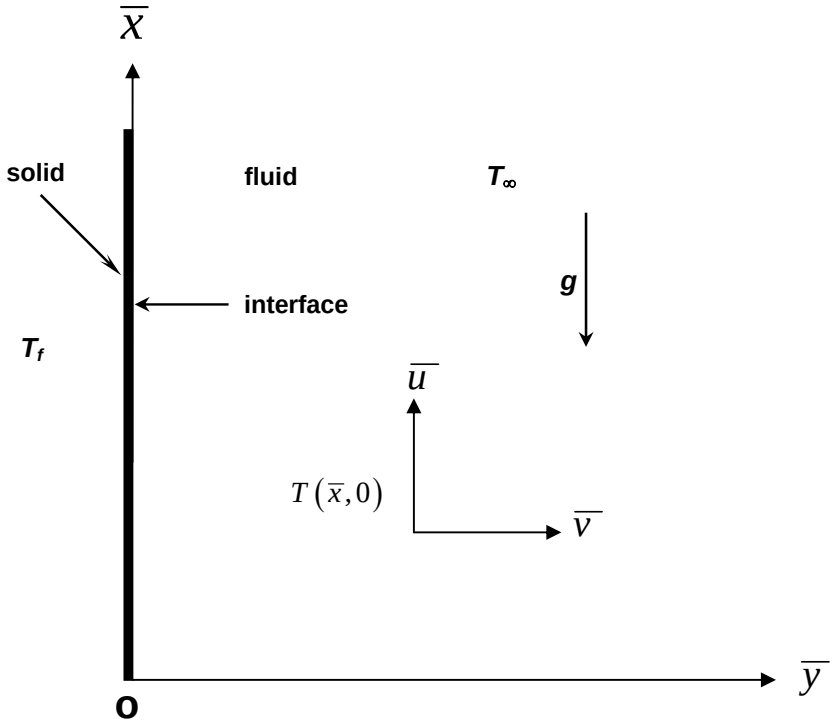

Fig.2.1: Physical model and coordinate system

Under the usual Boussinesq and boundary layer approximation, the equations for continuity, momentum, energy and concentration take the following form:

$$\frac{\partial \bar{u}}{\partial \bar{x}} + \frac{\partial \bar{v}}{\partial \bar{y}} = 0 \tag{2.1}$$

$$\bar{u}\frac{\partial \bar{u}}{\partial \bar{x}} + \bar{v}\frac{\partial \bar{u}}{\partial \bar{y}} = \nu \frac{\partial^2 \bar{u}}{\partial \bar{y}^2} + g\beta_T (T - T_\infty) + g\beta_c (c - c_\infty) \tag{2.2}$$

$$\bar{u}\frac{\partial T}{\partial \bar{x}} + \bar{v}\frac{\partial T}{\partial \bar{y}} = \frac{k_f}{\rho c_p}\frac{\partial^2 T}{\partial \bar{y}^2} \tag{2.3}$$

$$\bar{u}\frac{\partial c}{\partial \bar{x}} + \bar{v}\frac{\partial c}{\partial \bar{y}} = D\frac{\partial^2 c}{\partial \bar{y}^2} - k_1 c \tag{2.4}$$

with the boundary conditions

$$\begin{aligned} &\bar{u} = \bar{v} = 0, c = c_f, T = T_f(\bar{x},0) \text{ at } \quad \bar{y} = 0, \bar{x} > 0 \\ &\bar{u} \to 0, T \to T_\infty, c \to c_\infty \quad \text{ as } \quad \bar{y} \to \infty, \bar{x} > 0 \end{aligned} \tag{2.5}$$

where ρ is the density, k is the thermal conductivity, β_T is the coefficient of thermal expansion, β_c is the coefficient of concentration expansion, ν is the reference kinematics viscosity $(\nu = \mu/\rho)$, μ is the viscosity of the fluid, C_p is the specific heat due to constant pressure and D is molececular diffusivity of the species concentration.

Now introducing the following non-dimensional variables:

$$x = \frac{\bar{x}}{l},\ y = Gr^{1/4}\left(\frac{\bar{y}}{l}\right), \quad u = \frac{l}{\upsilon} Gr^{-1/2}\bar{u}, \quad v = \frac{l}{\upsilon} Gr^{-1/4}\bar{v}, \tag{2.6}$$

$$\theta = \frac{T - T_\infty}{T_f - T_\infty}, \qquad \phi = \frac{c - c_\infty}{c_f - c_\infty}, \qquad Gr = \frac{g\beta_T (T_f - T_\infty) l^3}{\nu^2} \tag{2.7}$$

where Gr is the Grashof number, θ is the non-dimensional temperature function, ϕ is the non-dimensional concentration temperature.

Substituting (2.6) and (2.7) into Equations (2.1), (2.2),(2.3) and (2.4) leads to the following non-dimensional equations

$$\frac{\partial u}{\partial x} + \frac{\partial v}{\partial y} = 0 \tag{2.8}$$

$$u\frac{\partial u}{\partial x} + v\frac{\partial u}{\partial y} = \frac{\partial^2 u}{\partial y^2} + \theta + N\phi \tag{2.9}$$

$$u\frac{\partial \theta}{\partial x} + v\frac{\partial \theta}{\partial y} = \frac{1}{Pr}\frac{\partial^2 \theta}{\partial y^2} \tag{2.10}$$

$$u\frac{\partial \phi}{\partial x} + v\frac{\partial \phi}{\partial y} = \frac{1}{S_c}\frac{\partial^2 \phi}{\partial y^2} - \gamma\phi \tag{2.11}$$

where $Pr = \frac{\upsilon c_p}{k}$ is the Prandtl number.

Now the boundary conditions (2.5) become

$$u = v = 0, \quad \theta = 1, \quad \phi = 1 \quad \text{at} \quad y = 0, \mathrm{x} > 0$$
$$\mathrm{u} \to 0, \quad \theta \to 0, \quad \phi \to 0 \quad \text{as} \quad \mathrm{y} \to \infty, \mathrm{x} > 0 \tag{2.12}$$

Equations (2.9), (2.10) and (2.11) are solved with the help of following variables

$$\psi = x^{\frac{4}{5}}(1+x)^{-\frac{1}{20}} f(x,\eta), \qquad \eta = yx^{-\frac{1}{5}}(1+x)^{-\frac{1}{20}}$$
$$\theta = x^{\frac{1}{5}}(1+x)^{\frac{1}{5}}\theta(x,\eta), \qquad \phi = x^{\frac{1}{5}}(1+x)^{\frac{1}{5}}\phi(x,\eta) \tag{2.13}$$

where η is a quasi-similarity variable and ψ is the non-dimensional stream function defined by

$$u = \frac{\partial \psi}{\partial y}, \quad v = -\frac{\partial \psi}{\partial x} \tag{2.14}$$

Then

$$u = \frac{\partial \psi}{\partial y} = x^{\frac{3}{5}}(1+x)^{-\frac{1}{10}} f', \text{ where } f' = \frac{\partial f}{\partial y}$$

$$\frac{\partial u}{\partial x} = x^{\frac{3}{5}}(1+x)^{-\frac{1}{10}}\frac{\partial f'}{\partial x} + \frac{3}{5}x^{-\frac{2}{5}}(1+x)^{-\frac{1}{10}} f' - \frac{1}{10}x^{\frac{3}{5}}(1+x)^{-\frac{11}{10}} f'$$

$$\frac{\partial u}{\partial y} = x^{\frac{2}{5}}(1+x)^{-\frac{3}{20}} f'', \quad \frac{\partial^2 u}{\partial y^2} = x^{\frac{1}{5}}(1+x)^{-\frac{1}{5}} f'''$$

$$u\frac{\partial u}{\partial x} = x^{\frac{6}{5}}(1+x)^{-\frac{1}{5}} f'\frac{\partial f'}{\partial x} + \frac{3}{5}x^{\frac{1}{5}}(1+x)^{-\frac{1}{5}} f'^2 - \frac{1}{10}x^{\frac{6}{5}}(1+x)^{-\frac{6}{5}} f'^2$$

$$v = -\frac{\partial \psi}{\partial x} = -x^{\frac{4}{5}}(1+x)^{-\frac{1}{20}}\frac{\partial f}{\partial x} - \frac{4}{5}x^{-\frac{1}{5}}(1+x)^{-\frac{1}{20}} f + \frac{1}{20}x^{\frac{4}{5}}(1+x)^{-\frac{21}{20}} f$$

$$v\frac{\partial u}{\partial y} = -x^{\frac{6}{5}}(1+x)^{-\frac{1}{5}} f''\frac{\partial f}{\partial x} - \frac{4}{5}x^{\frac{1}{5}}(1+x)^{-\frac{1}{5}} ff'' + \frac{1}{20}x^{\frac{6}{5}}(1+x)^{-\frac{6}{5}} ff''$$

Equation (2.9) becomes

$$f''' + \frac{16+15x}{20(1+x)} ff'' - \frac{6+5x}{10(1+x)} f'^2 + \theta + N\phi = x\left(f'\frac{\partial f'}{\partial x} - f''\frac{\partial f}{\partial x}\right) \tag{2.15}$$

Equation (2.10) becomes

$$\frac{1}{\Pr}\theta'' + \frac{16+15x}{20(1+x)} f\theta' - \frac{1}{5(1+x)} f'\theta = x(f'\frac{\partial\theta}{\partial x} - \theta'\frac{\partial f}{\partial x}) \tag{2.16}$$

Equation (2.11) becomes

$$\frac{1}{S_c}\phi'' + \frac{16+15x}{20(1+x)} f\phi' - \frac{1}{5(1+x)} f'\phi - \gamma x^{\frac{2}{5}}(1+x)^{\frac{1}{10}}\phi = x(f'\frac{\partial\phi}{\partial x} - \phi'\frac{\partial f}{\partial x}) \tag{2.17}$$

Along with boundary conditions

$$\begin{aligned} &f = f' = 0, \quad \theta = 1, \quad \phi = 1 \qquad \text{at} \quad \eta = 0 \\ &f' \to 0, \quad \theta \to 0, \quad \phi \to 0 \quad as \quad \eta \to \infty \end{aligned} \tag{2. 18}$$

where primes denote differentiation of the function with respect to η.

It can be seen that near the lower stagnation point of the sphere i.e. $x \approx 0$, Equations (2.15), (2.16) and (2.17) reduce to the following ordinary differential equations:

$$f''' + \frac{16}{20} ff'' - \frac{6}{10} f'^2 + \theta + N\phi = 0 \tag{2.19}$$

$$\frac{1}{Pr}\theta'' + \frac{16}{20} f\theta' - \frac{1}{5} f'\theta = 0 \tag{2.20}$$

$$\frac{1}{S_c}\phi'' + \frac{16}{20} f\phi' - \frac{1}{5} f'\phi = 0 \tag{2.21}$$

subject to the boundary conditions

$$\begin{aligned} &f(0) = f'(0) = 0, \quad \theta(0) = 1, \quad \phi(0) = 1 \\ &f' \to 0, \quad \theta \to 0, \quad \phi \to 0 \quad as \quad \eta \to \infty \end{aligned} \tag{2.22}$$

In practical applications, the physical quantities of principle interest are the shearing stress τ_w, the rate of heat transfer and the rate of concentration heat transfer in terms of the skin-friction coefficients C_f , Nusselt number *Nu* and Sherwood number *Sh* respectively, which can be written as

$$Nu = \frac{lGr^{-1/4}}{k_f(T_f - T_\infty)} q_w \ , \quad C_f = \frac{Gr^{-3/4} l^2}{\mu\upsilon} \tau_w \quad \text{and} \quad Sh = \frac{Gr^{-\frac{1}{4}} l}{D(c_f - c_\infty)} J_w \tag{2.23}$$

where $\tau_w = \mu\left(\frac{\partial \bar{u}}{\partial \bar{y}}\right)_{\bar{y}=0}$, $q_w = -k_f\left(\frac{\partial T}{\partial \bar{y}}\right)_{\bar{y}=0}$ and $J_w = -k_f\left(\frac{\partial c}{\partial \bar{y}}\right)_{\bar{y}=0}$, are the shearing stress, heat flux and concentration flux, respectively. (2.24)

Using the equations (2.14) and the boundary condition (2.22) into (2.23) and (2.24), we get the local skin friction coefficients, the local rate of heat transfer and the local rate of species concentration as

$$C_{f_x} = x^{\frac{2}{5}}(1+x)^{-\frac{3}{20}} f''(x,0) \tag{2.25}$$

$$Nu_x = -(1+x)^{-\frac{1}{4}}\theta'(x,0) \tag{2.26}$$

$$Sh_x = -(1+x)^{-\frac{1}{4}}\phi'(x,0) \tag{2.27}$$

We also discuss the effect of the chemical reaction parameter γ and buoyancy ratio parameter N on the velocity, temperature and concentration distribution. The values of the velocity, temperature and concentration distribution are calculated respectively from the following relations:

$$u = x^{\frac{3}{5}}(1+x)^{-\frac{1}{10}}\frac{\partial f}{\partial \eta}, \quad \theta = x^{\frac{1}{5}}(1+x)^{-\frac{1}{5}}\theta(x,0), \quad \phi = x^{\frac{1}{5}}(1+x)^{-\frac{1}{5}}\phi(x,0) \tag{2.28}$$

2.3 Results and discussion

Here we have investigated the conjugate effects of heat and mass transfer on natural convection flow along a vertical flat plate with chemical reaction that are obtained for fluids having Prandtl number Pr = 0.72 and for some test values of Pr = 1.0, 3.0, 5.0 and 7.0 against y for a wide range of values of buoyancy ratio parameter N, Schmidt number Sc and chemical reaction parameter γ. We have considered the values of Schmidt number Sc = 0.65, 0.85, 1.0, 1.2 and 1.4 with chemical reaction parameter γ=0.5, Prandtl number Pr = 0.72 and buoyancy ratio parameter N = 0.5.

The values of buoyancy ratio parameter N =0.0, 0.5, 0.7, 1.0 and 1.4 have been taken while γ= 0.5, Pr = 0.72 and Sc = 0.65. Different values of chemical reaction parameter γ = 0.0, 0.2, 0.5, 0.55 and 0.6 are considered while Sc = 0.65, Pr = 0.72 and N =0.5. Numerical values of local rate of heat transfer are calculated in terms of Nusselt number Nu_x for the surface of the sphere from lower stagnation point to upper stagnation point.

Figures 2.2-2.4 display results for the variation of the local skin friction coefficient C_{fx} ,local rate of heat transfer Nu_x and local rate of species concentration Sh_x for

different values of Prandtl number *Pr* for *Sc* = 0.65, *N* =0.5 and γ = 0.5. We can observe from these figures that as the Prandtl number *Pr* increases, both the skin friction coefficient and rate of species concentration decrease but the rates of heat transfer increase. For large values of Prandtl number Pr correspond to materials which are slightly conducting thermally and a increase in Pr corresponds to a decrease in the thermal conductivity. Then in any one point on the surface, the heat is not able to conduct easily into the fluid as Pr increases and therefore the thermal boundary layer becomes thinner, hence the corresponding temperature gradients are larger and the surface rate of heat transfer that means Nusselt number increases. The values of skin friction coefficient C_{fx} are recorded to be 1.30682, 1.17685, 0.97202, 0.88178, 0.82480 at x=3.5779. Also Nusselt number Nu_x and Sherwood number Sh_x are recorded to be 0.35694, 0.45640, 0.65192, 0.76095, 0.83997 and 0.13811, 0.13630, 0.12386, 0.12483, 0.12685 for *Sc* =0.65, 0.85, 1.0, 1.2, 1.4 respectively. Also it is observed that at x= 3.5779, the skin friction co-efficient C_{fx} and at x=0.0000, the local rate of species concentration Sh_x decrease by 58.54% and 8.88% respectively but at x=0.0000, the rates of heat transfer increase by 57.50% as *Pr* increases from 0.72 to 7.0.

Figures 2.7-2.9 show that both the skin friction coefficient C_{fx} and heat transfer coefficient Nu_x decrease respectively but the rate of species concentration Sh_x increases for increasing values of Schmidt number *Sc* in case of Prandtl number *Pr* = 0.72, buoyancy ratio parameter *N* =0.5 and chemical reaction parameter γ = 0.50. The values of skin friction coefficient C_{fx} are recorded to be 2.09904, 2.07593, 2.06727, 2.05607, 2.04155 at x=3.5779. Also Nusselt number Nu_x and Sherwood number Sh_x are recorded to be 0.47936, 0.46608, 0.45936, 0.44935, 0.43919 and 0.47936, 0.47937, 0.47939, 0.48567, 0.52498 for *Sc* =0.65, 0.85, 1.0, 1.2, 1.4 respectively which occur at the same point x = 0.00000. Here, it is observed that at x = 3.57779, the skin friction decreases by 2.816% and also Nusselt number Nu_x decreases by 8.379% & species concentration Sh_x increases by 8.689% as Schmidt number *Sc* changes from 0.65 to 1.4.

The effect of different values of chemical reaction parameter γ on the skin friction coefficient, the local rate of heat transfer and rate of species concentration while Prandtl number *Pr* = 0.72, buoyancy ratio parameter *N* = 0.5 and Schmidt number

Sc = 0.65 are shown in the figures 2.12- 2.14. Here, as the chemical reaction parameter γ increases, both the skin friction coefficient and heat transfer coefficient decrease and rate of species concentration increases. Here, it is observed that at x = 3.57779, the skin friction decreases by 21.818% and also Nusselt number Nu_x decreases by 9.646% & species concentration Sh_x increases by 9.646% as Schmidt number γ changes from 0.0 to 0.60.

From Figures 2.17 - 2.19, it can also easily be seen that an increase in buoyancy parameter N leads to increase in the local skin friction coefficient C_{fx} , the local rate of heat transfer Nu_x and the local rate of species concentration Sh_x while Prandtl number Pr = 0.72, chemical reaction parameter γ = 0.5 and Schmidt number Sc = 0.65. It is also observed that at any position of x, the skin friction coefficient C_{fx}, the local rate of species concentration Sh_x and the local Nusselt number Nu_x increase as N increases from 0.0 to 1.4. This phenomenon can easily be understood from the fact that when the buoyancy ratio parameter increases, the temperature of the fluid rises and the thickness of the velocity boundary layer grows, i.e., the thermal boundary layer becomes thinner than the velocity boundary layer. Therefore the skin friction coefficient C_{fx}, the local rate of species concentration Sh_x and the local Nusselt number Nu_x increase.The effect for different values of buoyancy ratio parameter N on the skin friction coefficient, the local rate of heat transfer and rate of species concentration in case of Prandtl number Pr = 0.72, Chemical reaction parameter γ = 0.5 and Schmidt number Sc=0.65 are shown in Figures 2.16, 2.17 and 2.18. Here, as buoyancy ratio parameter N increases, the skin friction coefficient, the local rate of heat transfer and rate of species concentration increase. The values of the local skin friction coefficient C_{fx}, the local Nusselt number Nu_x and Schmidt number Sc are recorded to be 1.24429, 1.68673, 1.85277, 2.09299, 2.39972 which occur at x=3.5779; 0.40305, 0.44608, 0.46027, 0.47936, 0.50172 and 0.40305, 0.44608, 0.46027, 0.47936, 0.50172 which occur at the same point at x=0.00000. It is here observed that the local skin friction, the Nusselt number and the Schmidt number increase by 48.148%, 19.666% and 19.666% respectively.

The effect of different values of Prandtl number Pr on the streamline and isotherm profiles while Schmidt number Sc = 0.65, buoyancy ratio parameter N = 0.5 and Chemical reaction parameter γ =0.5 are shown in Figures 2.5 and 2.6. From Figure

2.5(a), it is seen that when the Prandtl number *Pr*=0.72, the non- dimensional value of ψ_{max} within the computational domain is about 10.87 located at the upper stagnation point ($x \approx \pi$) of the vertical plate and when the thickness of the boundary layer reaches to the maximum level, but ψ_{max} again decreases with Pr and it attains about 7.34 for *Pr*= 3.0(see fig 2.5(b)), 6.39 for *Pr*=5.0(see fig 2.5(c)) and 6.01 for *Pr* =7.0(see fig 2.5(d)). This phenomenon fully coincides with the fluid properties that the fluid speeds down as *Pr* increases and the thickness of the velocity boundary layer grows substantially. Here, it is observed that the streamline profiles decrease by 80.865% as Prandtl number *Pr* changes from 0.72 to 7.0. The isotherm patterns for corresponding values are shown in Figure 2.6. From all these frames, we can see that the growth of the thermal boundary layer over the surface of the vertical flat plate is significant. As x increases from lower stagnation point ($x \approx 0$), the hot fluid raises down due to the gravity hence the thickness of the thermal boundary layer, y, is expected to grow. This phenomenon is very straightforward, as can be seen in frames 2.6, there is not appear deepness on the isotherms near to the surface of the vertical flat plate. The levels of isotherms are noticeably lower than the surface level and the fluid temperature not exceeds the level of surface temperature.

The development of streamlines and isotherms which are plotted for buoyancy ratio parameter *N* =0.5, Prandtl number *Pr* =0.72 and chemical reaction parameter γ = 0.5 for the different values of Schmidt number *Sc* (0.65, 0.85, 1.00, 1.20 and 1.40) are shown in Figure 2.10 and Figure 2.11. As *Sc* increases, the fluid speeds up and the thickness of the velocity boundary layer grows substantially. The isotherm patterns for corresponding values are shown in Figure 2.11. From all these frames, we can see that the growth of the thermal boundary layer over the surface of the vertical flat plate is significant. As x increases from lower stagnation point ($x \approx 0$), the hot fluid raises up due to the gravity hence the thickness of the thermal boundary layer, y, is expected to grow. But this phenomenon is not very straightforward, as can be seen in frames 2.11; there appear deepness on the isotherms near to the surface of the vertical plate. The levels of isotherms are noticeably lower than the surface level and the fluid temperature exceeds the level of surface temperature.

The development of streamlines and isotherms which are plotted for buoyancy ratio parameter *N* =0.5, Prandtl number *Pr* =0.72 and Schmidt number *Sc* = 0.65 for the

different values of chemical reaction parameter γ (0.00, 0.20, 0.50, 0.55 and 0.60) are shown in Figure 2.15 and Figure 2.16. As γ increases, the fluid speeds up and the thickness of the velocity boundary layer grows substantially. The isotherm patterns for corresponding values are shown in Figure 2.16. From all these frames, we can see that as x increases from lower stagnation point ($x \approx 0$), the hot fluid raises up due to the gravity hence the thickness of the thermal boundary layer, y, is expected to grow. But this phenomenon is not very straightforward, as can be seen in frames 2.16; there appear deepness on the isotherms near to the surface of the vertical plate. The levels of isotherms are noticeably lower than the surface level and the fluid temperature not exceeds the level of surface temperature.

Figures 2.20 and figures 2.21 illustrate the effect of the buoyancy ratio parameter N on the development of streamlines and isotherms which are plotted for Prandtl number Pr =0.72, Schmidt number Sc =0.65 and chemical reaction parameter γ = 0.5. From Figure 2.20(a), it is seen that when the buoyancy ratio parameter N=0.0, the non- dimensional value of ψ_{max} within the computational domain is about 12.76 located at the upper stagnation point ($x \approx \pi$) of the vertical plate and when the thickness of the boundary layer reaches to the maximum level, but ψ_{max} again increase with N and it attains about 14.04 for N= 0.5(see fig 2.20(b), 15.19 for N= 1.0(see fig 2.20(c) and 16.80 for N =1.4(see fig 2.20(d). This phenomenon fully coincides with the fluid properties that the fluid speeds down as N increases and the thickness of the velocity boundary layer grows substantially. The isotherm patterns for corresponding values are shown in Figure 2.21. From all these frames, we can see that the growth of the thermal boundary layer over the surface of the vertical flat plate is significant. As x increases from lower stagnation point ($x \approx 0$), the hot fluid raises down due to the gravity hence the thickness of the thermal boundary layer, y, is expected to grow. This phenomenon is very straightforward, as can be seen in frames 2.21, there is not appear deepness on the isotherms near to the surface of the vertical flat plate. The levels of isotherms are noticeably lower than the surface level and the fluid temperature not exceeds the level of surface temperature.

Numerical values of skin friction coefficient C_{fx} , rate of heat transfer Nu_x and species concentration Sh_x are calculated from equations (2.25), (2.26) and (2.27) for

the surface of the sphere from lower stagnation point at x = 0^o to x = 90^o. Numerical values of C_{fx}, Nu_x and Sh_x are depicted in Table 2.1.

Table 2.1: Skin friction coefficient, rate of heat transfer and rate of species concentration against x for different values of Prandtl number Pr with other controlling parameters Sc = 0.65, N = 0.5, γ =0.5.

x	Pr=0.72			Pr=3.0			Pr=7.0		
	C_{fx}	Nu_x	Sh_x	C_{fx}	Nu_x	Sh_x	C_{fx}	Nu_x	Sh_x
0.00000	0.00000	0.35694	0.13811	0.00000	0.65192	0.12386	0.00000	0.83997	0.12685
0.2618	0.54256	0.33022	0.10480	0.40326	0.60434	0.10202	0.34202	0.77907	0.10345
0.5236	0.69940	0.31077	0.10146	0.51988	0.56956	0.09684	0.44097	0.73450	0.09663
0.7854	0.80631	0.29560	0.09629	0.59941	0.54234	0.09223	0.50845	0.69959	0.09060
1.0472	0.88902	0.28332	0.09364	0.66094	0.52024	0.08931	0.56068	0.67123	0.08832
1.3090	0.95708	0.27308	0.08996	0.71159	0.50178	0.08632	0.60367	0.64753	0.08496
1.5708	1.01523	0.26436	0.08818	0.75487	0.48603	0.08415	0.64041	0.62730	0.08316
1.8326	1.06618	0.25680	0.08519	0.79280	0.47236	0.08192	0.67262	0.60973	0.08072
2.0944	1.11165	0.25016	0.08407	0.82666	0.46033	0.08021	0.70136	0.59427	0.07925
2.3562	1.15279	0.24427	0.08138	0.85730	0.44963	0.07845	0.72738	0.58051	0.07735
2.6180	1.19044	0.23897	0.08085	0.88534	0.44002	0.07705	0.75118	0.56814	0.07613
2.8798	1.22519	0.23418	0.07820	0.91121	0.43131	0.07560	0.77316	0.55694	0.07458
3.1416	1.25749	0.22982	0.07828	0.93527	0.42337	0.07443	0.79359	0.54673	0.07354
3.4034	1.29736	0.22456	0.07687	0.95778	0.41609	0.07320	0.81270	0.53735	0.07223
3.5779	1.30682	0.22333	0.07453	0.97202	0.41155	0.07248	0.82480	0.53151	0.07153

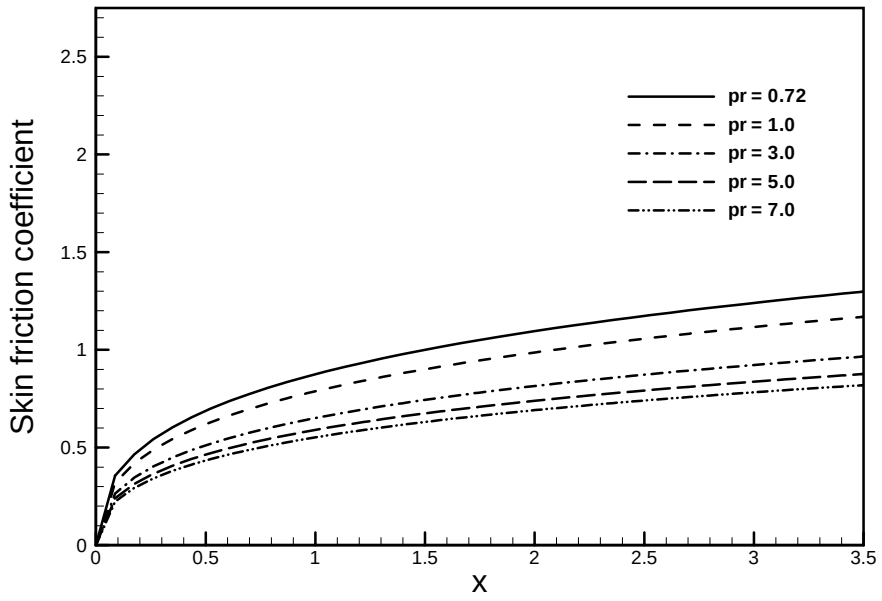

Figure 2.2: Skin friction for different values of *Pr* with *Sc* = 0.65, γ =0.50 and *N* =0.5

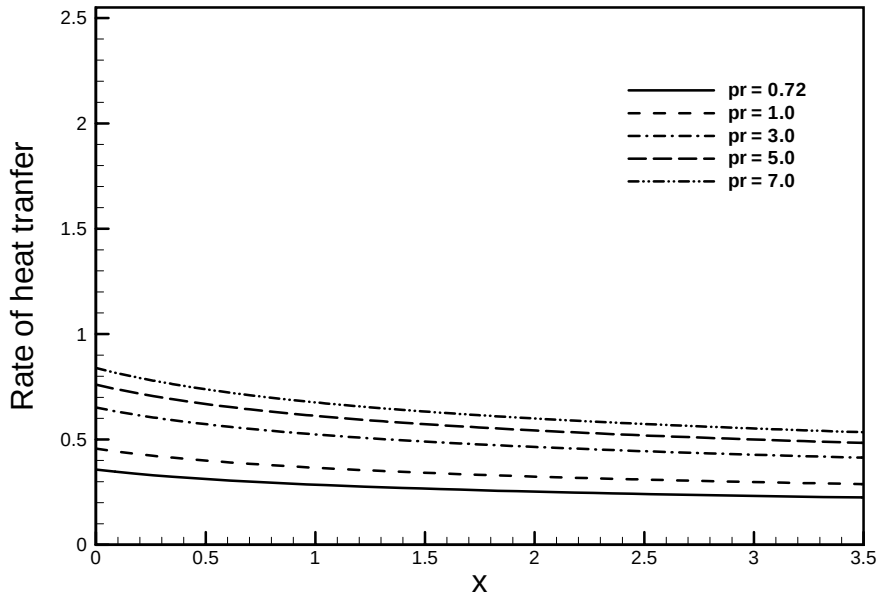

Figure2.3: Rate of heat transfer for different values of *Pr* with Sc= 0.65, γ = 0.50, *N* = 0.5

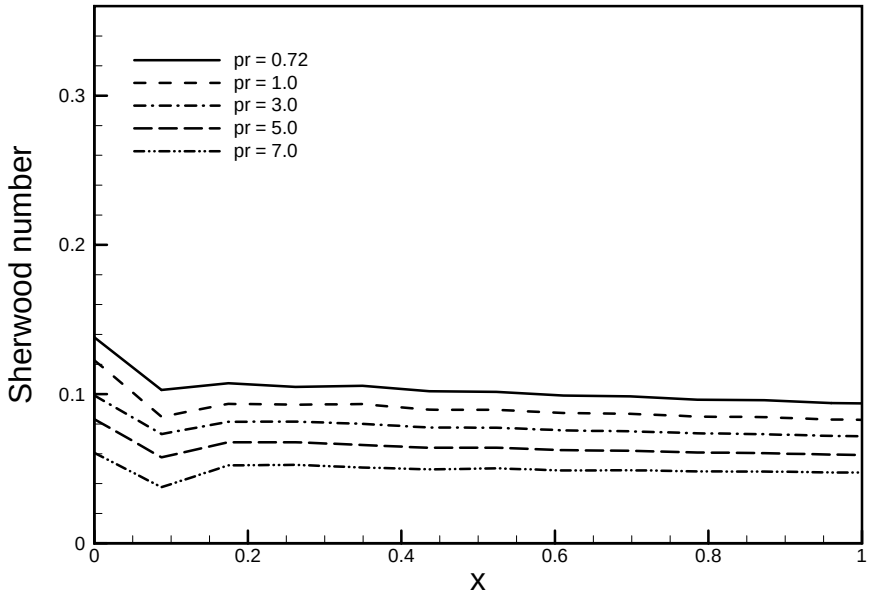

Figure 2.4: Rate of species concentration for different values of *Pr* with Sc= 0.65, γ = 0.50, N =0.5.

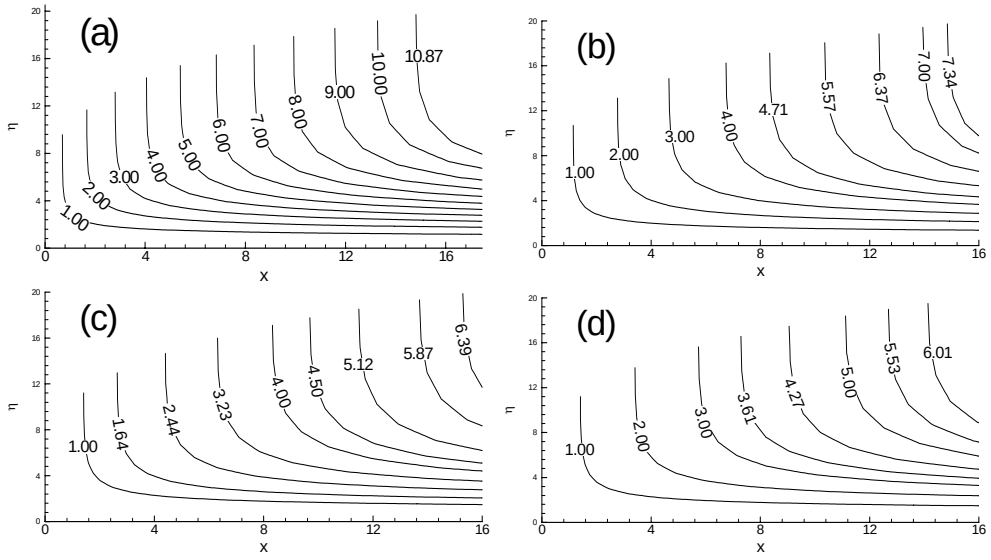

Figure 2.5: Streamlines for a) *Pr* = 0.5 b) *Pr*= 3.0 c) *Pr* = 5.0 d) *Pr* = 7.0 in case of Sc = 0.65, γ =0.50 and N =0.5

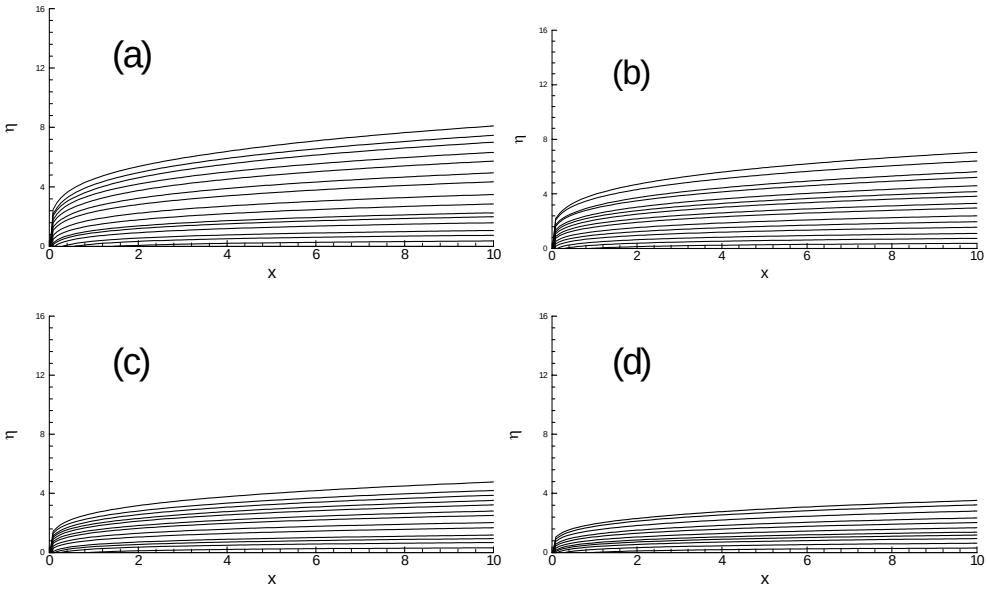

Figure 2.6: Isotherms for a) Pr = 0.72 b) Pr= 3.0 c) Pr = 5.0 d) Pr = 7.0 in case of Sc = 0.65, γ =0.50 and N =0.5

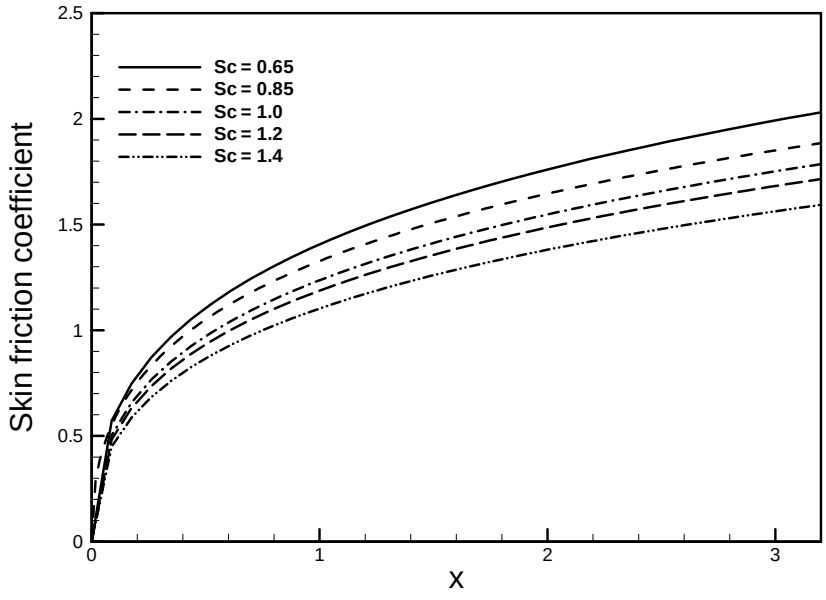

Figure 2.7: Skin friction for different values of Sc with Pr = 0.72, γ =0.50 and N =0.5

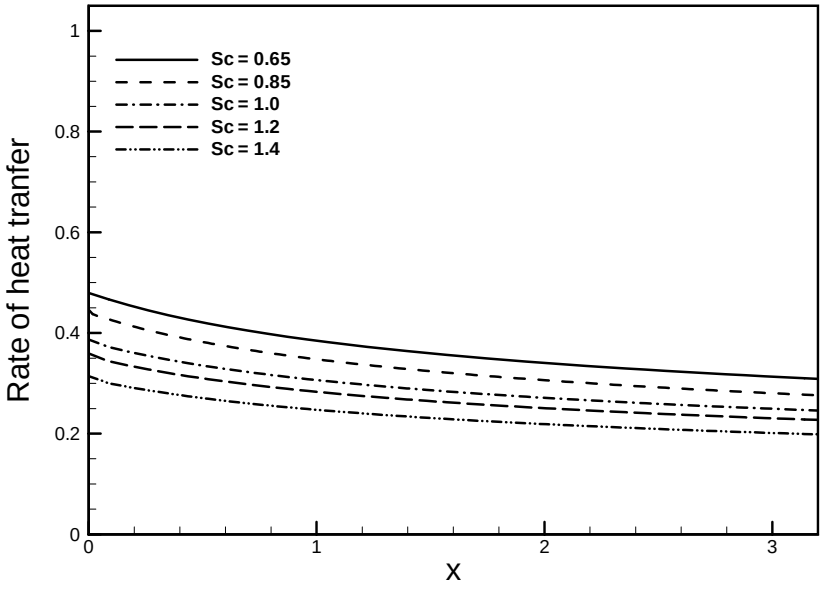

Figure 2.8: Rate of heat transfer for different values of *Sc* with *Pr* = 0.72, γ =0.50 and *N* =0.5

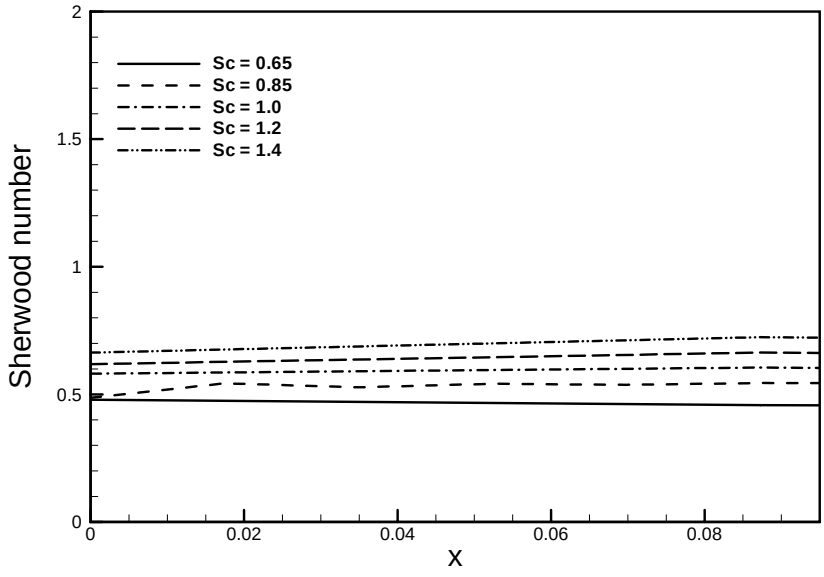

Figure 2.9: Rate of species concentration for different values of *Sc* with *Pr* = 0.72, γ =0.50 and *N* =0.5

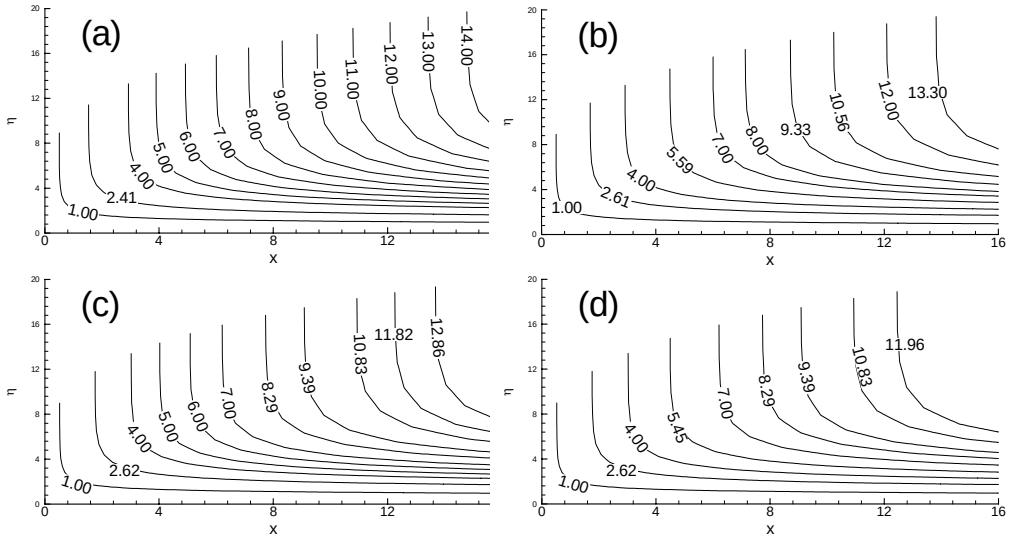

Figure 2.10: Streamlines for a) *Sc*=0.65 b) *Sc*= 0.85 c) *Sc*=1.0 d) *Sc*=1.4 in case of *Pr* = 0.72, γ =0.50 and *N* =0.5

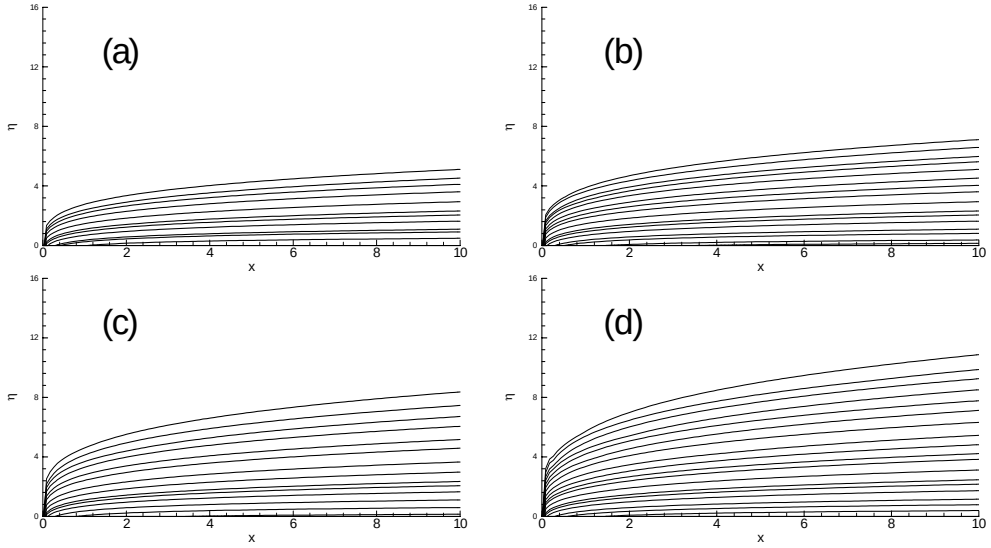

Figure 2.11: Isotherm for a) *Sc*=0.65 b) *Sc*= 0.85 c) *Sc*=1.0 d) *Sc*= 1.4 in case of *Pr* = 0.72, γ =0.50 and *N* =0.5.

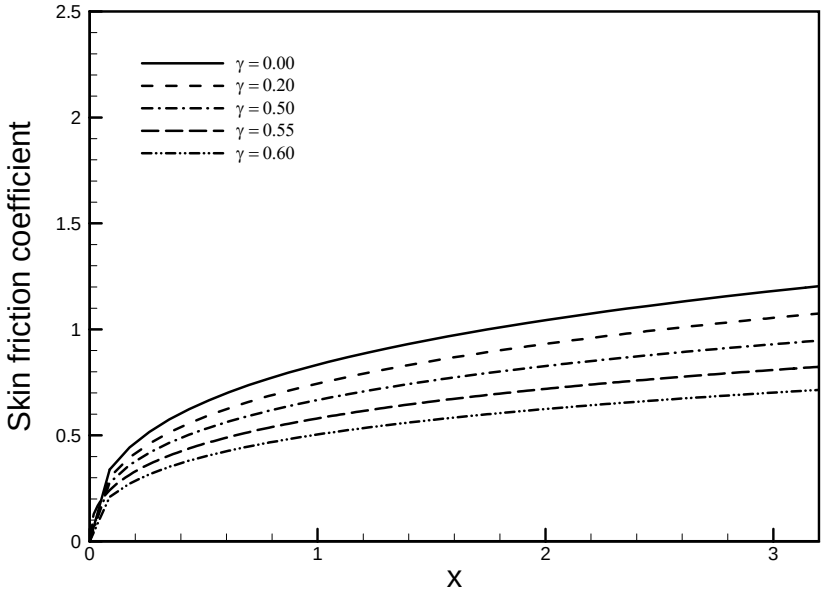

Figure 2.12: Skin friction coefficient for different values of γ with Sc = 0.65, Pr =0.72 and N =0.5.

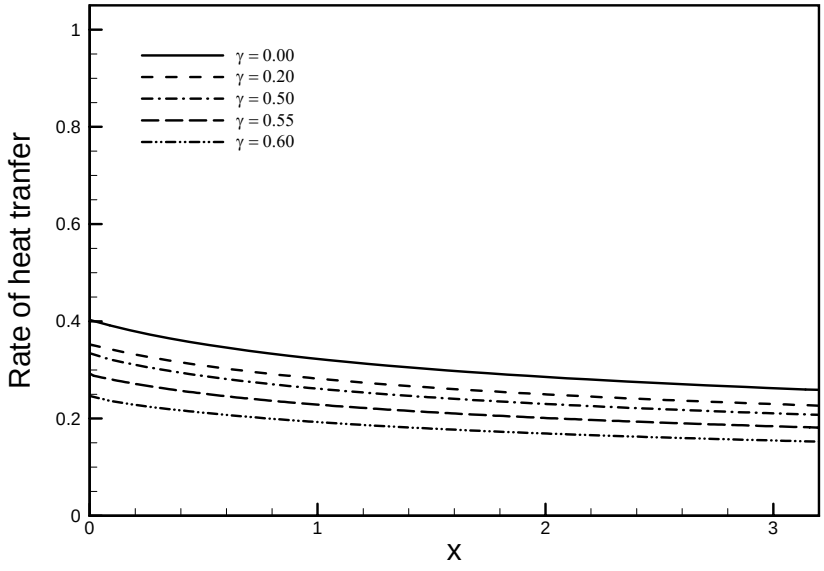

Figure 2.13: Rate of heat transfer for different values of γ with Sc = 0.65, N =0.5 and Pr =0.72.

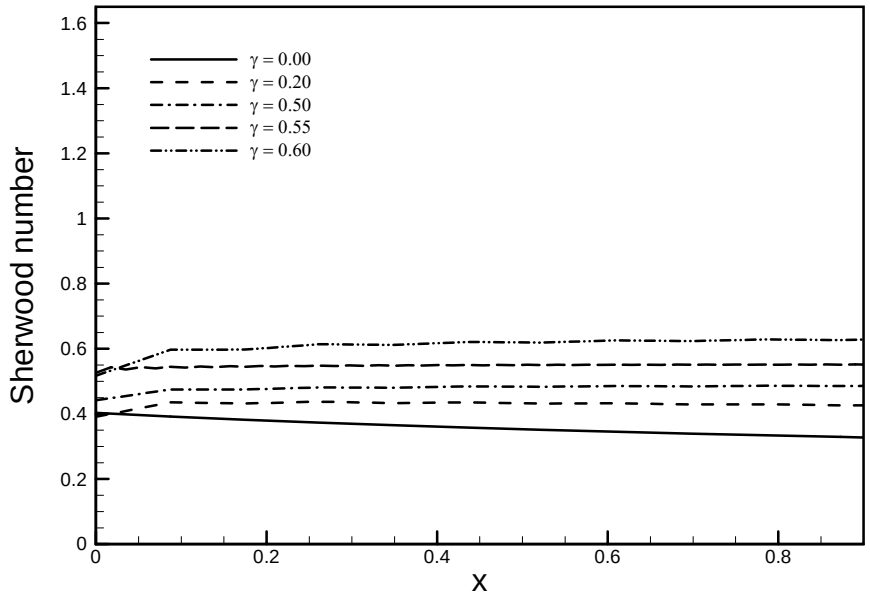

Figure 2.14: Rate of species concentration for different values of γ with Sc = 0.65, N =0.5 and Pr =0.72.

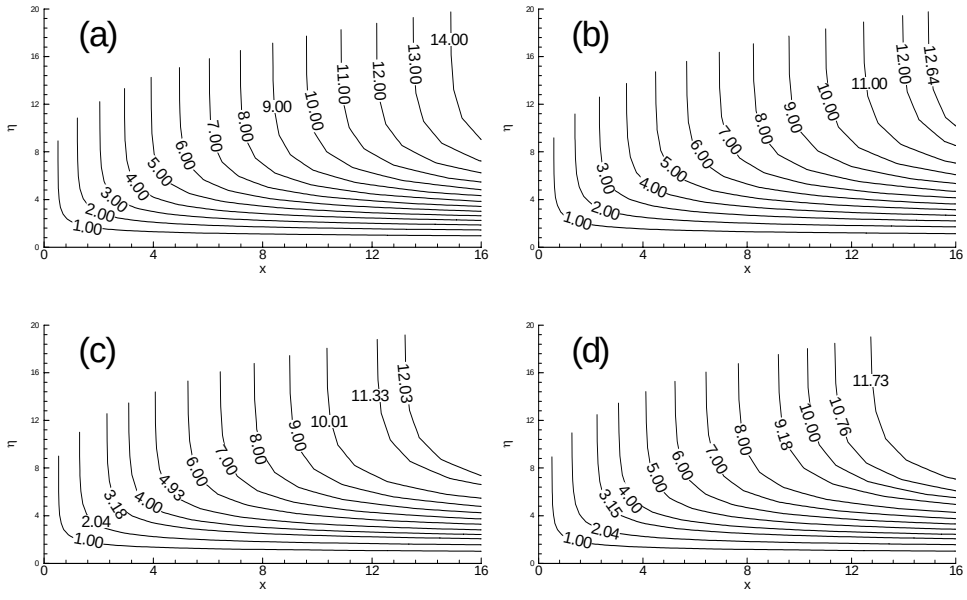

Figure 2.15: Streamlines for a) γ= 0.0 b) γ =0.20 c) γ = 0.50 d) γ= 0.60 in case of Sc = 0.65, N =0.5 and Pr=0.72.

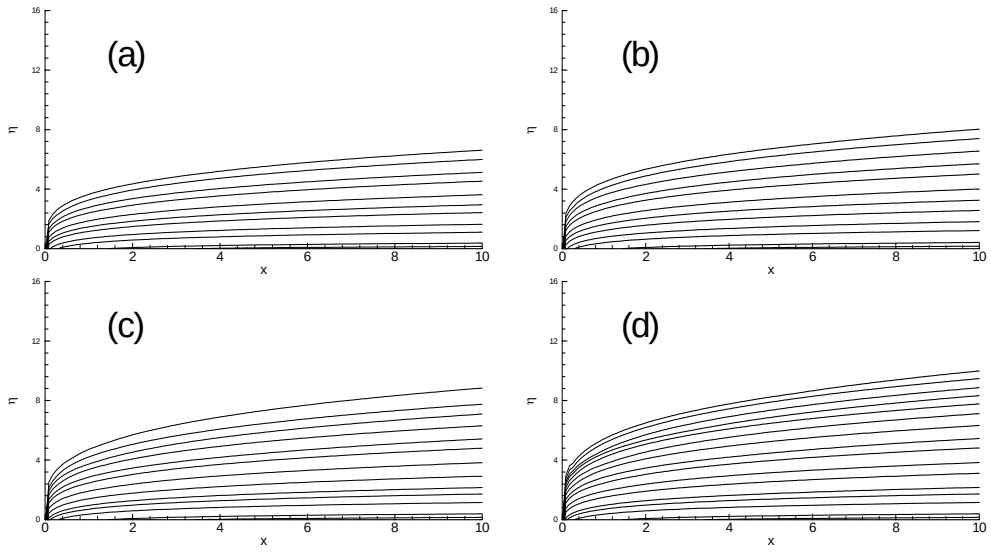

Figure 2.16: Isotherms for a) γ= 0.0 b) γ =0.20 c) γ = 0.50 d) γ= 0.60 in case of Sc = 0.65, N =0.5 and Pr=0.72.

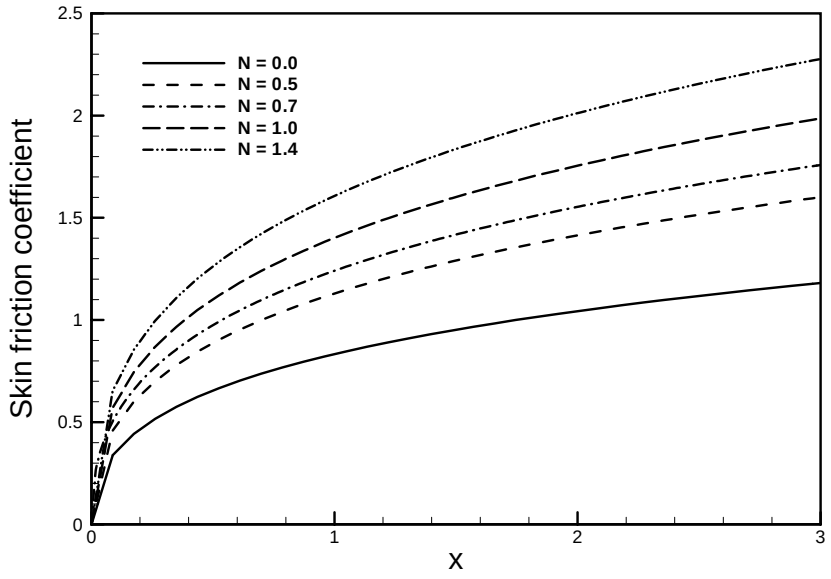

Figure 2.17: Skin friction coefficient for different values of N with Sc = 0.65, γ =0.50 and Pr=0.72.

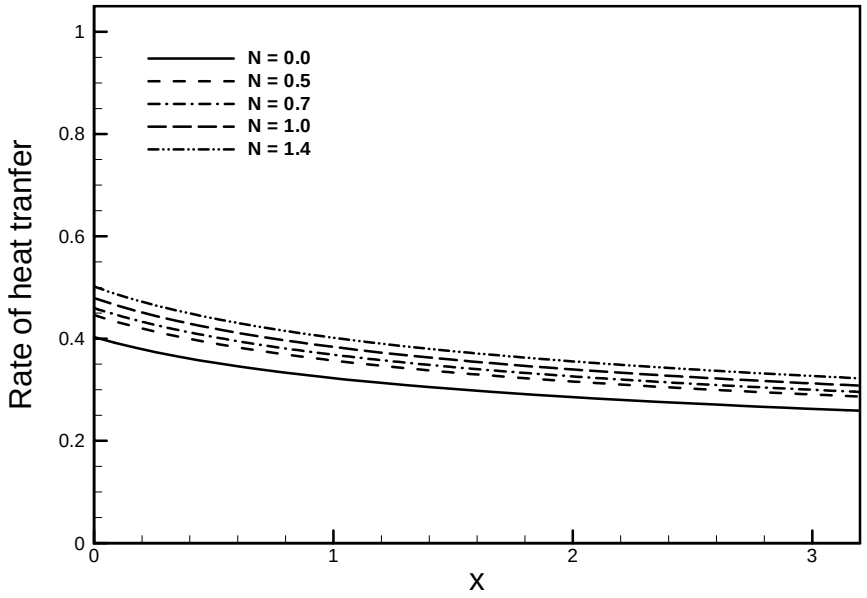

Figure 2.18: Rate of heat transfer for different values of N with Sc = 0.65, γ =0.50 and Pr=0.72.

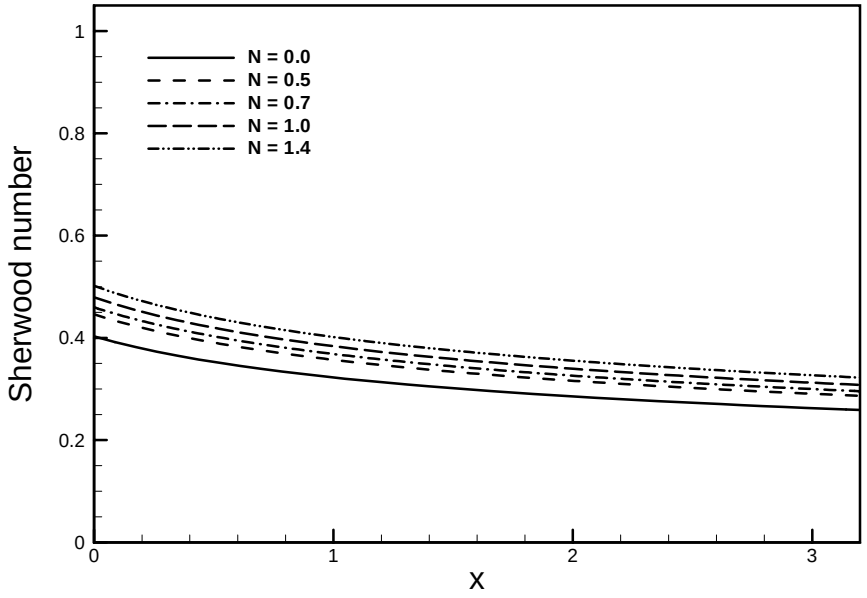

Figure 2.19: Rate of species concentration for different values of N with Sc = 0.65, Pr=0.72 and γ =0.50.

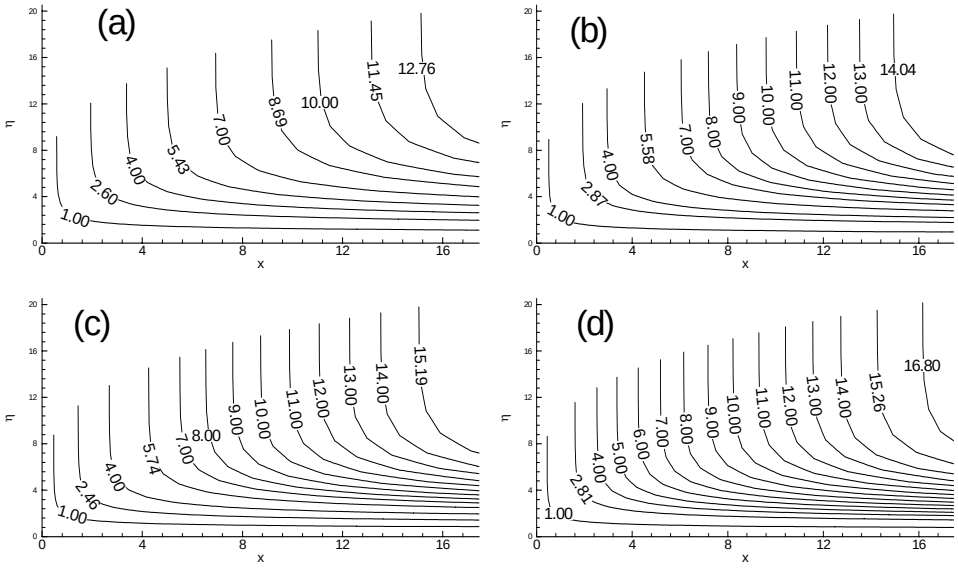

Figure 2.20: Streamlines for a) N=0.0 b) N = 0.50 c) N= 1.0 d) N=1.40 in case of Sc = 0.65, Pr=0.72 and γ =0.50**.**

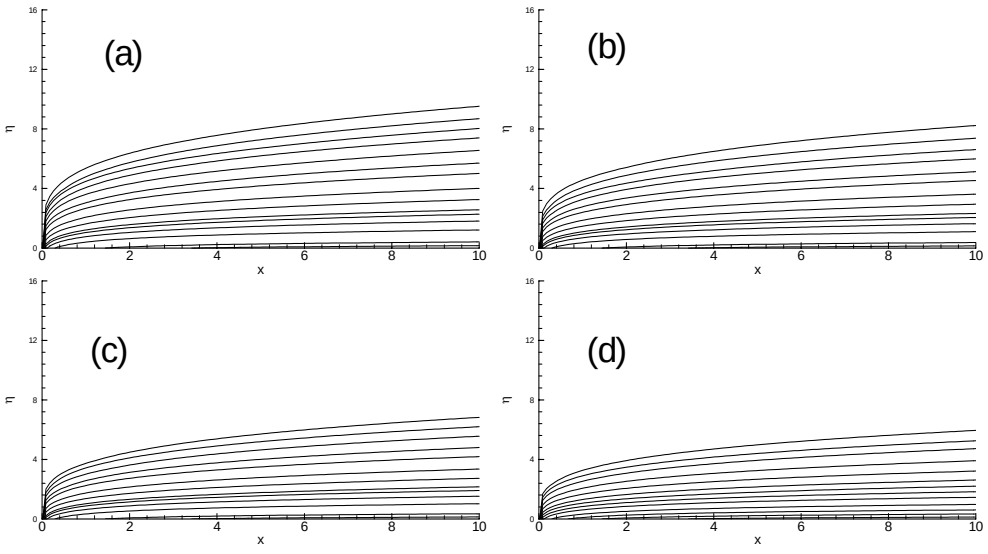

Figure 2.21: Isotherm for a) N=0.0 b) N = 0.50 c) N= 1.0 d) N=1.40 in case of Sc = 0.65, Pr=0.72 and γ =0.50.

2.4 Conclusion

The conjugate effects of heat and mass transfer on natural convection flow along a vertical flat plate with chemical reaction has been investigated for different values of relevant physical parameters including Prandtl number *Pr* and schimdt number S_c.

The governing boundary layer equations of motion are transformed into a non-dimensional form and the resulting non-linear systems of partial differential equations are reduced to local non-similarity boundary layer equations, which are solved numerically by using implicit finite difference method together with the Keller-box scheme. From the present investigation, following conclusions may be drawn:

- Significant effects of Prandtl number *Pr* on skin friction, the rate of heat transfer and the rate of species concentration have been found in this investigation. An increase in the values of Prandtl number *Pr* leads to an increase in both the local skin friction coefficient C_{fx} and the local rate of species concentration Sh_x decrease at different position of y but the local rate of heat transfer Nu_x increases at different position of x.
- The increase in the values of Schmidt number *Sc* leads to decrease in the local skin friction coefficient C_{fx} and the local rate of heat transfer Nu_x but increases in the local rate of species concentration Sh_x.
- Both the local skin friction coefficient C_{fx} and the local rate of heat transfer Nu_x decrease significantly when the values of Chemical reaction parameter γ increase. But for increase values of Chemical reaction parameter γ, the local rate of species concentration Sh_x increase.
- The entire local skin friction coefficient C_{fx}, the local rate of heat transfer Nu_x and the local rate of species concentration Sh_x increase when the buoyancy ratio parameter *N* increases.
- Streamlines and isotherms have changed significantly with the increasing values of parameters.

Chapter 3

Conjugate Effects of Heat and Mass Transfer on Natural Convection Flow along a flat plate in Presence of Heat Generation with Chemical Reaction

3.1 Introduction

In this chapter, the description of the conjugate effects of heat and mass transfer on natural convection flow on a vertical flat plate in presence of heat generation with chemical reaction has been focused. The governing boundary layer equations are first transformed into a non-dimensional form and the resulting nonlinear system of partial differential equations are then solved numerically using a very efficient finite-difference method known as the Keller-box scheme. Here the attention has been given on the evolution of the surface shear stress in terms of local skin friction Cf_x, the rate of heat transfer in terms of local Nusselt number Nu_x and the rate of species concentration in terms of Sherwood number Sh_x and also on streamline profiles and isotherm profiles for a selection of parameter sets consisting of heat generation parameter Q, Prandlt number Pr, Chemical reaction parameter γ and Buoyancy ratio parameter N.

3.2 Formulation of the problem

A steady two-dimensional natural convection boundary layer flow from a flat plate of length l, which is immersed in a viscous and incompressible optically dense fluid with heat generation, is considered. It is assumed that the surface temperature of the sphere, T_f, is constant, where $T_f > T_\infty$. Here T_∞ is the ambient temperature of the fluid, T is the temperature of the fluid in the boundary layer, g is the acceleration due to gravity and $\left(\bar{u}, \bar{v}\right)$ are velocity components along the $\left(\bar{x}, \bar{y}\right)$ axes. The physical configuration considered is as shown in Fig. 3.1:

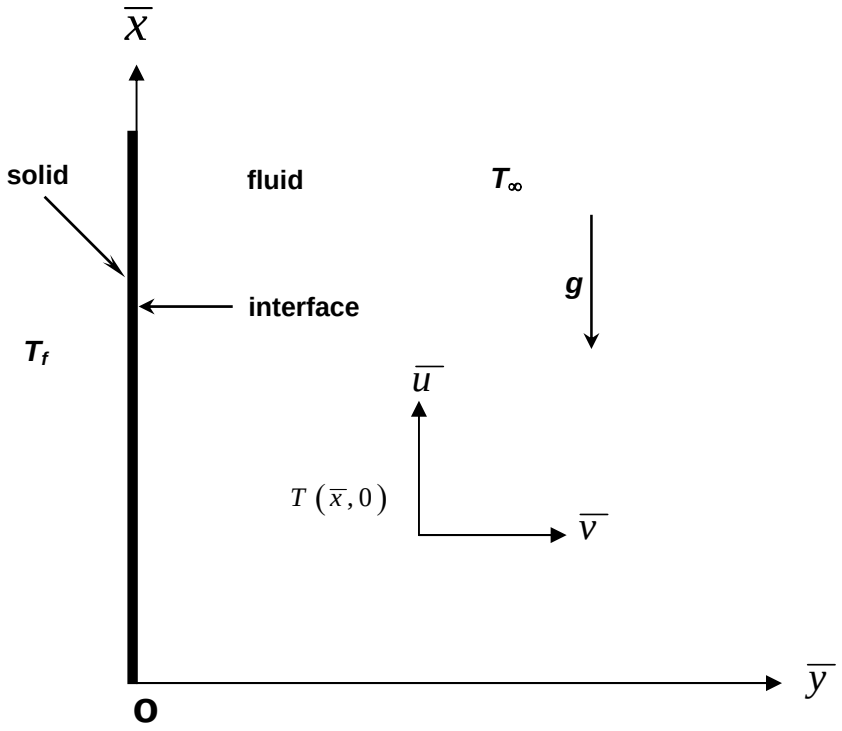

Fig.3.1: Physical model and coordinate system

Under the above assumptions, the governing equations for steady two-dimensional laminar boundary layer flow problem under consideration can be written as

$$\frac{\partial \bar{u}}{\partial \bar{x}} + \frac{\partial \bar{v}}{\partial \bar{y}} = 0 \tag{3.1}$$

$$\bar{u}\frac{\partial \bar{u}}{\partial \bar{x}} + \bar{v}\frac{\partial \bar{u}}{\partial \bar{y}} = \nu \frac{\partial^2 \bar{u}}{\partial \bar{y}^2} + g\beta_T (T - T_\infty) + g\beta_c (c - c_\infty) \tag{3.2}$$

$$\bar{u}\frac{\partial T}{\partial \bar{x}} + \bar{v}\frac{\partial T}{\partial \bar{y}} = \frac{k_f}{\rho c_p}\frac{\partial^2 T}{\partial \bar{y}^2} + \frac{Q_0}{\rho c_p}(T_f - T_\infty) \tag{3.3}$$

$$\bar{u}\frac{\partial c}{\partial \bar{x}} + \bar{v}\frac{\partial c}{\partial \bar{y}} = D\frac{\partial^2 c}{\partial \bar{y}^2} - k_1 c \tag{3.4}$$

with the boundary conditions

$$\bar{u} = \bar{v} = 0, c = c_f, T = T_f(\bar{x},0) \text{ at } \bar{y} = 0, \bar{x} > 0$$
$$\bar{u} \to 0, T \to T_\infty, c \to c_\infty \quad \text{as} \quad \bar{y} \to \infty, \bar{x} > 0 \tag{3.5}$$

where $\frac{Q_0}{\rho c_p}(T_f - T_\infty)$, being a constant represents the amount of generated or absorbed heat from per unit volume. Heat is generated or absorbed from the source term according as Q_0 is positive or negative.

Here ρ is the density, k is the thermal conductivity, β_T is the coefficient of thermal expansion, β_c is the coefficient of concentration expansion, ν is the reference kinematic viscosity $(\nu = \mu/\rho)$, μ is the viscosity of the fluid, C_p is the specific heat due to constant pressure and D is molececular diffusivity of the species concentration.

The above equations are further non-dimensionalised using the new variables:

$$x = \frac{\bar{x}}{l},\ y = Gr^{1/4}\left(\frac{\bar{y}}{l}\right), \quad u = \frac{l}{\upsilon}Gr^{-1/2}\bar{u}, \quad v = \frac{l}{\upsilon}Gr^{-1/4}\bar{v}, \tag{3.6}$$

$$\theta = \frac{T - T_\infty}{T_f - T_\infty}, \quad \phi = \frac{c - c_\infty}{c_f - c_\infty}, \quad Gr = \frac{g\beta_T(T_f - T_\infty)l^3}{\nu^2} \tag{3.7}$$

where Gr is the Grashof number, θ is the non-dimensional temperature function, T_f is the constant temperature at the surface, ϕ is the concentration temperature function.

Substituting (3.6) and (3.7) into equations (3.1), (3.2), (3,3) and (3.4) leads to the following non-dimensional equations

$$\frac{\partial u}{\partial x} + \frac{\partial v}{\partial y} = 0 \tag{3.8}$$

$$u\frac{\partial u}{\partial x} + v\frac{\partial u}{\partial y} = \frac{\partial^2 u}{\partial y^2} + \theta + N\phi \tag{3.9}$$

$$u\frac{\partial\theta}{\partial x}+v\frac{\partial\theta}{\partial y}=\frac{1}{Pr}\frac{\partial^2\theta}{\partial y^2}+\theta Q \tag{3.10}$$

$$u\frac{\partial\phi}{\partial x}+v\frac{\partial\phi}{\partial y}=\frac{1}{S_c}\frac{\partial^2\phi}{\partial y^2}-\gamma\phi \tag{3.11}$$

where $Pr=\frac{\upsilon c_p}{k_f}$ is the Prandtl number and $Q=\frac{Q_o l^2}{\mu c_p Gr^{1/2}}$ is the heat generation parameter.

The corresponding boundary conditions (3.5) become

$$\begin{aligned} &u=v=0,\quad \theta=1,\ \phi=1 \quad \text{at} \quad y=0,\ \text{x}>0\\ &u\to 0,\quad \theta\to 0,\quad \phi\to 0 \ \text{as} \ y\to\infty,\ \text{x}>0 \end{aligned} \tag{3.12}$$

Equations (3.9), (3.10) and (3.11) are solved with the help of following variables

$$\begin{aligned} &\psi = x^{\frac{4}{5}}(1+x)^{-\frac{1}{20}} f(x,\eta), \qquad \eta = yx^{-\frac{1}{5}}(1+x)^{-\frac{1}{20}}\\ &\theta = x^{\frac{1}{5}}(1+x)^{\frac{1}{5}}\theta(x,\eta), \qquad \phi = x^{\frac{1}{5}}(1+x)^{\frac{1}{5}}\phi(x,\eta) \end{aligned} \tag{3.13}$$

where ψ is the stream function defined by

$$u = \frac{\partial\psi}{\partial y}, \qquad v = -\frac{\partial\psi}{\partial x} \tag{3.14}$$

$$u=\frac{\partial\psi}{\partial y}=x^{\frac{3}{5}}(1+x)^{-\frac{1}{10}} f', \ \textit{where} \quad f'=\frac{\partial f}{\partial y}$$

$$\frac{\partial u}{\partial x}=x^{\frac{3}{5}}(1+x)^{-\frac{1}{10}}\frac{\partial f'}{\partial x}+\frac{3}{5}x^{-\frac{2}{5}}(1+x)^{-\frac{1}{10}} f'-\frac{1}{10}x^{\frac{3}{5}}(1+x)^{-\frac{11}{10}} f'$$

$$\frac{\partial u}{\partial y} = x^{\frac{2}{5}}(1+x)^{-\frac{3}{20}} f'', \quad \frac{\partial^2 u}{\partial y^2} = x^{\frac{1}{5}}(1+x)^{-\frac{1}{5}} f'''$$

$$u\frac{\partial u}{\partial x} = x^{\frac{6}{5}}(1+x)^{-\frac{1}{5}} f'\frac{\partial f'}{\partial x}+\frac{3}{5}x^{\frac{1}{5}}(1+x)^{-\frac{1}{5}} f'^2-\frac{1}{10}x^{\frac{6}{5}}(1+x)^{-\frac{6}{5}} f'^2$$

$$v = -\frac{\partial \psi}{\partial x} = -x^{\frac{4}{5}}(1+x)^{-\frac{1}{20}}\frac{\partial f}{\partial x} - \frac{4}{5}x^{-\frac{1}{5}}(1+x)^{-\frac{1}{20}} f + \frac{1}{20}x^{\frac{4}{5}}(1+x)^{-\frac{21}{20}} f$$

$$v\frac{\partial u}{\partial y} = -x^{\frac{6}{5}}(1+x)^{-\frac{1}{5}} f''\frac{\partial f}{\partial x} - \frac{4}{5}x^{\frac{1}{5}}(1+x)^{-\frac{1}{5}} ff'' + \frac{1}{20}x^{\frac{6}{5}}(1+x)^{-\frac{6}{5}} ff''$$

Equation (3.9) becomes

$$f''' + \frac{16+15x}{20(1+x)} ff'' - \frac{6+5x}{10(1+x)} f'^2 + \theta + N\phi = x(f'\frac{\partial f'}{\partial x} - f''\frac{\partial f}{\partial x}) \tag{3.15}$$

Equation (3.10) becomes

$$\frac{1}{\Pr}\theta'' + \frac{16+15x}{20(1+x)} f\theta' - \frac{1}{5(1+x)} f'\theta + Qx^{\frac{2}{5}}(1+x)^{\frac{1}{10}}\theta = x(f'\frac{\partial \theta}{\partial x} - \theta'\frac{\partial f}{\partial x}) \tag{3.16}$$

Equation (3.11) becomes

$$\frac{1}{S_c}\phi'' + \frac{16+15x}{20(1+x)} f\phi' - \frac{1}{5(1+x)} f'\phi - \gamma x^{\frac{2}{5}}(1+x)^{\frac{1}{10}}\phi = x(f'\frac{\partial \phi}{\partial x} - \phi'\frac{\partial f}{\partial x}) \tag{3.17}$$

Along with boundary conditions

$$\begin{aligned} &f = f' = 0, \quad \theta = 1, \quad \phi = 1 \quad \text{at} \quad \eta = 0, \ \text{x} > 0 \\ &f' \to 0, \quad \theta \to 0, \quad \phi \to 0 \quad \text{as} \quad \eta \to \infty \end{aligned} \tag{3.18}$$

where primes denote differentiation of the function with respect to η.

Near the lower stagnation point of the sphere, i.e., $x \approx 0$, the following ordinary differential equations are obtained from equations (3.15), (3.16) and (3.17).

$$f''' + \frac{16}{20} ff'' - \frac{6}{10} f'^2 + \theta + N\phi = 0 \tag{3.19}$$

$$\frac{1}{Pr}\theta'' + \frac{16}{20} f\theta' - \frac{1}{5} f'\theta = 0 \tag{3.20}$$

$$\frac{1}{S_c}\phi'' + \frac{16}{20} f\phi' - \frac{1}{5} f'\phi = 0 \tag{3.21}$$

with the boundary conditions

$$f(0) = f'(0) = 0, \quad \theta(0) = 1, \quad \phi(0) = 1$$
$$f' \to 0, \quad \theta \to 0, \quad \phi \to 0 \text{ as } \eta \to \infty \tag{3.22}$$

In practical applications, the physical quantities of principle interest are the shearing stress τ_w, the rate heat transfer and the rate of species concentration in terms of the skin-friction coefficients C_f, Nusselt number *Nu* and Sherwood number *Sh*, which can be written in non- dimensional form as

$$Nu = \frac{lGr^{-1/4}}{k_f(T_f - T_\infty)} q_w, \quad C_f = \frac{Gr^{-3/4} l^2}{\mu\upsilon} \tau_w \text{ and } Sh = \frac{Gr^{-\frac{1}{4}} l}{D(c_f - c_\infty)} J_w \tag{3.23}$$

where $\tau_w = \mu \left(\frac{\partial \bar{u}}{\partial \bar{y}} \right)_{\bar{y}=0}$, $q_w = -k_f \left(\frac{\partial T}{\partial \bar{y}} \right)_{\bar{y}=0}$ *and* $J_w = -k_f \left(\frac{\partial c}{\partial \bar{y}} \right)_{\bar{y}=0}$, are the shearing stress, heat flux and concentration flux, respectively.

Putting the above values in Equations (3.23), we have

$$Nu_x = \frac{lGr^{-1/4}}{k(T_f - T_\infty)} \times -\frac{k(T_f - T_\infty)}{lGr^{-1/4}} \left(\frac{\partial \theta}{\partial y} \right)_{y=0} = -\left(\frac{\partial \theta}{\partial y} \right)_{y=0}$$

$$\therefore Nu_x = -\left(\frac{\partial \theta}{\partial y} \right)_{y=0} \tag{3.24}$$

$$C_{f_x} = \frac{Gr^{-3/4} l^2}{\mu\nu} \times \frac{\mu\nu}{l^2 Gr^{-3/4}} \left(\frac{\partial u}{\partial y} \right)_{y=0} = \left(\frac{\partial u}{\partial y} \right)_{y=0} = x^{\frac{2}{5}} (1+x)^{-\frac{3}{20}} \left(\frac{\partial^2 f}{\partial \eta^2} \right)_{y=0},$$

since $u = x^{\frac{3}{5}} (1+x)^{-\frac{1}{10}} \frac{\partial f}{\partial \eta}$

$$\therefore C_{f_x} = x^{\frac{2}{5}} (1+x)^{-\frac{3}{20}} \left(\frac{\partial^2 f}{\partial \eta^2} \right)_{y=0} \tag{3.25}$$

and $Sh_x = \frac{Gr^{-\frac{1}{4}} l}{D(c_f - c_\infty)} \times -\frac{k_f (c_f - c_\infty)}{lGr^{-\frac{1}{4}}} \left(\frac{\partial \phi}{\partial y} \right)_{y=0} = -\left(\frac{\partial \phi}{\partial y} \right)_{y=0}$

$$\therefore Sh_x = -\left(\frac{\partial \phi}{\partial y}\right)_{y=0} \tag{3.26}$$

We discuss temperature profiles, streamlines and isotherms for a selection of parameter sets consisting of heat generation parameter, the Prandlt number, Chemical reaction parameter, Schmidt number and buoyancy ratio parameter N at different position of *x*.

3.3 Results and discussion

We have here investigated analytically the conjugate effects of heat and mass transfer on natural convection in presence of heat generation with chemical reaction. Solutions are obtained for fluids having Prandtl number Pr = 0.72 (air) and for some values of Pr = 1.0, 3.0, 5.0 and 7.0 against η for a wide range of values of buoyancy ratio parameter N, Schmidt number Sc, Chemical reaction parameter γ and heat generation parameter Q. We have considered the values of Schmidt number S_c = 0.73, 0.80, 1.00, 1.10 and 1.30 with chemical reaction parameter γ=0.60, Prandtl number Pr = 0.72, buoyancy ratio parameter N = 0.50 and heat generation parameter Q = 0.10.

The values of buoyancy ratio parameter N =0.1, 0.3, 0.5, 0.7 and 0.9 have been taken in case of γ= 0.60, Pr = 0.72, S_c = 0.73 and Q = 0.10. The different values of chemical reaction parameter γ = 0.00, 0.20, 0.40, 0.60 and 0.70 are considered with S_c = 0.73, Pr = 0.72, N =0.5 and Q =0.10. Different values of heat generation parameter Q =0.01, 0.03, 0.05, 0.08 and 0.10 have been taken in case of S_c = 0.73, Pr = 0.72, N =0.50 and γ =0.60. Numerical values of local rate of heat transfer are calculated in terms of Nusselt number Nu_x for the surface of the sphere from lower stagnation point to upper stagnation point. The effect for different values of heat generation parameter Q and chemical reaction parameter γ on local skin friction coefficient C_{fx}, the local Nusselt number Nu_x and the Sherwood number Sh_x , as well as streamline and isotherm profiles with the Prandtl number Pr = 0.72, buoyancy ratio parameter N =0.50 and Schmidt number Sc = 0.73, are also observed.

Figures 3.2-3.4 display results for the variation of the local skin friction coefficient C_{fx}, local rate of heat transfer Nu_x and local rate of species concentration Sh_x for different values of Prandtl number Pr for Sc = 0.73, N =0.50 , γ = 0.60 and Q = 0.10. We can observe from these figures that as the Prandtl number Pr increases, both the skin friction

coefficient and rate of species concentration decrease but the rates of heat transfer increase. Also it is observed that at x= 3.5779, the skin friction co-efficient C_{fx} and at x=0.0000, the local rate of species concentration Sh_x decrease by 4.835% and 2.791% respectively but at x=0.0000, the rates of heat transfer increase by 12.748% as Pr increases from 0.72 to 7.0.

Figures 3.7-3.9 show that both the skin friction coefficient C_{fx} and heat transfer coefficient Nu_x decrease respectively but the rate of species concentration Sh_x increases for increasing values of Schmidt number Sc in case of Prandtl number Pr = 0.72, buoyancy ratio parameter N =0.50,chemical reaction parameter γ = 0.60 and heat generation parameter Q =0.10. The values of skin friction coefficient C_{fx} are recorded to be 1.65166, 1.64810, 1.64006, 1.63688, 1.62892 at x=3.5779. Also Nusselt number Nu_x and Sherwood number Sh_x are recorded to be 0.40941, 0.40868, 0.40677, 0.40608, 0.40498 and 0.61148, 0.62404, 0.65494, 0.66746, 0.68550 for Sc =0.73, 0.80, 1.00, 1.10, 1.30 respectively which occur at the same point x = 3.57792. Here, it is observed that at x = 3.57779, the skin friction decreases by 1.396% and also Nusselt number Nu_x decreases by 1.094% & species concentration Sh_x increases by 10.798% as Schmidt number Sc changes from 0.73 to 1.30.

The effect of different values of chemical reaction parameter γ on the skin friction coefficient, the local rate of heat transfer and rate of species concentration while Prandtl number Pr = 0.72, buoyancy ratio parameter N = 0.50, Schmidt number Sc = 0.73 and heat generation parameter Q =0.10 are shown in the figures 3.12- 3.14. Here, as the chemical reaction parameter γ increases, both the skin friction coefficient and heat transfer coefficient decrease and rate of species concentration increases. It is here observed that at x = 3.57779, the skin friction coefficient decreases by 6.8045% and also Nusselt number Nu_x decreases by 1.046% & species concentration Sh_x increases by 1.046% as Schmidt number γ changes from 0.0 to 0.70.

From Figures 3.17 - 3.19, it can also easily be seen that an increase in buoyancy parameter N leads to increase in the local skin friction coefficient C_{fx}, the local rate of heat transfer Nu_x and the local rate of species concentration Sh_x while Prandtl number Pr = 0.72, chemical reaction parameter γ = 0.60, heat generation parameter Q =0.10 and Schmidt number Sc = 0.73. It is also observed that at any position of x, the skin friction coefficient

C_{fx}, the local rate of species concentration Sh_x and the local Nusselt number Nu_x increase as N increases from 0.10 to 0.90. This phenomenon can easily be understood from the fact that when the buoyancy ratio parameter increases, the temperature of the fluid rises and the thickness of the velocity boundary layer grows, i.e., the thermal boundary layer becomes thinner than the velocity boundary layer. Therefore the skin friction coefficient C_{fx}, the local rate of species concentration Sh_x and the local Nusselt number Nu_x increase. It is here observed that, the local skin friction coefficient C_{fx}, the local rate of species concentration Sh_x and the local Nusselt number Nu_x increase by 28.144%, 12.777% and 12.777% respectively.

The effect for different values of heat generation parameter Q on the local skin friction coefficient C_{fx} , the local rate of heat transfer Nu_x and the local rate of species concentration Sh_x while Prandtl number Pr = 0.72, buoyancy ratio parameter N = 0.50, Schmidt number Sc = 0.73 and chemical reaction parameter γ = 0.60, are shown in figures 3.22, 3.23 and 3.24. Here, as the heat generation parameter Q increases, the local rate of heat transfer Nu_x and the local rate of species concentration Sh_x increase but the local Nusselt number Nu_x decreases. Howe. The values of skin friction coefficient C_{fx} are recorded to be 1.24325, 1.27159, 1.29386, 1.830921, 1.85480 at x=3.5779. Also Nusselt number Nu_x and Sherwood number Sh_x are recorded to be 0.39480, 0.45640, 0.38392, 0.37569, 0.37018 and 0.10543, 0.11029, 0.11706, 0.11708, 0.11996 for Q = 0.01,0.03, 0.05, 0.08, 0.10 respectively. Also it is observed that at x= 3.5779, the skin friction co-efficient C_{fx} increases by 32.9712% and at x=0.17453, the local rate of species concentration Sh_x increases by 12.1124% but at x=0.08727, the local rates of heat transfer Nu_x decreases by -6.6508% as Q increases from 0.01 to 0.10.

Figures 3.5 and figures 3.6 illustrate the effect of the Prandtl number Pr on the development of streamlines and isotherms which are plotted for buoyancy ratio parameter N =0.50, heat generation parameter Q = 0.10, Schmidt number Sc =0.73 and chemical reaction parameter γ = 0.60. From Figure 3.5(a), it is seen that when the Prandtl number Pr=0.72, the non- dimensional value of ψ_{max} within the computational domain is about 15.00 located at the upper stagnation point (x $\approx\pi$) of the vertical plate and when the thickness of the boundary layer reaches to the maximum level, but ψ_{max} again decrease with Pr and it attains about 13.64 for Pr= 3.0(see fig 3.5(b), 12.66 for Pr= 5.0(see fig

3.5(c) and 11.69 for *Pr* =7.0(see fig 3.5(d). This phenomenon fully coincides with the fluid properties that the fluid speeds down as *Pr* decreases and the thickness of the velocity boundary layer grows substantially. The isotherm patterns for corresponding values are shown in Figure 3.6. From all these frames, we can see that the growth of the thermal boundary layer over the surface of the vertical flat plate is significant. As x increases from lower stagnation point ($x \approx 0$), the hot fluid raises down due to the gravity hence the thickness of the thermal boundary layer, y, is expected to grow. This phenomenon is very straightforward, as can be seen in frames 3.6, there is not appear deepness on the isotherms near to the surface of the vertical flat plate. The levels of isotherms are noticeably lower than the surface level and the fluid temperature not exceeds the level of surface temperature.

The development of streamlines and isotherms which are plotted for buoyancy ratio parameter *N* =0.50, heat generation parameter *Q* = 0.10, Prandtl number *Pr* =0.72 and chemical reaction parameter γ = 0.60 for the different values of Schmidt number *Sc* (0.73, 0.80, 1.00, 1.10 and 1.30) are shown in Figure 3.10 and Figure 3.11. As *Sc* increases, the fluid speeds up and the thickness of the velocity boundary layer grows substantially. The isotherm patterns for corresponding values are shown in Figure 3.11. From all these frames, we can see that the growth of the thermal boundary layer over the surface of the vertical flat plate is significant. As x increases from lower stagnation point ($x \approx 0$), the hot fluid raises up due to the gravity hence the thickness of the thermal boundary layer, y, is expected to grow. But this phenomenon is not very straightforward, as can be seen in frames 3.11; there appear deepness on the isotherms near to the surface of the vertical plate. The levels of isotherms are noticeably lower than the surface level and the fluid temperature exceeds the level of surface temperature.

The development of streamlines and isotherms which are plotted for buoyancy ratio parameter *N* =0.50, heat generation parameter *Q* = 0.10, Prandtl number *Pr* =0.72 and Schmidt number *Sc* = 0.73 for the different values of chemical reaction parameter γ (0.00, 0.20, 0.40, 0.60 and 0.70) are shown in Figure 3.15 and Figure 3.16. As γ increases, the fluid speeds up and the thickness of the velocity boundary layer grows substantially. The isotherm patterns for corresponding values are shown in Figure 3.22. From all these frames, we can see that as x increases from lower stagnation point ($x \approx 0$), the hot fluid

raises up due to the gravity hence the thickness of the thermal boundary layer, y, is expected to grow. But this phenomenon is not very straightforward, as can be seen in frames 3.22; there appear deepness on the isotherms near to the surface of the vertical plate. The levels of isotherms are noticeably lower than the surface level and the fluid temperature not exceeds the level of surface temperature.

Figures 3.21 and figures 3.22 illustrate the effect of the buoyancy ratio parameter *N* on the development of streamlines and isotherms which are plotted for Prandtl number *Pr* =0.72, heat generation parameter *Q* = 0.10, Schmidt number *Sc* =0.73 and chemical reaction parameter γ = 0.60. From Figure 3.15(a), it is seen that when the buoyancy ratio parameter *N*=0.10, the non- dimensional value of ψ_{max} within the computational domain is about 13.51 located at the upper stagnation point (x $\approx\pi$) of the vertical plate and when the thickness of the boundary layer reaches to the maximum level, but ψ_{max} again increase with *N* and it attains about 14.41 for *N*= 0.30(see fig 3.15(b), 14.89 for *N*= 0.50(see fig 3.15(c) and 15.05 for *N* =0.90(see fig 3.15(d). This phenomenon fully coincides with the fluid properties that the fluid speeds down as *N* increases and the thickness of the velocity boundary layer grows substantially. The isotherm patterns for corresponding values are shown in Figure 3.16. From all these frames, we can see that the growth of the thermal boundary layer over the surface of the vertical flat plate is significant. As x increases from lower stagnation point (x $\approx$0), the hot fluid raises down due to the gravity hence the thickness of the thermal boundary layer, y, is expected to grow. This phenomenon is very straightforward, as can be seen in frames 3.16, there is not appear deepness on the isotherms near to the surface of the vertical flat plate. The levels of isotherms are noticeably lower than the surface level and the fluid temperature not exceeds the level of surface temperature.

Figures 3.25 and figures 3.26 illustrate the effect of the heat generation parameter *Q* on the development of streamlines and isotherms which are plotted for Prandtl number *Pr* =0.72, buoyancy ratio parameter *N* = 0.50, Schmidt number *Sc* =0.73 and chemical reaction parameter γ = 0.60. From Figure 3.25(a), it is seen that when the heat generation parameter *Q*=0.01, the non- dimensional value of ψ_{max} within the computational domain is about 11.71 located at the upper stagnation point (x $\approx\pi$) of the vertical plate and when the thickness of the boundary layer reaches to the maximum level, but ψ_{max} again increase with

Q and it attains about 12.82 for Q= 0.03(see fig 3.25(b), 14.00 for Q= 0.08(see fig 3.25(c) and 18.82for Q =0.10(see fig 3.25(d)). This phenomenon fully coincides with the fluid properties that the fluid speeds up as N increases and the thickness of the velocity boundary layer grows substantially. The isotherm patterns for corresponding values are shown in Figure 3.26. we can see from all these frames that as x increases from lower stagnation point ($x \approx 0$), the hot fluid raises up due to the gravity hence the thickness of the thermal boundary layer, y, is expected to grow. This phenomenon is very straightforward, as can be seen in frames 3.26, there is appear deepness on the isotherms near to the surface of the vertical flat plate. The levels of isotherms are noticeably higher than the surface level and the fluid temperature exceeds the level of surface temperature.

Numerical values of skin friction coefficient C_{fx} , rate of heat transfer Nu_x and rate of species concentration Sh_x are calculated from Equations (3.23) and (3.24) from the surface of the vertical flat plate. Numerical values of C_{fx} ,Nu_x and Sh_x are shown in table 3.1.

Table 3.1: Skin friction coefficient, rate of heat transfer and rate of species concentration against x for different values of heat generation parameter Q with other controlling parameters Pr = 0.72, Sc = 0.73, N =0.50 and γ = 0.60.

x	Q=0.01			Q=0.05			Q=0.10		
	C_{fx}	Nu_x	Sh_x	C_{fx}	Nu_x	Sh_x	C_{fx}	Nu_x	Sh_x
0.00000	0.00000	0.40909	0.13436	0.00000	0.40909	0.13436	0.00000	0.40909	0.13436
0.26180	0.51415	0.37491	0.10403	0.52051	0.34828	0.09366	0.54186	0.25954	0.09964
0.52360	0.66316	0.35191	0.10024	0.67411	0.31911	0.10475	0.71155	0.20714	0.10333
0.78540	0.76488	0.33378	0.09533	0.77996	0.29495	0.09209	0.83237	0.16056	0.09523
1.04720	0.84366	0.31929	0.09254	0.86262	0.27701	0.09561	0.92934	0.09650	0.09532
1.30900	0.90856	0.30707	0.08915	0.93120	0.26086	0.08710	1.01182	0.08983	0.12826
1.57080	0.96406	0.29677	0.08712	0.99024	0.24804	0.08976	1.08445	0.07245	0.08992
1.83260	1.01273	0.28774	0.08452	1.04235	0.23602	0.08275	1.14992	0.04785	0.08550
2.09440	1.05621	0.27989	0.08302	1.08916	0.22615	0.08562	1.20991	0.02839	0.08595
2.35619	1.09558	0.27282	0.08086	1.13179	0.21663	0.07907	1.26557	0.00805	0.08200
2.61799	1.13163	0.26654	0.07974	1.17103	0.20864	0.08251	1.31773	-0.00849	0.08287
2.87979	1.16493	0.26079	0.07786	1.20745	0.20079	0.07587	1.36697	-0.02601	0.07905

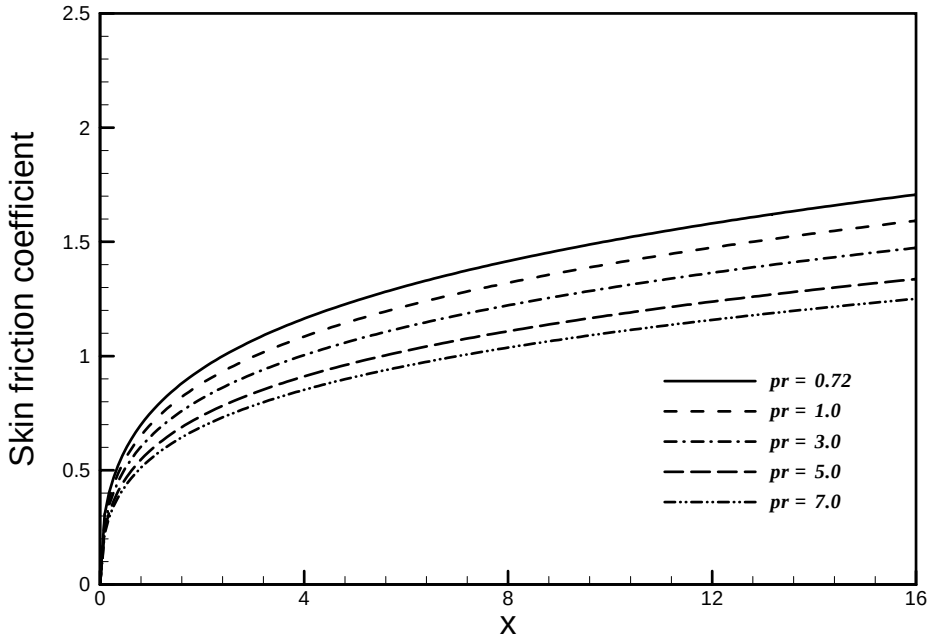

Figure 3.2: Skin friction coefficient for different values of *Pr* in case of *Sc* = 0.73, *N* =*0*.50, *Q* = 0.10 and γ = 0.60.

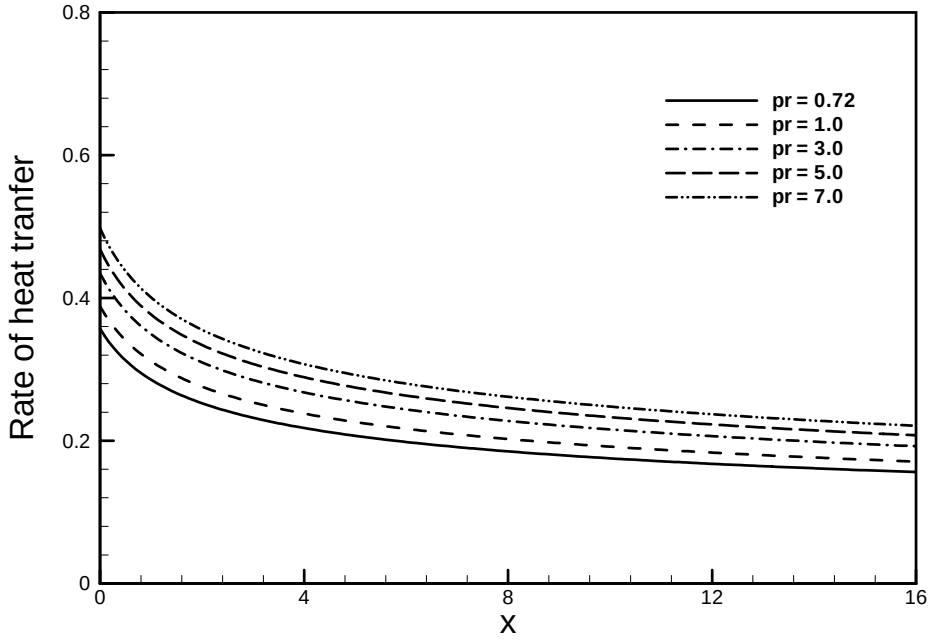

Figure 3.3: Rate of heat transfer for different values of *Pr* in case of *Sc* = 0.73, *N* =*0*.50, *Q* = 0.10 and γ = 0.60.

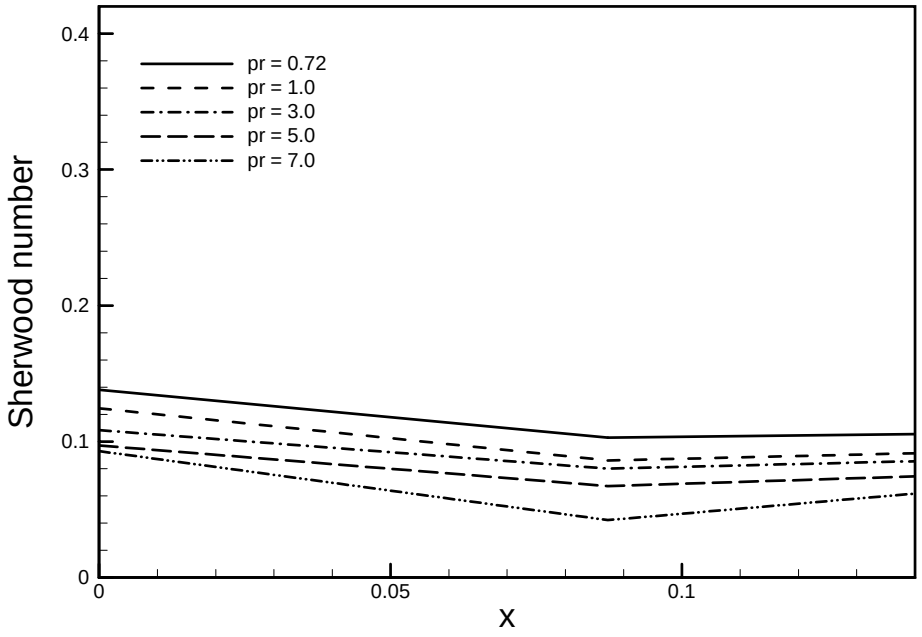

Figure 3.4: Rate of species concentration for different values of *Pr* in case of *Sc* = 0.73, *N* =*0*.50, *Q* = 0.10 and γ = 0.60.

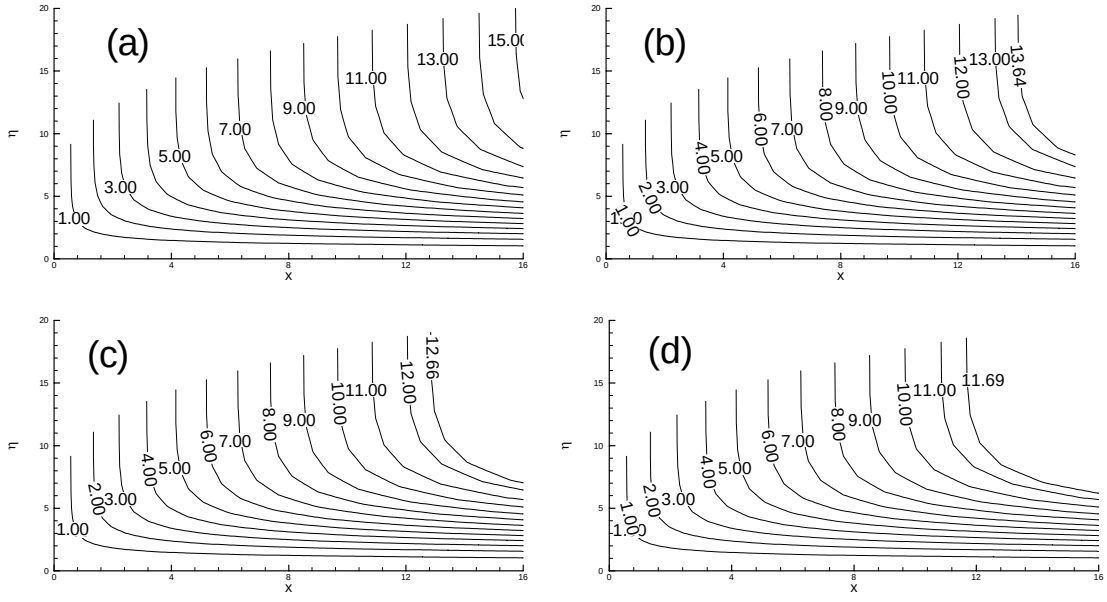

Figure 3.5: Streamlines for a) *Pr* =0.72 b) *Pr* = 3.0 c) *Pr* = 5.0 *d) Pr* = 7.0 in case of *Sc* = 0.73, *N* =*0*.50, *Q* = 0.10 and γ = 0.60.

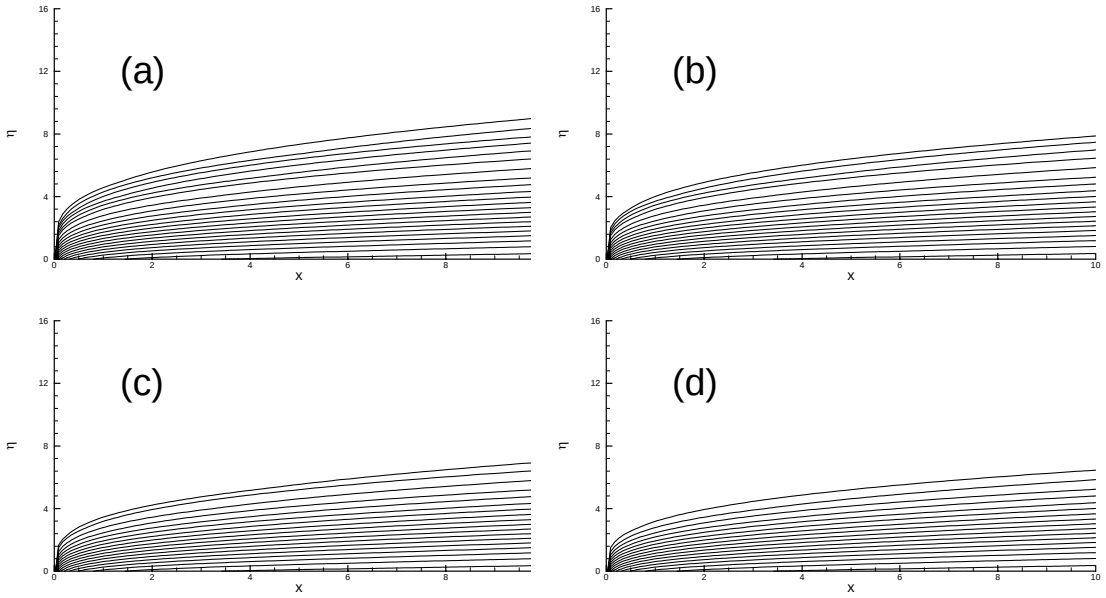

Figure 3.6: Isotherms for a) *Pr* =0.72 b) *Pr* = 3.0 c) *Pr* = 5.0 *d) Pr* = 7.0 in case of *Sc* = 0.73, *N =0*.50, *Q* = 0.10 and γ = 0.60

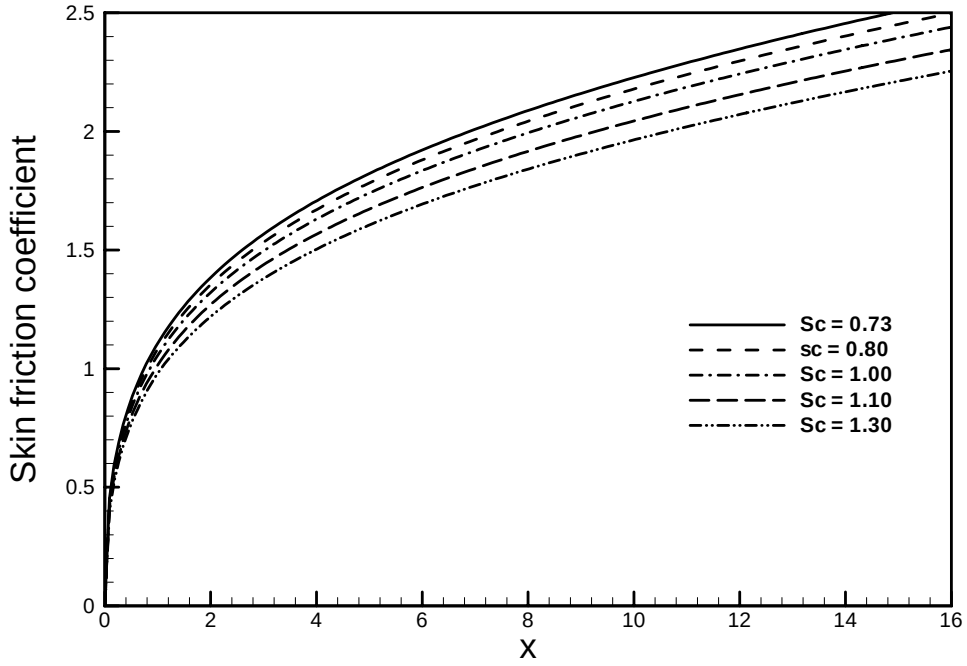

Figure 3.7: Skin friction coefficient for different values of *Sc* in case of *Pr* = 0.72, *N =0*.50, *Q* = 0.10 and γ = 0.60.

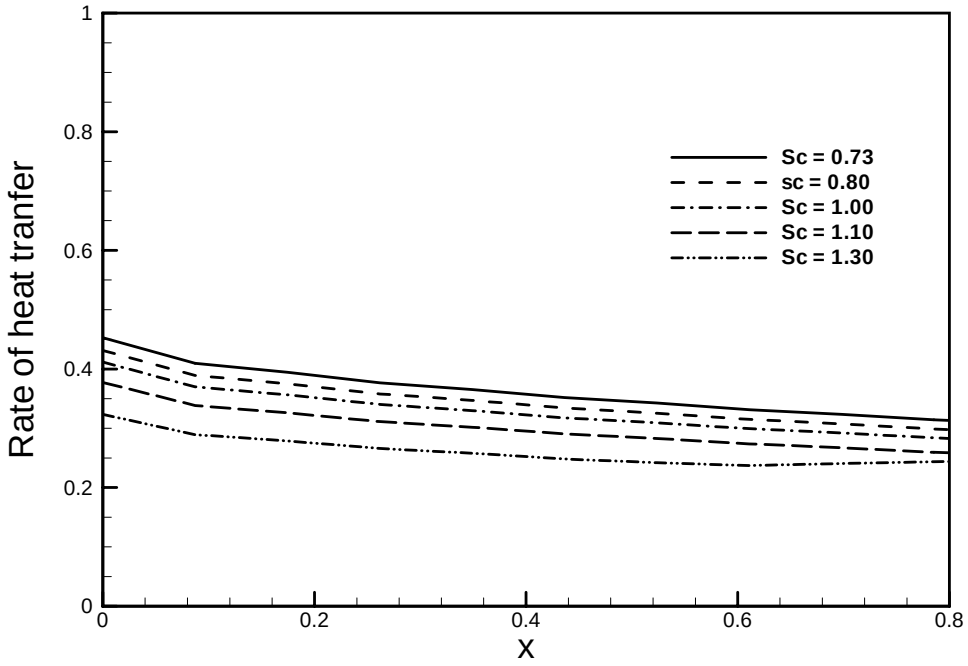

Figure 3.8: Rate of heat transfer for different values of *Sc* in case of *Pr* = 0.72, *N* =*0*.50, *Q* = 0.10 and γ = 0.60.

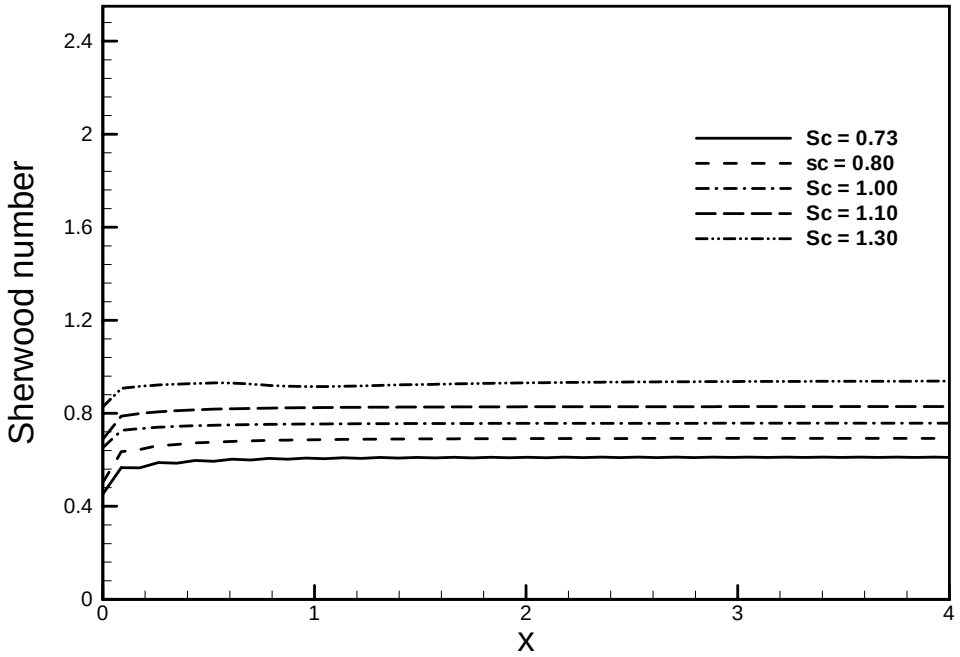

Figure 3.9: Rate of species concentration for different values of *Sc* in case of *Pr* = 0.72, *N* =*0*.50, *Q* = 0.10 and γ = 0.60.

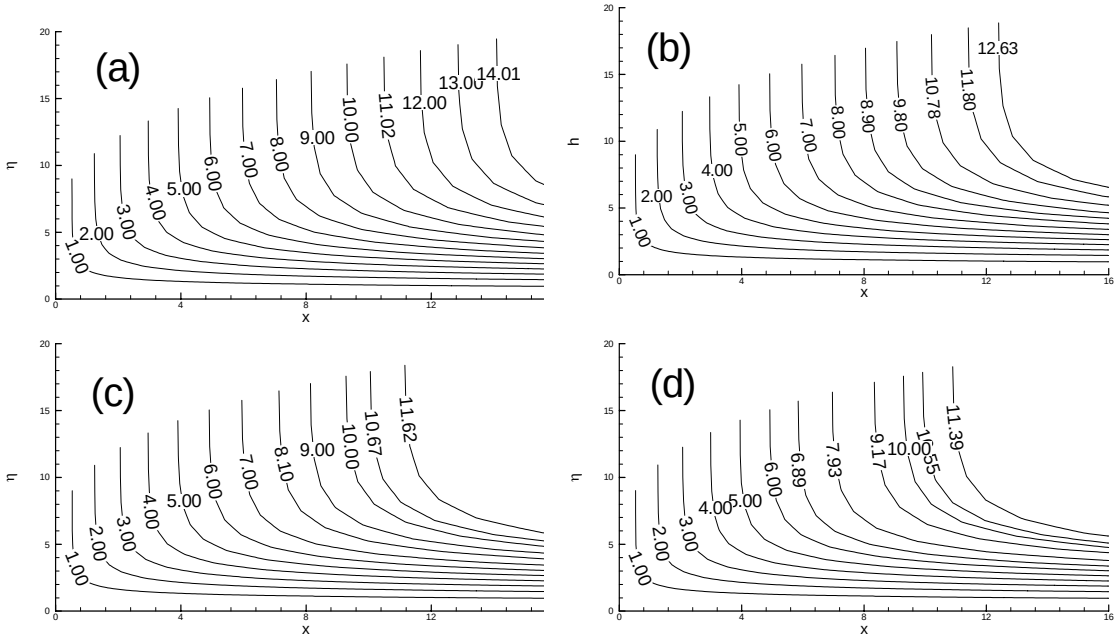

Figure 3.10: Streamlines for a) *Sc*= 0.73 b) *Sc*= 0.80 c) *Sc* = 1.00 d) *Sc* =1.30 in case of *Pr* = 0.72, *N* =*0*.50, *Q* = 0.10 and γ = 0.60.

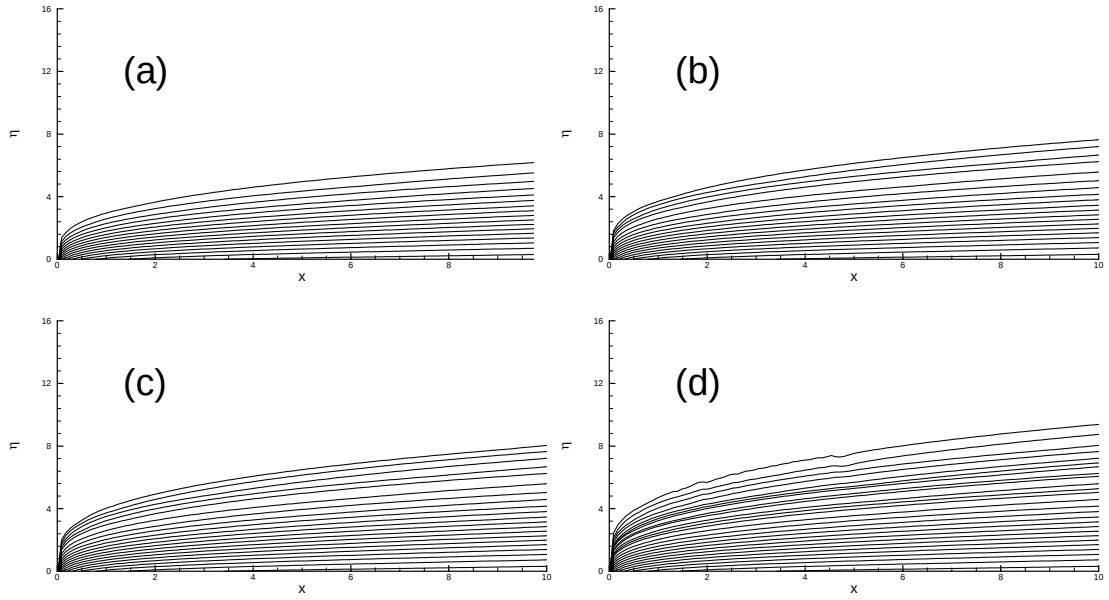

Figure 3.11: Isotherm for a) *Sc*= 0.72 b) *Sc*= 0.80 c) *Sc* = 1.0 d) *Sc* =1.30 in case of *Pr* = 0.72, *N* =*0*.5, *Q* = 0.40 and γ = 0.60.

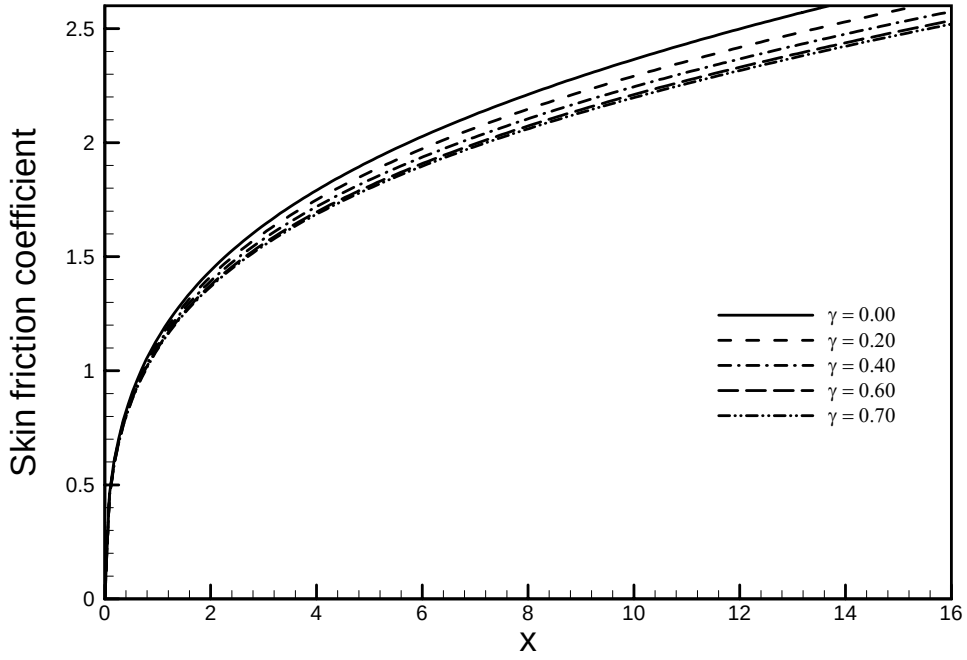

Figure 3.12: Skin friction coefficient for different values of γ in case of Sc = 0.73, N =*0*.5, Q = 0.40 and Pr = 0.72.

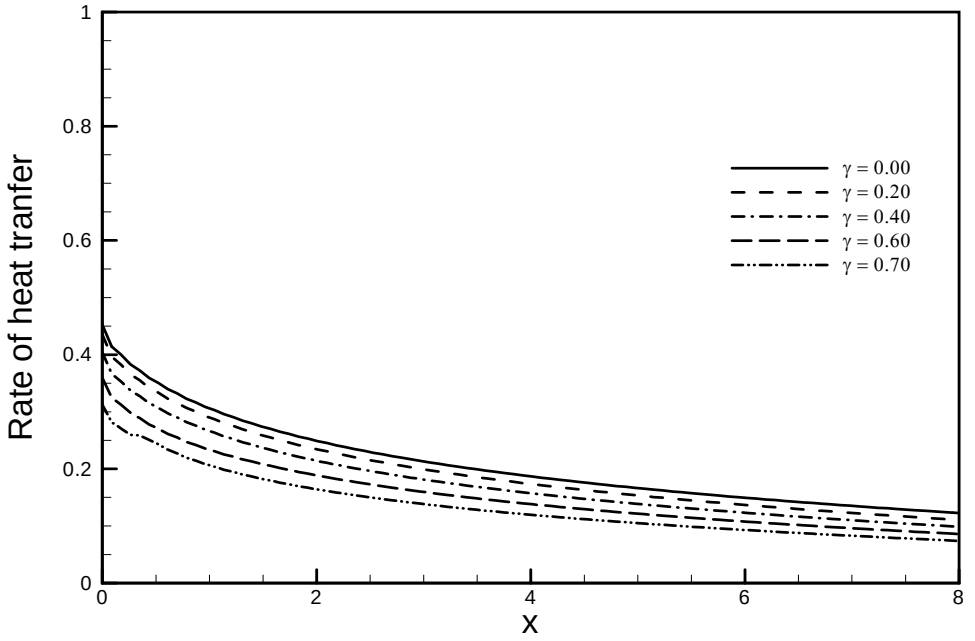

Figure 3.13: Rate of heat transfer for different values of γ in case of Sc = 0.73, N =*0*.5, Q = 0.40 and Pr = 0.72.

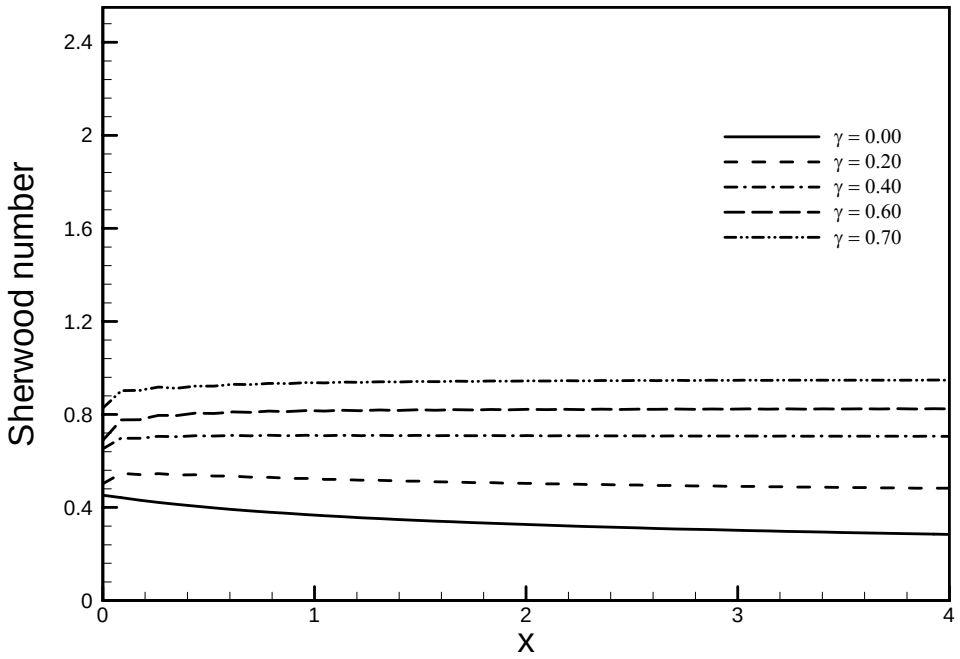

Figure 3.14: Rate of species concentration for different values of γ in case of Sc = 0.73, N =*0*.5, Q = 0.40 and Pr = 0.72.

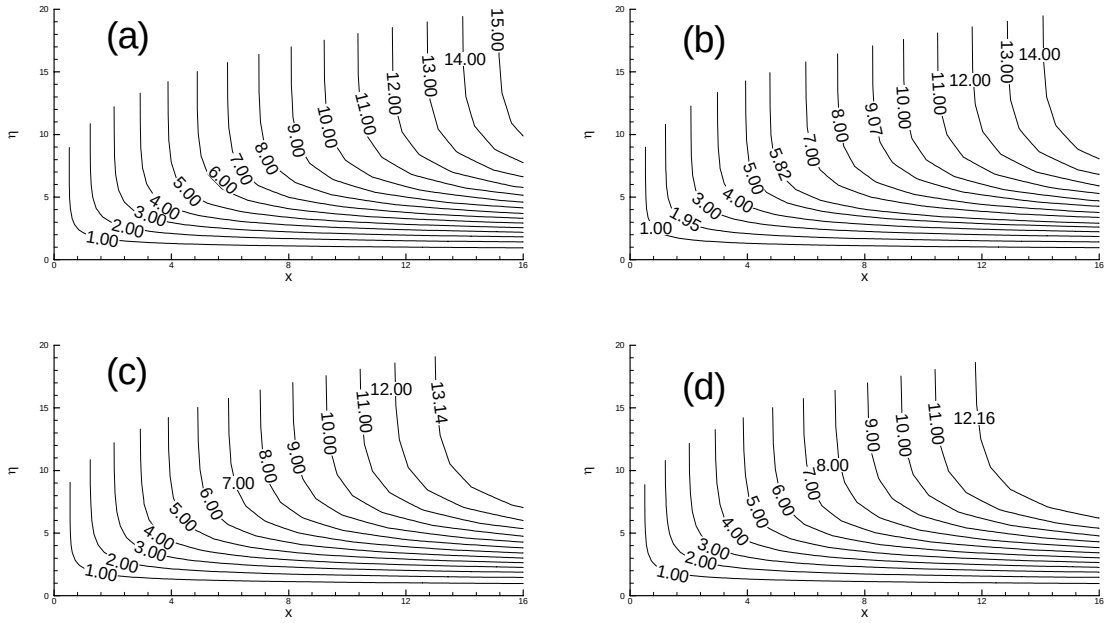

Figure 3.15: Streamlines for a) γ =0.20 *b)* γ = 0.40 c) γ = 0.60 d) γ = 0.70 in case of Sc = 0.73, N =*0*.5, Q = 0.40 and Pr = 0.72.

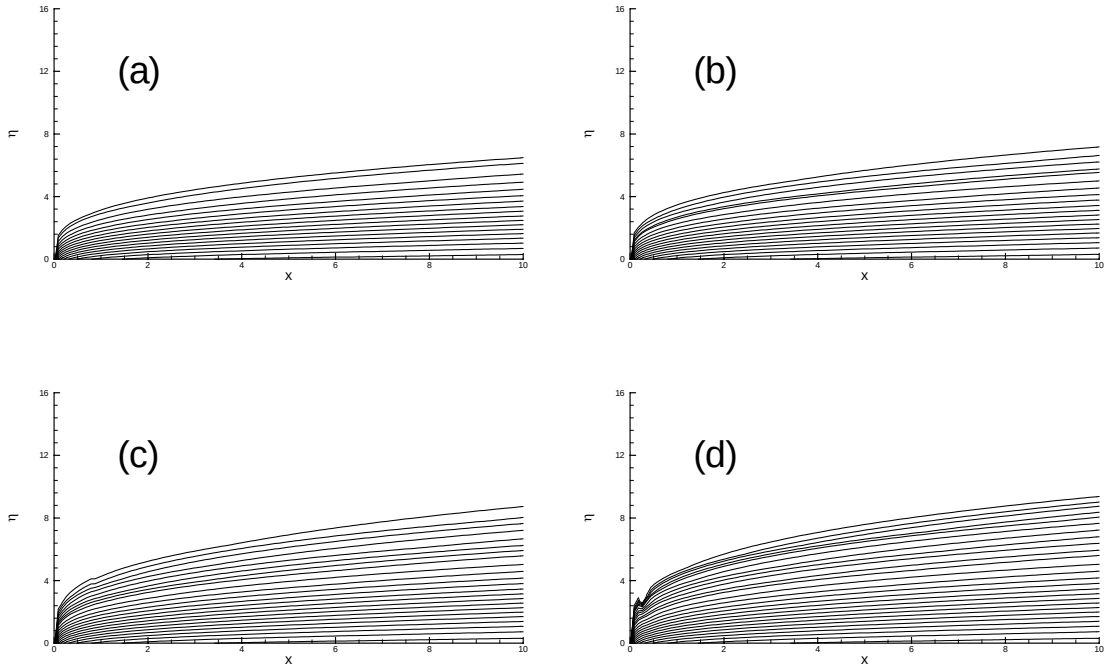

Figure 3.16: Isotherms for a) γ =0.20 *b)* γ = 0.40 c) γ = 0.60 d) γ = 0.70 in case of *Sc* = 0.73, *N* =*0*.5, *Q* = 0.40 and *Pr* = 0.72.

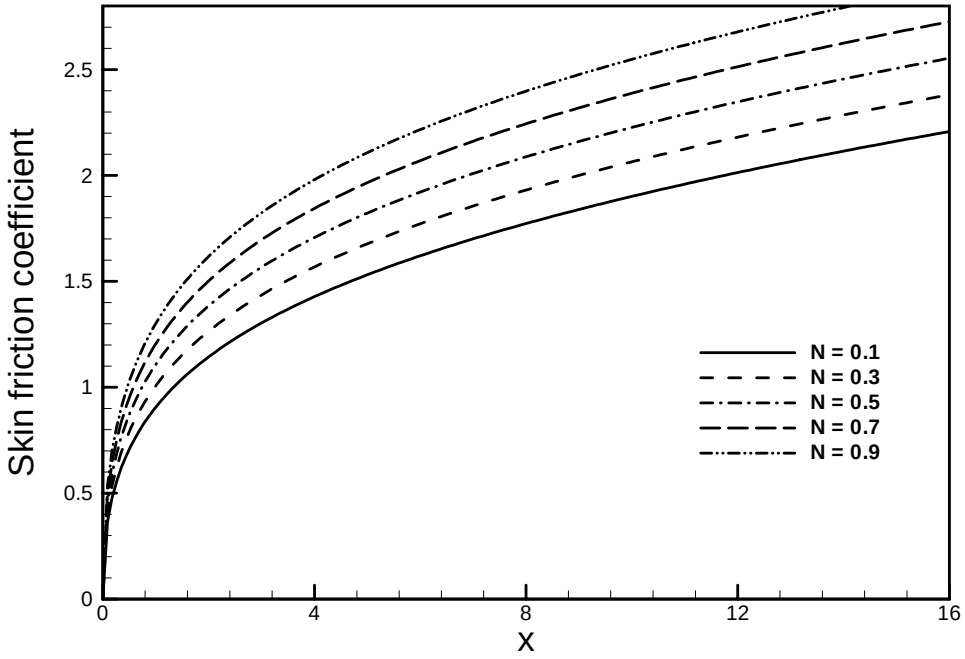

Figure 3.17: Skin friction coefficient for different values of *N* in case of *Sc* = 0.73, *Pr* =*0*.5, *Q* = 0.40 and γ = 0.60.

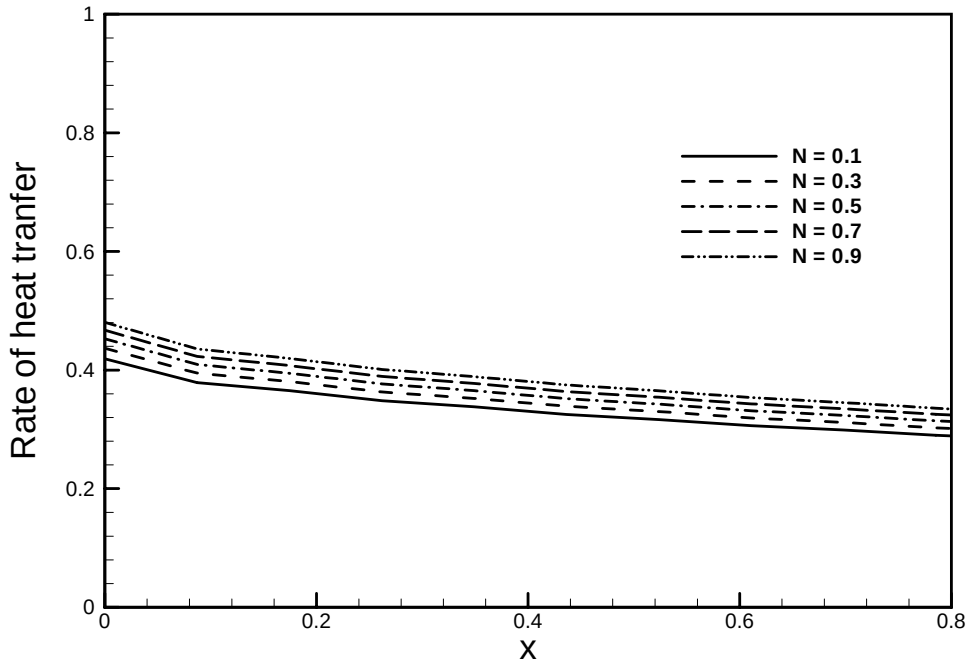

Figure 3.18: Rate of heat transfer for different values of N in case of Sc = 0.73, Pr =0.72, Q = 0.40 and γ = 0.60.

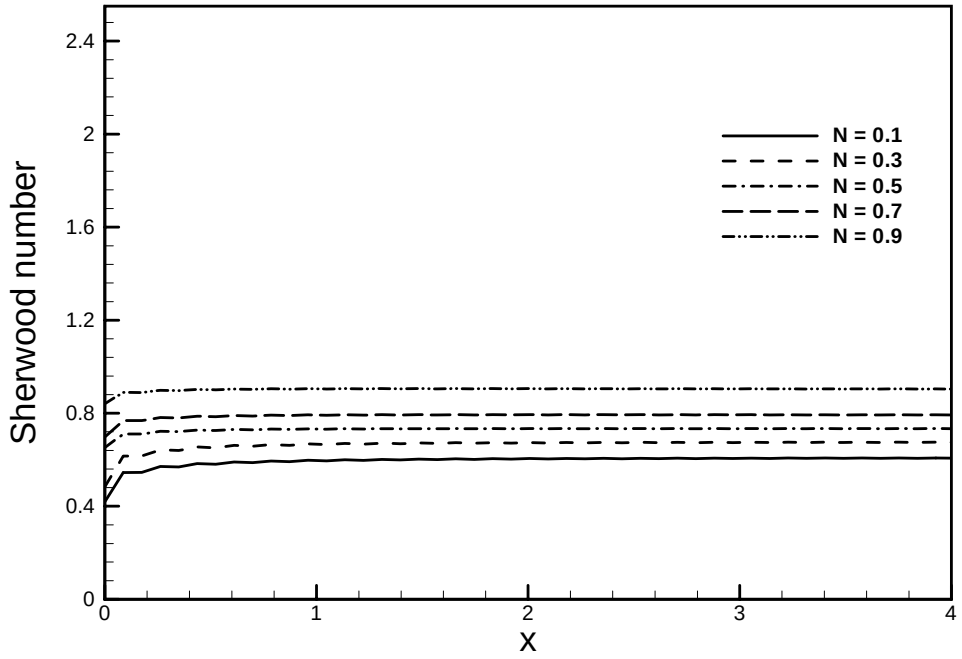

Figure 3.19: Rate of species concentration for different values of N in case of Sc = 0.73, Pr =0.72, Q = 0.40 and γ = 0.60.

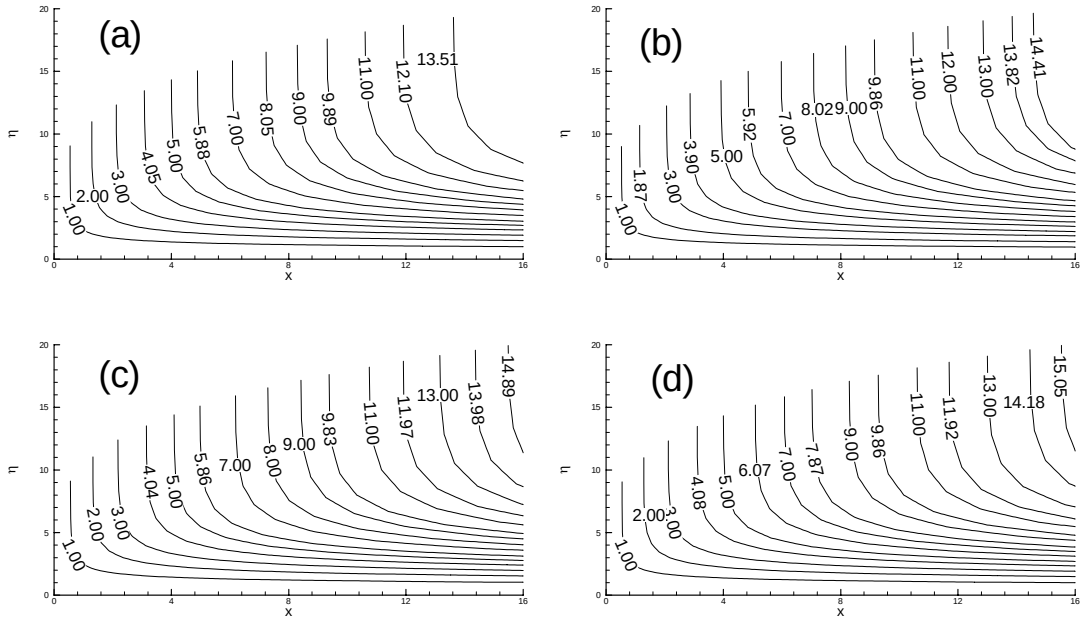

Figure 3.20: Streamlines for a) $N = 0.10$ *b)* $N = 0.30$ *c)* $N = 0.50$ *d)* $N = 0.90$ in case of $Sc = 0.73$, $Pr = 0.72$, $Q = 0.40$ and $\gamma = 0.60$.

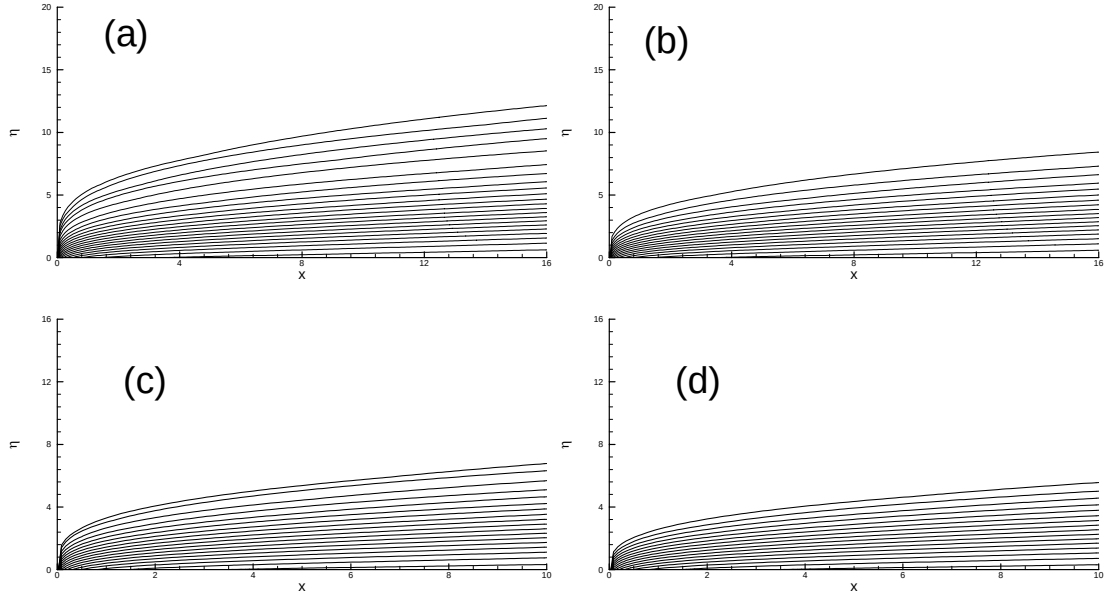

Figure 3.21: Isotherms for a) $N = 0.10$ *b)* $N = 0.30$ *c)* $N = 0.50$ *d)* $N = 0.90$ in case of $Sc = 0.72$, $Pr = 0.72$, $Q = 0.40$ and $\gamma = 0.5$.

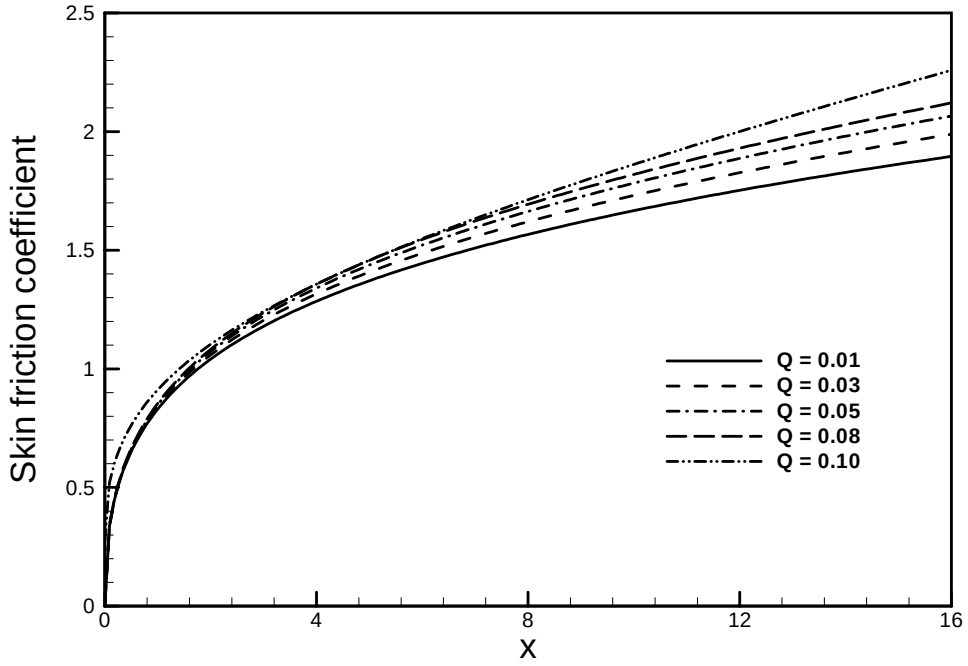

Figure 3.22: Skin friction coefficient for different values of Q in case of $Sc = 0.73$, $Pr = 0.72$, $N = 0.50$ and $\gamma = 0.60$.

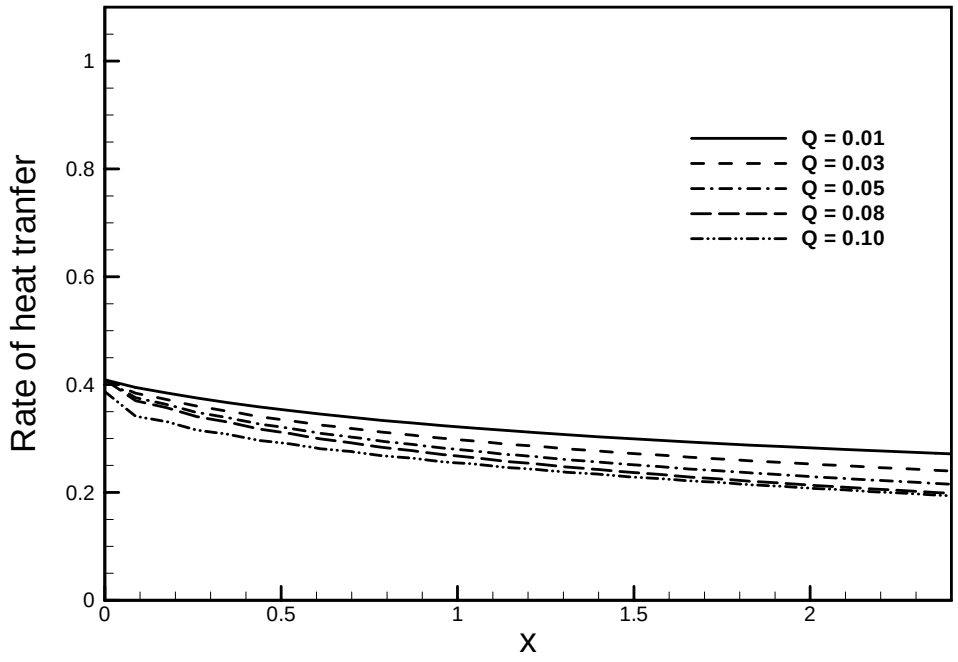

Figure 3.23: Rate of heat transfer for different values of Q in case of $Sc = 0.73$, $Pr = 0.72$, $N = 0.50$ and $\gamma = 0.60$.

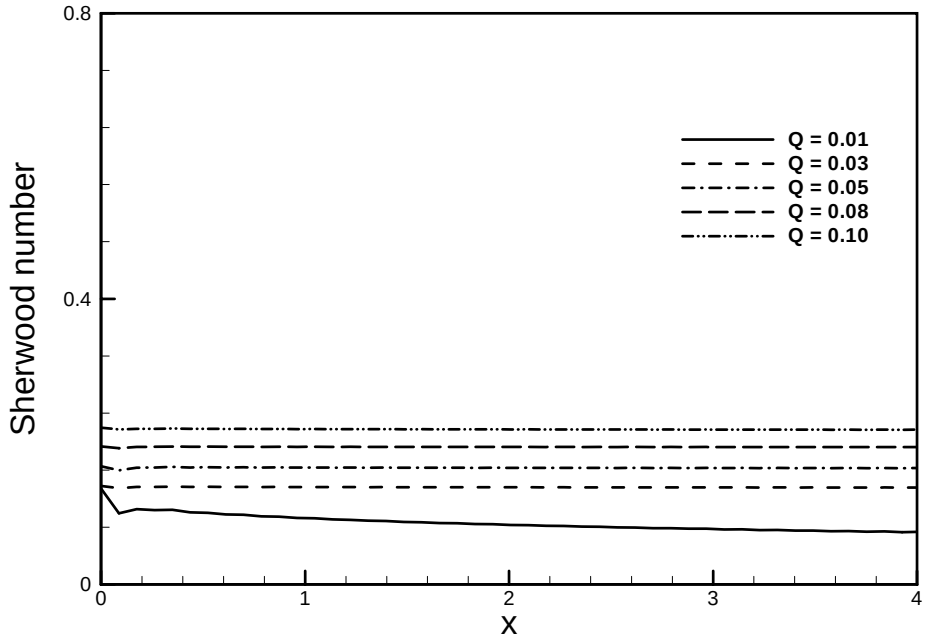

Figure 3.24: Rate of species concentration for different values of Q in case of Sc = 0.73, Pr =0.72, N = 0.50 and γ = 0.60.

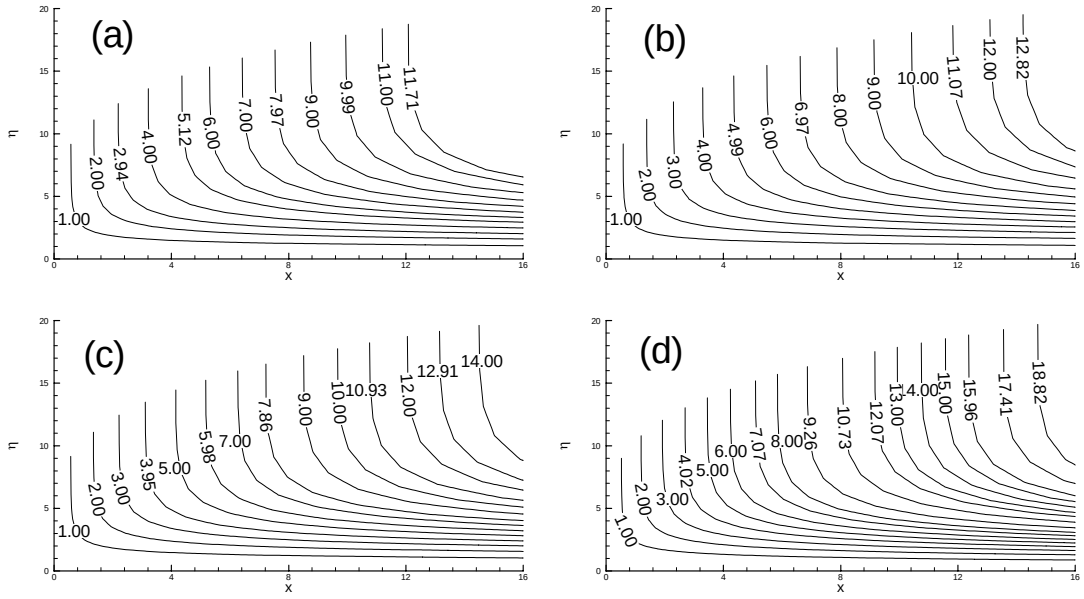

Figure 3.25: Streamlines for a) Q = 0.03 b) Q = 0.05 c) Q =0.08 d) Q = 1.0 in case of Sc = 0.73, Pr =0.72, N = 0.50 and γ = 0.60.

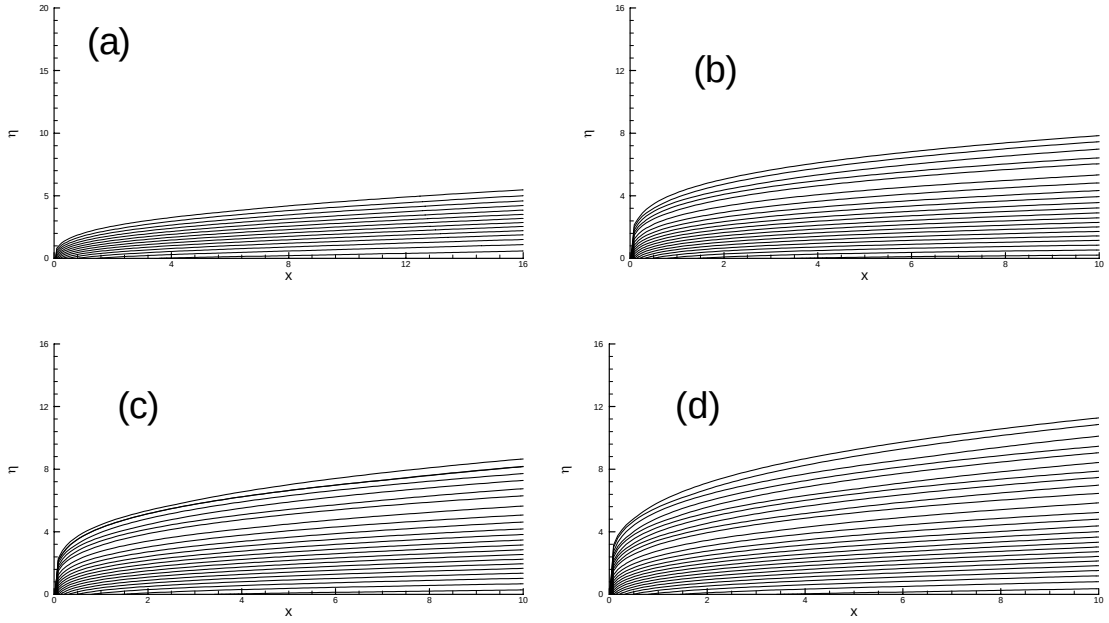

Figure 3.26: Isotherms for a) Q = 0.03 b) Q = 0.05 c) Q =0.08 d) Q = 1.0 Sc = 0.73, Pr =*0*.72, N = 0.50 and γ = 0.60.

3.4 Conclusion

For different values of relevant physical parameters including the heat generation parameter Q, the conjugate effects of heat and mass transfer on natural convection flow along a vertical flat plate has been investigated. The governing boundary layer equations of motion are transformed into a non-dimensional form and the resulting non-linear systems of partial differential equations are reduced to local non-similarity boundary layer equations, which are solved numerically by using implicit finite difference method together with the Keller-box scheme. From the present investigation the following conclusions may be drawn:

- Significant effects of heat generation parameter Q on skin friction coefficient $C_{fx,,}$ the rate of heat transfer Nu_x and the rate of species concentration Sh_x have been found in this investigation but the effect of heat generation parameter Q on skin friction

coefficient and the rate of species concentration are more significant. An increase in the values of heat generation parameter Q leads to an increase in the local skin friction coefficient C_{fx} and the rate of species concentration Sh_x at different position of η but the local rate of heat transfer Nu_x decreases at different position of x for Pr =0.72.

- All the local skin friction coefficient C_{fx}, the local rate of heat transfer Nu_x and the local rate of species concentration Sh_x increase significantly when the values of buoyancy ratio parameter N increases.
- As the Chemical reaction parameter γ increases, both the skin friction coefficient C_{fx} and the local rate of heat transfer Nu_x decrease significantly but the local rate of species concentration Sh_x increases.
- Increasing values of Prandtl number Pr lead to decrease the local skin friction coefficient C_{fx} and the local rate of species concentration Sh_x but increase the local rate of heat transfer Nu_x.
- An increase in the values of Sc leads to an increase in the values of the local rate of species concentration Sh_x but both the local skin friction coefficient C_{fx} and the local rate of heat transfer Nu_x decrease when Sc increases.
- Streamlines and isotherms have changed significantly with the increasing values of parameters.

Chapter 4

4.1 Comparison of the results

In this context we have investigated analytically the conjugate effects of heat and mass transfer first in absence of heat generation and then in presence of heat generation with chemical reaction. Figure 4.1 to 4.6 depicts the comparisons of the numerical results of the Skin friction $C_{fx,}$ Nusselt number Nu_x and Sherwood number Sh_x in the First chapter(when heat generation parameter Q absent) with those in the Second chapter(when heat generation parameter Q present).

Here, the chemical reaction parameter γ = 0.5, buoyancy ratio parameter N=0.5 and Schmidt number Sc = 0.72 are chosen in case of Pr = 0.72 (Q = 0.0), Pr = 0.72 (Q=0.10) and Pr = 7.0 (Q=0.0), Pr = 7.0(Q=0.10) respectively. A careful study of the results and it helped me to take decision that the present results agree well with the solutions.

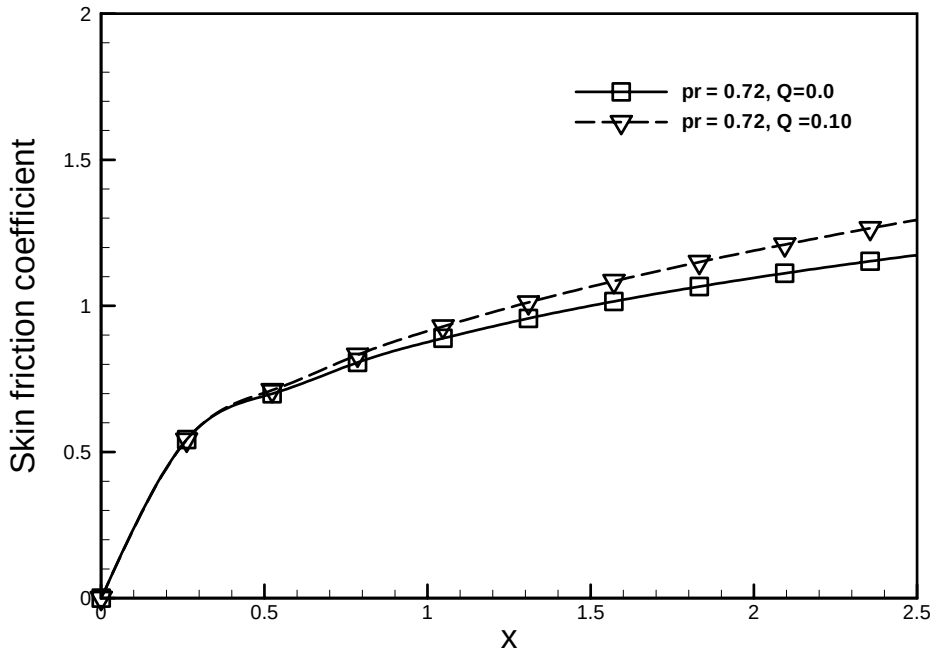

Figure 4.1: Comparisons of the numerical results of Skin friction C_{fx} for the Prandtl numbers Pr =0.72 with those obtained by Q =0.0 and Q = 0.10.

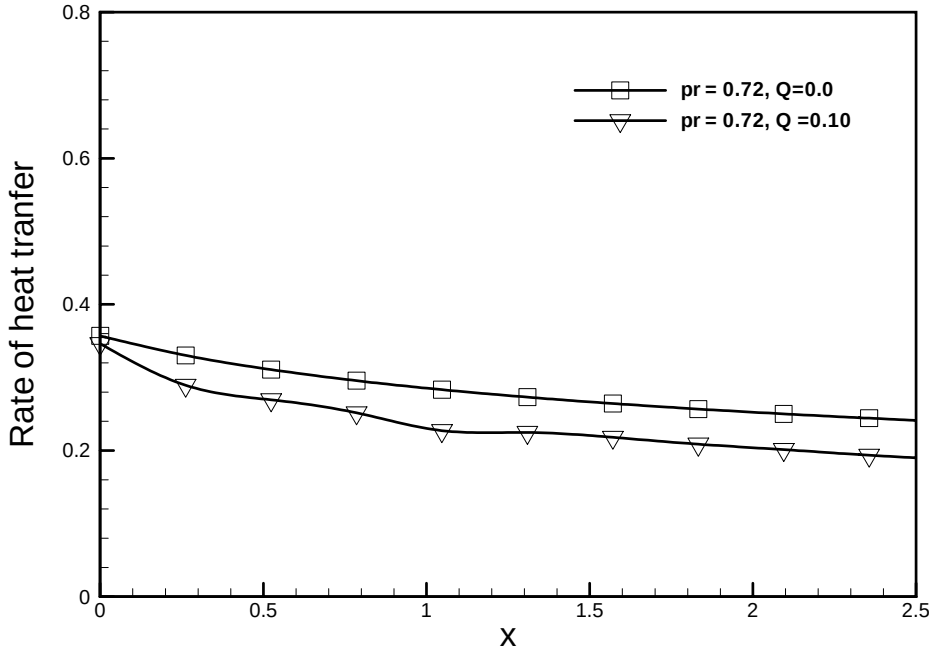

Figure 4.2: Comparisons of the numerical results of Nusselt number Nu_x for the Prandtl numbers Pr =0.72 with those obtained by Q =0.0 and Q = 0.10.

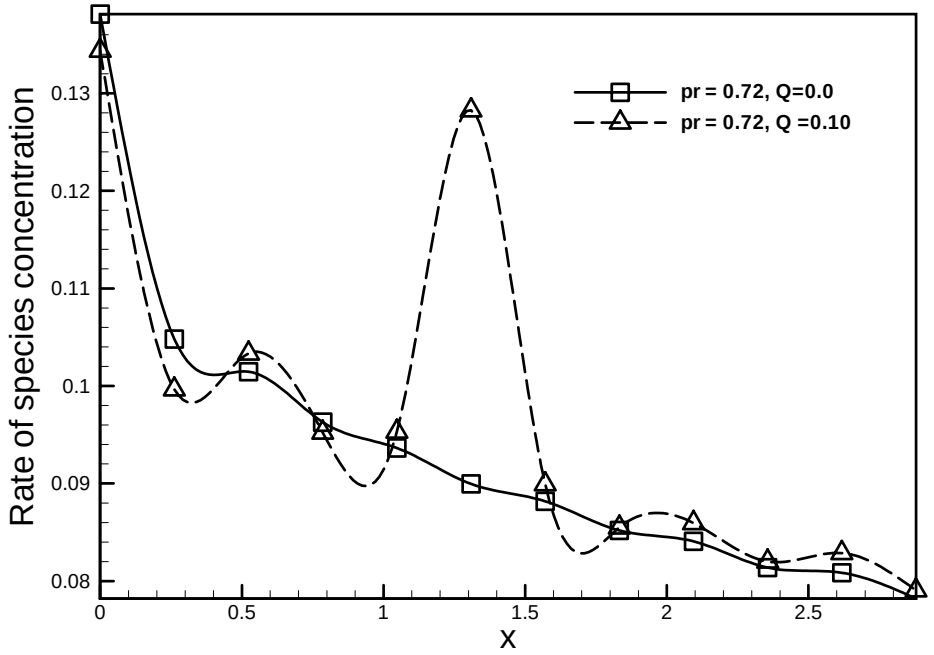

Figure 4.3: Comparisons of the numerical results of Schmidt number Sc for the Prandtl numbers Pr =0.72 with those obtained by Q =0.0 and Q = 0.10.

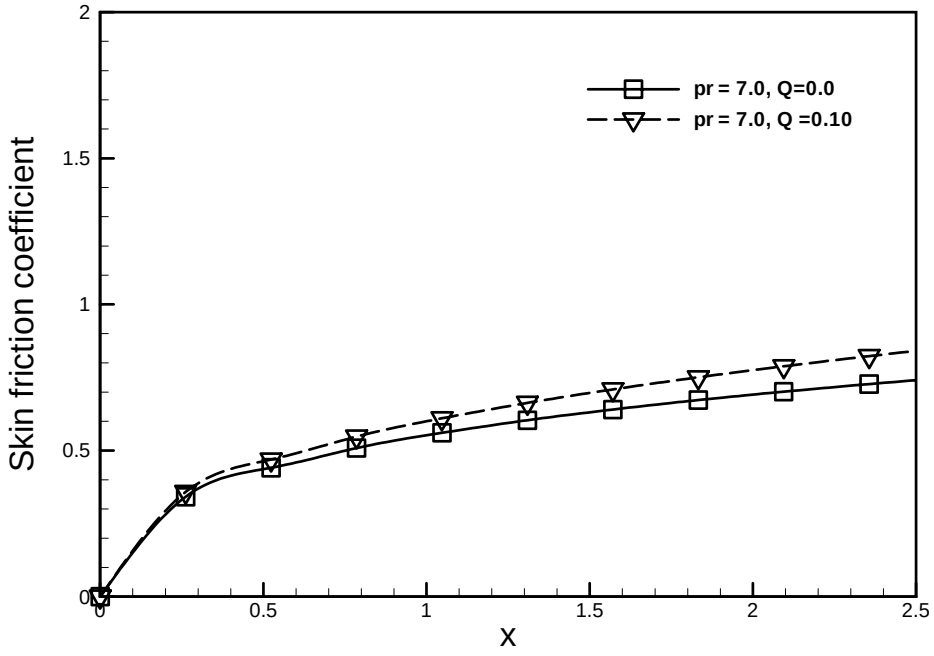

Figure 4.4: Comparisons of the numerical results of skin friction C_{fx} for the Prandtl numbers Pr =7.0 with those obtained by Q =0.0 and Q = 0.10.

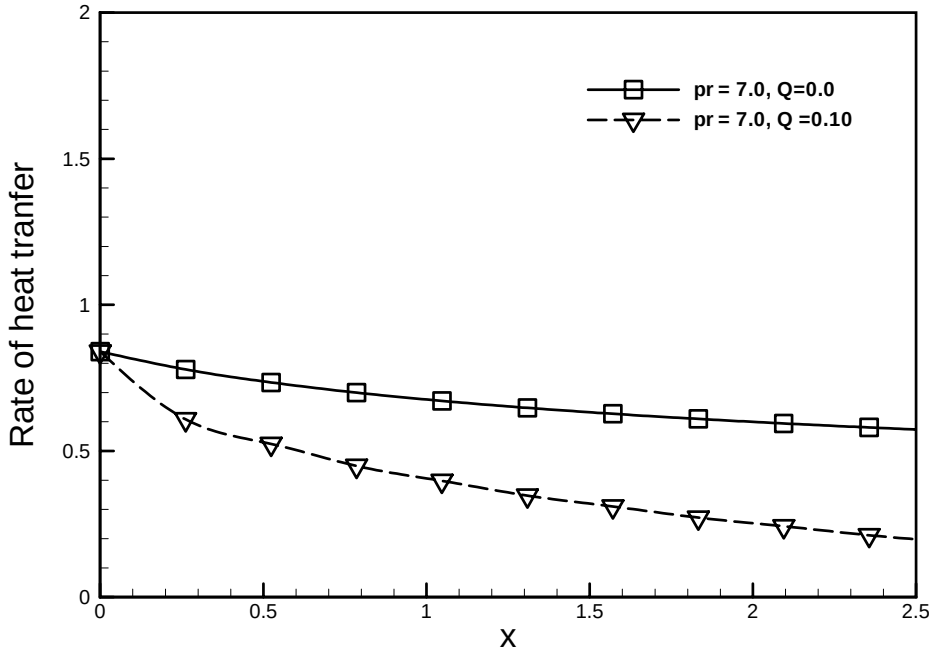

Figure 4.5: Comparisons of the numerical results of Nusselt number Nu_x for the Prandtl numbers Pr =7.0 with those obtained by Q =0.0 and Q = 0.10.

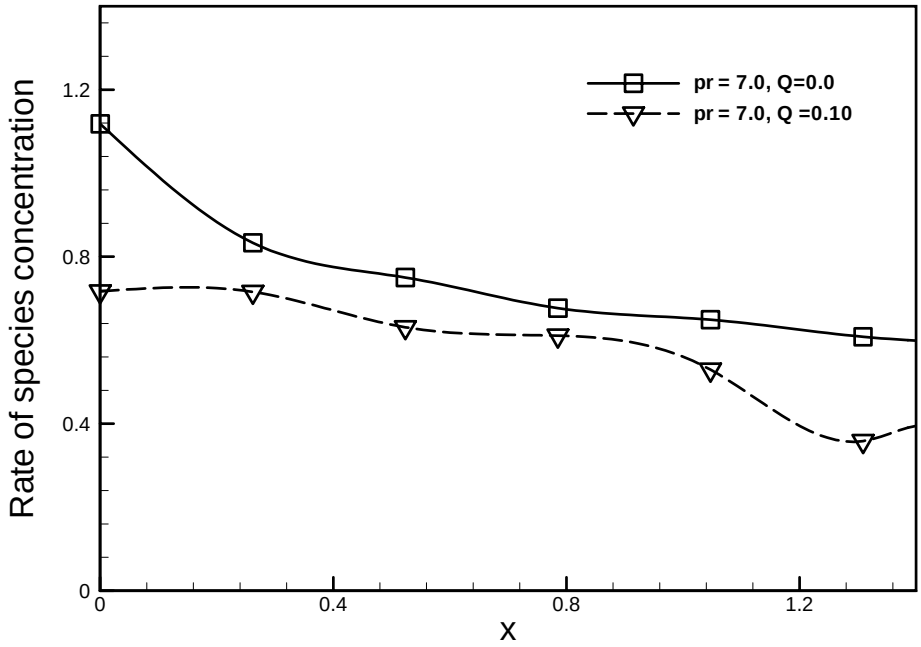

Figure 4.6: Comparisons of the numerical results of Schmidt number *Sc* for the Prandtl numbers *Pr* = 7.0 with those obtained by *Q* =0.0 and *Q* = 0.10.

Figure 4.1 and 4.4 show the comparisons of the numerical results of the skin friction coefficients C_{fx} at Q = 0.0 and Q = 0.10 for Prandtl number Pr = 0.72 and 7.0. Here, the chemical reaction parameter γ = 0.5, the buoyancy ratio N =0.5 and Schmidt numbers Sc = 0.72 have been chosen. In presence of the heat generation parameter, the thermal conductivity increases. Therefore the thermal boundary layer becomes thicker, hence the corresponding temperature gradients are smaller and the surface local rate of heat transfer decreases but the local rate of species concentration and the local skin friction coefficient increase.

Figure 4.2 and 4.5 shows the comparisons of the numerical results of the Nusselt number Nu_x at Q =0.0 and Q = 0.10 for different values of Prandtl number Pr = 0.72 and 7.0. Here, the chemical reaction parameter γ = 0.5, the buoyancy ratio N =0.5 and Schmidt numbers Sc = 0.72 have been chosen. The comparison shows fairly good agreement between the results.

Figure 4.3 and 4.6 show the comparisons of the numerical results of the Sherwood number Sh_x at Q = 0.0 and Q = 0.10 for different values of Prandtl number Pr = 0.72 and 7.0. Here, the chemical reaction parameter γ = 0.5, the buoyancy ratio N =0.5 and Schmidt numbers

Sc = 0.72 have been chosen. The comparison shows fairly good agreement between the results.

4.2 Extension of this work

In this work, we considered constant viscosity and constant thermal conductivity but they are functions of temperature.

- If we consider the viscosity and thermal conductivity as functions of temperature then we can extend our problem.
- Also taking the non-uniform surface temperature, the problem can be extended.
- If we consider the magnetohydrodynamic natural convection then we can extend our problem.

Appendix A

Implicit Finite Difference Method

Implicit finite difference method in conjunction with Keller- box elimination technique is engaged to dig up the solutions of the transformed governing equations with the corresponding boundary conditions. This practice is well documented and widely used by Keller and Cebeci (1971) and recently by Hossain et al. (1990, 1992, 1996, 1997 and 1998).

Accompanied by Keller – box elimination scheme, an epigrammatic discussion on the advancement of algorithm on implicit finite difference method is given below taking into account the following Equations (A1-A3).

$$f''' + \frac{16+15x}{20(1+x)} ff'' - \frac{6+5x}{10(1+x)} f'^2 + (\theta + N\phi) = x\left(f' \frac{\partial f'}{\partial x} - f'' \frac{\partial f}{\partial x}\right) \qquad \text{(A1)}$$

and

$$\frac{1}{\Pr}\theta'' + \frac{16+15x}{20(1+x)} f\theta' - \frac{1}{5(1+x)} f'\theta + Qx^{2/5}(1+x)^{1/10}\theta = x\left(f' \frac{\partial \theta}{\partial x} - \theta' \frac{\partial f}{\partial x}\right) \qquad \text{(A2)}$$

and

$$\frac{1}{Sc}\phi'' + \frac{16+15x}{20(1+x)} f\phi' - \frac{1}{5(1+x)} f'\phi - \gamma x^{2/5}(1+x)^{1/10}\phi = x\left(f' \frac{\partial \phi}{\partial x} - \phi' \frac{\partial f}{\partial x}\right) \qquad \text{(A3)}$$

To apply the aforementioned method, we first convert Equations (A1)-(A3) into the following system of first order equations with dependent variables $u(\xi,\eta)$, $v(\xi,\eta)$, $p(\xi,\eta)$, $g(\xi,\eta)$, $w(\xi,\eta)$ and $q(\xi,\eta)$ as

$$f' = u\ ,\ u' = v,\quad g = \theta,\quad \theta' = p,\quad w = \phi \quad and \quad \phi' = q \qquad \text{(A4)}$$

$$v' + p_1 fv - p_2 u^2 + p_3 g + p_4 w = \xi\left(u\frac{\partial u}{\partial \xi} - \frac{\partial f}{\partial \xi} v\right) \qquad \text{(A5)}$$

$$\frac{1}{\Pr} p' + p_1 fp - p_5 ug + p_7 Qg = \xi\left(u\frac{\partial g}{\partial \xi} - p\frac{\partial f}{\partial \xi}\right) \qquad \text{(A6)}$$

$$\frac{1}{Sc}q' + p_1 fq - p_5 uw + p_6 \gamma w = \xi\left(u\frac{\partial w}{\partial \xi} - q\frac{\partial f}{\partial \xi}\right) \tag{A7}$$

where

$$x = \xi,\ p_1 = \frac{16+15x}{20(1+x)},\ p_2 = \frac{6+5x}{10(1+x)},\ p_3 = 1,\ p_4 = an,\ p_5 = \frac{1}{5(1+x)},$$
$$p_6 = (1+x)^{1/10},\ p_7 = x^{2/5}(1+x)^{1/10} \tag{A8}$$

The corresponding boundary conditions are

$$f(\xi,0) = 0,\ u(\xi,0) = 0,\ g(\xi,0) = 0 \text{ and } w(\xi,\eta) = 0$$
$$u(\xi,\infty) \to 0,\ g(\xi,\infty) \to 0,\ w(\xi,\eta) \to 0 \tag{A9}$$

We now consider the net rectangle on the (ξ,η) plane and denote the net point by

$$\eta_0 = 0,\quad \eta_j = \eta_{j-1} + h_j,\qquad j = 1,2,\ldots J$$
$$\xi^0 = 0,\quad \xi^n = \xi^{n-1} + k_n,\quad n = 1,2,\ldots N \tag{A10}$$

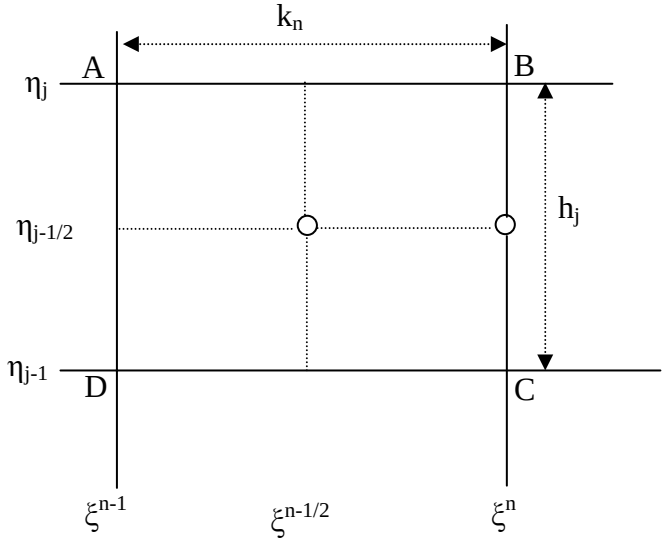

Figure A1: Net rectangle for difference approximations for the Box scheme

Here '*n*' and '*j*' are just sequence of numbers on the (ξ,η) plane, k_n and h_j are the variable mesh widths.

We approximate the quantities (*f*, *u*, *v*, *p*, *q*) at the points (ξ^n,η_j) of the net by $(f_j^n,u_j^n,v_j^n,p_j^n,q_j^n)$ which we call net function. We also employ the notation g_j^n and w_j^n for the quantities midway between net points shown in Figure (A1) and for any net function as

$$\xi^{n-1/2} = \tfrac{1}{2}(\xi^n + \xi^{n-1}) \tag{A11}$$

$$\eta_{j-1/2} = \tfrac{1}{2}(\eta_j - \eta_{j-1}) \tag{A12}$$

$$g_j^{n-1/2} = \tfrac{1}{2}(g_j^n + g_j^{n-1}) \tag{A13}$$

$$g_{j-1/2}^n = \tfrac{1}{2}(g_j^n + g_{j-1}^n) \tag{A14}$$

$$w_j^{n-1/2} = \frac{1}{2}(w_j^n + w_j^{n-1}) \tag{A15}$$

$$w_{j-1/2}^n = \frac{1}{2}(w_j^n + w_{j-1}^n) \tag{A16}$$

Now we write the difference equations that are to approximate Equations (A4) - (A7) by considering one mesh rectangle for the mid point $(\xi^n, n_{j-1/2})$ to obtain

$$\frac{f_j^n - f_{j-1}^n}{h_j} = u_{j-1/2}^n \tag{A17}$$

$$\frac{u_j^n - u_{j-1}^n}{h_j} = v_{j-1/2}^n \tag{A18}$$

$$\frac{g_j^n - g_{j-1}^n}{h_j} = p_{j-1/2}^n \tag{A19}$$

$$\frac{w_j^n - w_{j-1}^n}{h_j} = q_{j-1/2}^n \tag{A20}$$

$$\frac{1}{2}\left(\frac{v_j^n - v_{j-1}^n}{h_j} + \frac{v_j^{n-1} - v_{j-1}^{n-1}}{h_j}\right) + (p_1 fv)_{j-\frac{1}{2}}^{n-\frac{1}{2}} - (p_2 u^2)_{j-\frac{1}{2}}^{n-\frac{1}{2}} + (p_3 g)_{j-\frac{1}{2}}^{n-\frac{1}{2}} + (p_4 w)_{j-\frac{1}{2}}^{n-\frac{1}{2}}$$
$$= (\xi)_{j-\frac{1}{2}}^{n-\frac{1}{2}} \left((u)_{j-\frac{1}{2}}^{n-\frac{1}{2}} \frac{u_j^n - u_{j-1}^n}{k_n} + (v)_{j-\frac{1}{2}}^{n-\frac{1}{2}} \frac{f_j^{n-1} - f_{j-1}^{n-1}}{k_n}\right) \tag{A21}$$

$$\frac{1}{\Pr}\frac{1}{2}\left(\frac{g_j^n - g_{j-1}^n}{h_j} + \frac{g_j^{n-1} - g_{j-1}^{n-1}}{h_j}\right) + \left(p_1 fp\right)_{j-\frac{1}{2}}^{n-\frac{1}{2}} - \left(p_5 ug\right)_{j-\frac{1}{2}}^{n-\frac{1}{2}} + Q(p_7 g)_{j-\frac{1}{2}}^{n-\frac{1}{2}}$$
$$= \xi_{j-\frac{1}{2}}^{n-\frac{1}{2}} \left\{ u_{j-\frac{1}{2}}^{n-\frac{1}{2}} \left(\frac{g^n_{j-\frac{1}{2}} - g^{n-1}_{j-\frac{1}{2}}}{k_n} \right) + p_{j-\frac{1}{2}}^{n-\frac{1}{2}} \left(\frac{f^n_{j-\frac{1}{2}} - f^{n-1}_{j-\frac{1}{2}}}{k_n} \right) \right\} \tag{A22}$$

$$\frac{1}{Sc}\frac{1}{2}\left(\frac{w_j^n - w_{j-1}^n}{h_j} + \frac{w_j^{n-1} - w_{j-1}^{n-1}}{h_j}\right) + \left(p_1 fq\right)_{j-\frac{1}{2}}^{n-\frac{1}{2}} - \left(p_5 uw\right)_{j-\frac{1}{2}}^{n-\frac{1}{2}} + \gamma(p_7 w)_{j-\frac{1}{2}}^{n-\frac{1}{2}}$$
$$= \xi_{j-\frac{1}{2}}^{n-\frac{1}{2}} \left\{ u_{j-\frac{1}{2}}^{n-\frac{1}{2}} \left(\frac{w^n_{j-\frac{1}{2}} - w^{n-1}_{j-\frac{1}{2}}}{k_n} \right) + q_{j-\frac{1}{2}}^{n-\frac{1}{2}} \left(\frac{f^n_{j-\frac{1}{2}} - f^{n-1}_{j-\frac{1}{2}}}{k_n} \right) \right\} \tag{A23}$$

Similarly Equations (A5) – (A7) are approximate by centering about the mid point$(\xi^{n-1/2}, n_{j-1/2})$. Centering the Equations (A11) about the point $(\xi^{n-1/2}, n)$ without specifying η to obtain the algebraic equations. The difference approximation to Equations (A5)-(A7) become

$$h_j^{-1}(v_j^n - v_{j-1}^n) + \{(p_1)_{j-1/2}^n + \alpha_n\}(f v)_{j-1/2}^n - \{(p_2)_{j-1/2}^n + \alpha_n\}(u^2)_{j-1/2}^n + (p_3 g)_{j-1/2}^n$$
$$+ (p_4 w)_{j-1/2}^n + \alpha_n\{f_{j-1/2}^n v_{j-1/2}^{n-1} - v_{j-1/2}^n f_{j-1/2}^{n-1}\} = R_{j-1/2}^{n-1}$$

where

$$L_{j-\frac{1}{2}}^{n-1} = (p_1)_{j-\frac{1}{2}}^{n-1}(fv)_{j-\frac{1}{2}}^{n-1} - (p_2)_{j-\frac{1}{2}}^{n-1}(u^2)_{j-\frac{1}{2}}^{n-1} + (p_3 g)_{j-\frac{1}{2}}^{n-1}$$
$$- (p_4 w)_{j-\frac{1}{2}1}^{n-1} + h_j^{-1}(v_j^{n-1} - v_{j-1}^{n-1}) \qquad \text{(A24)}$$

And

$$R_{j-\frac{1}{2}}^{n-1} = -L_{j-\frac{1}{2}}^{n-1} + \alpha_n\left\{-(u^2)_{j-\frac{1}{2}}^{n-1} + (fv)_{j-\frac{1}{2}}^{n-1}\right\}$$

$$\frac{1}{\mathrm{Pr}}[h_j^{-1}(p_j^n - p_{j-1}^n)] + (p_1)_{j-1/2}^n (f p)_{j-1/2}^n - (p_5)_{j-1/2}^n (ug)_{j-1/2}^n + Q(p_7)_{j-1/2}^n g_{j-1/2}^n - \frac{1}{\mathrm{Pr}}[h_j^{-1}(p_j^{n-1} - p_{j-1}^{n-1}]$$
$$-[(p_1)_{j-1/2}^{n-1}(fp)_{j-1/2}^{n-1} - (p_5)_{j-1/2}^{n-1}(ug)_{j-1/2}^{n-1} + Q(p_7)_{j-1/2}^{n-1} g_{j-1/2}^{n-1}] = \alpha_n[\{(ug)_{j-1/2}^n - (ug)_{j-1/2}^{n-1} - u_{j-1/2}^n g_{j-1/2}^{n-1}$$
$$+ u_{j-1/2}^{n-1} g_{j-1/2}^n\} - \{(f p)_{j-1/2}^n - (f p)_{j-1/2}^{n-1} - p_{j-1/2}^n f_{j-1/2}^{n-1} + p_{j-1/2}^{n-1} f_{j-1/2}^n\}]$$
$$\frac{1}{\mathrm{Pr}}[h_j^{-1}(p_j^n - p_{j-1}^n)] + (p_1)_{j-1/2}^n (f\ p)_{j-1/2}^n - (p_5)_{j-1/2}^n (ug)_{j-1/2}^n + Q(p_7)_{j-1/2}^n g_{j-1/2}^n = -M_{j-1/2}^{n-1} \qquad \text{(A25)}$$
$$+ \alpha_n\ [-(ug)_{j-1/2}^{n-1} + (f\ p)_{j-1/2}^{n-1}] + \alpha_n\ [(ug)_{j-1/2}^n - (f\ p)_{j-1/2}^n - u_{j-1/2}^n\ g_{j-1/2}^{n-1} + u_{j-1/2}^{n-1}\ g_{j-1/2}^n\}$$
$$+ p_{j-1/2}^n f_{j-1/2}^{n-1} - p_{j-1/2}^{n-1} f_{j-1/2}^n]$$

$$\frac{1}{\mathrm{Pr}}[h_j^{-1}(p_j^n - p_{j-1}^n)] + \{(p_1)_{j-1/2}^n + \alpha_n\}(f\ p)_{j-1/2}^n - (p_5)_{j-1/2}^n (ug)_{j-1/2}^n + Q(p_7)_{j-1/2}^n g_{j-1/2}^n$$
$$- \alpha_n\ [\{(ug)_{j-1/2}^n - (ug)_{j-1/2}^{n-1} - u_{j-1/2}^n\ g_{j-1/2}^{n-1} + u_{j-1/2}^{n-1}\ g_{j-1/2}^n\} + p_{j-1/2}^n f_{j-1/2}^{n-1} - p_{j-1/2}^{n-1} f_{j-1/2}^n\}] \qquad \text{(A26)}$$
$$= T_{j-1/2}^{n-1}$$

where

$$M^{n-1}_{j-1/2} = \frac{1}{\mathrm{Pr}}[h_j^{-1}(p_j^{n-1} - p_{j-1}^{n-1})] -$$

$$[(p_1)^{n-1}_{j-1/2}(fp)^{n-1}_{j-1/2} + (p_5)^{n-1}_{j-1/2}(ug)^{n-1}_{j-1/2} + Q(p_7)^{n-1}_{j-1/2} g^{n-}_{j-}$$

$$T^{n-1}_{j-1/2} = -M^{n-1}_{j-1/2} + \alpha_n[(f\ p)^{n-1}_{j-1/2} - (u\ g)^{n-1}_{j-1/2}]$$

$$\frac{1}{Sc}[h_j^{-1}(q_j^n - q_{j-1}^n)] + (p_1)^n_{j-1/2}(f\ q)^n_{j-1/2} - (p_5)^n_{j-1/2}(uw)^n_{j-1/2} - \frac{1}{\mathrm{Pr}}[h_j^{-1}(q_j^{n-1} - q_{j-1}^{n-1}] - [(p_1)^{n-1}_{j-1/2}(fq)^{n-1}_{j-1/2}$$
$$-(p_5)^{n-1}_{j-1/2}(uw)^{n-1}_{j-1/2}] = \alpha_n[\{(uw)^n_{j-1/2} - (uw)^{n-1}_{j-1/2} - u^n_{j-1/2} w^{n-1}_{j-1/2} + u^{n-1}_{j-1/2} w^n_{j-1/2}\} - \{(f\ q)^n_{j-1/2}$$
$$-(f\ q)^{n-1}_{j-1/2} - q^n_{j-1/2} f^{n-1}_{j-1/2} + q^{n-1}_{j-1/2} f^n_{j-1/2}\}] \qquad \text{(A27)}$$

$$\frac{1}{Sc}[h_j^{-1}(q_j^n - q_{j-1}^n)] + (p_1)^n_{j-1/2}(f\ q)^n_{j-1/2} - (p_5)^n_{j-1/2}(uw)^n_{j-1/2} = -N^{n-1}_{j-1/2} + \alpha_n\ [-(uw)^{n-1}_{j-1/2}$$
$$+(f\ q)^{n-1}_{j-1/2}] + \alpha_n\ [(uw)^n_{j-1/2} - (f\ q)^n_{j-1/2} - u^n_{j-1/2}\ w^{n-1}_{j-1/2} + u^{n-1}_{j-1/2}\ w^n_{j-1/2}\}$$
$$+q^n_{j-1/2} f^{n-1}_{j-1/2} - q^{n-1}_{j-1/2} f^n_{j-1/2}] \qquad \text{(A28)}$$

$$\frac{1}{Sc}[h_j^{-1}(q_j^n - q_{j-1}^n)] + \{(p_1)^n_{j-1/2} + \alpha_n\}(f\ q)^n_{j-1/2} - (p_5)^n_{j-1/2}(uw)^n_{j-1/2}$$
$$-\alpha_n\ [\{(uw)^n_{j-1/2} - (uw)^{n-1}_{j-1/2} - u^n_{j-1/2}\ w^{n-1}_{j-1/2} + u^{n-1}_{j-1/2}\ w^n_{j-1/2}\} + q^n_{j-1/2} f^{n-1}_{j-1/2} - q^{n-1}_{j-1/2} f^n_{j-1/2}\}] \qquad \text{(A29)}$$
$$= S^{n-1}_{j-1/2}$$

where

$$N^{n-1}_{j-1/2} = \frac{1}{Sc}[h_j^{-1}(q_j^{n-1} - q_{j-1}^{n-1})] -$$

$$[(p_1)^{n-1}_{j-1/2}(fq)^{n-1}_{j-1/2} + (p_5)^{n-1}_{j-1/2}(uw)^{n-1}_{j-1/2}]$$

$$S^{n-1}_{j-1/2} = -N^{n-1}_{j-1/2} + \alpha_n[(f\ q)^{n-1}_{j-1/2} - (u\ w)^{n-1}_{j-1/2}]$$

The corresponding boundary conditions (A9) become

$$f_0^n = 0, \quad u_0^n = 0, \quad g_0^n = 1$$
$$u_J^n = 0, \quad g_J^n = 0, \quad w_J^n = 0 \tag{A30}$$

If we assume (f_j^{n-1}, u_j^{n-1}, v_j^{n-1}, g_j^{n-1}, w_j^{n-1}, p_j^{n-1}, q_j^{n-1}), i = 0, 1, 2, 3, ⋯ ⋯ , IMAX with initial values equal to those at the proviso x stations. For higher iterates we get

$$f_j^{(i+1)} = f_j^{(i)} + \delta f_j^{(i)}$$
$$u_j^{(i+1)} = u_j^{(i)} + \delta u_j^{(i)} \tag{A31a}$$
$$v_j^{(i+1)} = v_j^{(i)} + \delta v_j^{(i)} \tag{A31b}$$
$$g_j^{(i+1)} = g_j^{(i)} + \delta g_j^{(i)} \tag{A31c}$$
$$w_j^{(i+1)} = w_j^{(i)} + \delta w_j^{(i)} \tag{A31d}$$
$$p_j^{(i+1)} = p_j^{(i)} + \delta p_j^{(i)} \tag{A31e}$$
$$q_j^{(i+1)} = q_j^{(i)} + \delta q_j^{(i)} \tag{A31f}$$

We then insert the right side of the expression (A31) in place of f_j^n, u_j^n, v_j^n, g_j^n and w_j^n in Equations (A17)-(A20) dropping the terms that are quadratic in δf_j^i , δu_j^i, δv_j^i , δp_j^i and δq_j^i . This procedure yields the following linear system of algebraic equations:

$$f_j^{(i)} + \delta f_j^{(i)} - f_{j-1}^{(i)} - \delta f_{j-1}^{(i)} = \frac{h_j}{2}\left\{u_j^{(i)} + \delta u_j^{(i)} + u_{j-1}^{(i)} + \delta u_{j-1}^{(i)}\right\}$$

$$\delta f_j^{(i)} - \delta f_{j-1}^{(i)} - \frac{h_j}{2}(\delta u_j^{(i)} + \delta u_{j-1}^{(i)}) = (r_1)_j \tag{A32}$$

$$\delta u_j^{(i)} - \delta u_{j-1}^{(i)} - \frac{h_j}{2}(\delta v_j^{(i)} + \delta v_{j-1}^{(i)}) = (r_4)_j \tag{A33}$$

$$\delta g_j^{(i)} - \delta g_{j-1}^{(i)} - \frac{h_j}{2}(\delta g_j^{(i)} + \delta g_{j-1}^{(i)}) = (r_5)_j \tag{A34}$$

$$\delta w_j^{(i)} - \delta w_{j-1}^{(i)} - \frac{h_j}{2}(\delta w_j^n + \delta w_{j-1}^{(i)}) = (r_6)_j \tag{A35}$$

Momentum equation becomes:

$$h_j^{-1}(v_j^i+\delta v_j^i-v_{j-1}^i-\delta v_{j-1}^i)+\{(p_1)_{j-1/2}^n+\alpha_n\}\{(fv)_{j-1/2}^i+\delta(fv)_{j-1/2}^i\}$$
$$-\{(p_2)_{j-1/2}^n+\alpha_n\}\{(u^2)_{j-1/2}^i+\delta(u^2)_{j-1/2}^i\}+\{(p_3)_{j-1/2}^n\}\{g_{j-1/2}^i+\delta g_{j-1/2}^i\}$$
$$+\{(p_4)_{j-1/2}^n\{w_{j-1/2}^i+\delta w_{j-1/2}^i\}+\alpha_n\{v_{j-1/2}^{n-1}(f_{j-1/2}^i+\delta f_{j-1/2}^i)$$
$$-f_{j-1/2}^{n-1}(v_{j-1/2}^i+\delta v_{j-1/2}^i)\}=R_{j-1/2}^{n-1}$$

$$(s_1)_j\,\delta v_j^{(i)}+(s_2)_j\,\delta v_{j-1}^{(i)}+(s_3)_j\,\delta f_j^{(i)}+(s_4)_j\,\delta f_{j-1}^{(i)}+(s_5)_j\,\delta u_j^{(i)}$$
$$+(s_6)_j\,\delta u_{j-1}^{(i)}+(s_7)_j\,\delta g_j^{(i)}+(s_8)_j\,\delta g_{j-1}^{(i)}+(s_9)_j\,\delta w_j^{(i)}+(s_{10})_j\,\delta w_{j-1}^{(i)} \qquad \text{(A36)}$$
$$+(s_{11})\delta p_j^{(i)}+(s_{12})_j\,\delta p_{j-1}^{(i)}=(r_2)_j$$

Energy equation becomes:

$$\frac{1}{\mathrm{Pr}}[h_j^{-1}(p_j^i+\delta p_j^i-p_{j-1}^i-\delta p_{j-1}^i)-$$
$$(p_5)_{j-1/2}^n\{(ug)_{j-1/2}^i+\delta(ug)_{j-1/2}^i\}+(p_7)_{j-1/2}^n\left\{(g)_{j-1/2}^i+\delta(g)_{j-1/2}^i\right\}$$
$$+\{(p_1)_{j-1/2}^n+\alpha_n\}\{(fp)_{j-1/2}^i+\delta(fp)_{j-1/2}^i\}-\alpha_n\,[\{(ug)_{j-1/2}^i+\delta(ug)_{j-1/2}^i\}$$
$$+(p_{j-1/2}^i+\delta p_{j-1/2}^i)f_{j-1/2}^{n-1}-p_{j-1/2}^{n-1}(f_{j-1/2}^i+\delta f_{j-1/2}^i\}-\{(u)_{j-1/2}^i+\delta(u)_{j-1/2}^i\}g_{j-1/2}^{n-1}\}$$
$$\{(g)_{j-1/2}^i+\delta(g)_{j-1/2}^i\}u_{j-1/2}^{n-1}\}]=T_{j-1/2}^{n-1}$$

$$(t_1)_j\,\delta p_j^{(i)}+(t_2)_j\,\delta p_{j-1}^{(i)}+(t_3)_j\,\delta q_j^{(i)}+(t_4)_j\,\delta q_{j-1}^{(i)}+(t_5)_j\,\delta f_j^{(i)}+(t_6)_j\,\delta f_{j-1}^{(i)}$$
$$+(t_7)_j\,\delta u_j^{(i)}+(t_8)_j\,\delta u_{j-1}^{(i)}+(t_9)_j\,\delta g_j^{(i)}+(t_{10})_j\,\delta g_{j-1}^{(i)}+(t_{11})_j\,\delta w_j^{(i)}+(t_{12})_j\,\delta w_{j-1}^{(i)} \qquad \text{(A37)}$$
$$=(r_3)_j$$

Concentration equation becomes:

$$\frac{1}{Sc}[h_j^{-1}(q_j^i+\delta q_j^i-q_{j-1}^i-\delta q_{j-1}^i)+$$
$$(p_5)_{j-1/2}^n\{(uw)_{j-1/2}^i+\delta(uw)_{j-1/2}^i\}+\{(p_1)_{j-1/2}^n+\alpha_n\}\{(f\,q)_{j-1/2}^i+\delta(f\,q)_{j-1/2}^i\}$$
$$-\alpha_n\,[\{(uw)_{j-1/2}^i+\delta(uw)_{j-1/2}^i\}+(q_{j-1/2}^i+\delta q_{j-1/2}^i)f_{j-1/2}^{n-1}$$
$$-q_{j-1/2}^{n-1}(f_{j-1/2}^i+\delta f_{j-1/2}^i\}-\{(u)_{j-1/2}^i+\delta(u)_{j-1/2}^i\}w_{j-1/2}^{n-1}\}$$
$$\{(w)_{j-1/2}^i+\delta(w)_{j-1/2}^i\}u_{j-1/2}^{n-1}\}]=S_{j-1/2}^{n-1}$$

$$(l_1)_j\,\delta p_j^{(i)}+(l_2)_j\,\delta p_{j-1}^{(i)}+(l_3)_j\,\delta q_j^{(i)}+(l_4)_j\,\delta q_{j-1}^{(i)}+(l_5)_j\,\delta f_j^{(i)}+(l_6)_j\,\delta f_{j-1}^{(i)}$$
$$+(l_7)_j\,\delta u_j^{(i)}+(l_8)_j\,\delta u_{j-1}^{(i)}+(l_9)_j\,\delta g_j^{(i)}+(l_{10})_j\,\delta g_{j-1}^{(i)}+(l_{11})_j\,\delta w_j^{(i)}+(l_{12})_j\,\delta w_{j-1}^{(i)} \qquad \text{(A38)}$$
$$=(r_4)_j$$

Where

$$(r_1)_j=f_{j-1}^{(i)}-f_j^{(i)}+h_j u_{j-1/2}^{(i)} \qquad \text{(A39a)}$$
$$(r_4)_j=u_{j-1}^{(i)}-u_j^{(i)}+h_j v_{j-1/2}^{(i)} \qquad \text{(A39b)}$$
$$(r_5)_j=g_{j-1}^{(i)}-g_j^{(i)}+h_j p_{j-1/2}^{(i)} \qquad \text{(A39c)}$$
$$(r_2)_j=R_{j-1/2}^{n-1}-\left\{h_j^{-1}(v_j^i-v_{j-1}^i)+\{(p_1)_{j-\frac{1}{2}}^n+\alpha_n\}(fv)_{j-1/2}^i\right\}-$$
$$\{(p_2)_{j-\frac{1}{2}}^n+\alpha_n\}(u^2)_{j-1/2}^{(i)}+g_{j-\frac{1}{2}}^i-\xi_{j-\frac{1}{2}}^n u_{j-\frac{1}{2}}^n++\alpha_n(f_{j-1/2}^i v_{j-1/2}^{n-1}-f_{j-1/2}^{n-1}v_{j-1/2}^i) \qquad \text{(A39d)}$$

$$(r_3)_j=T_{j-1/2}^{n-1}-\frac{1}{P_r}\{h_j^{-1}(p_j^{(i)}-p_{j-1}^{(i)})\}+(p_5)_{j-1/2}^n(ug)_{j-1/2}^i-(p_7)_{j-1/2}^i(g)_{j-1/2}^i-$$
$$\{(p_1)_{j-1/2}^n+\alpha_n\}(f\,p)_{j-1/2}^i-\alpha_n\,[\{(ug)_{j-1/2}^i+p_{j-1/2}^i f_{j-1/2}^{n-1}-p_{j-1/2}^{n-1}f_{j-1/2}^i-(u)_{j-1/2}^i g_{j-1/2}^{n-1} \qquad \text{(A39e)}$$
$$+(g)_{j-1/2}^i u_{j-1/2}^{n-1}\}]$$

$$(r_4)_j=S_{j-1/2}^{n-1}-\frac{1}{S_c}\{h_j^{-1}(q_j^{(i)}-q_{j-1}^{(i)})\}-(p_5)_{j-1/2}^n(uw)_{j-1/2}^i+$$
$$\{(p_1)_{j-1/2}^n+\alpha_n\}(f\,q)_{j-1/2}^i-\alpha_n\,[\{(uw)_{j-1/2}^i+q_{j-1/2}^i f_{j-1/2}^{n-1}-q_{j-1/2}^{n-1}f_{j-1/2}^i-(u)_{j-1/2}^i w_{j-1/2}^{n-1} \qquad \text{(A39f)}$$
$$+(w)_{j-1/2}^i u_{j-1/2}^{n-1}\}]$$

Thus the coefficients of momentum equation are

$$(s_1)_j = h_j^{-1} + \frac{1}{2}\left\{(p_1)^n_{j-\frac{1}{2}} + \alpha_n\right\} f_j^{(i)} - \frac{\alpha_n}{2}\ f_{j-1/2}^{n-1} \tag{A40a}$$

$$(s_2)_j = -h_j^{-1} + \frac{1}{2}\left\{(p_1)^n_{j-\frac{1}{2}} + \alpha_n\right\} f_{j-1}^{(i)} - \frac{\alpha_n}{2}\ f_{j-1/2}^{n-1} \tag{A40b}$$

$$(s_3)_j = \frac{1}{2}\left\{(p_1)^n_{j-\frac{1}{2}} + \alpha_n\right\} v_j^{(i)} - \frac{\alpha_n}{2} v_{j-1/2}^{n-1} \tag{A40c}$$

$$(s_4)_j = \frac{1}{2}\left\{(p_1)^n_{j-\frac{1}{2}} + \alpha_n\right\} v_j^{(i)} - \frac{\alpha_n}{2} v_{j-1/2}^{n-1} \tag{A40d}$$

$$(s_5)_j = -\frac{1}{2}\{(p_2)^n_{j-\frac{1}{2}} + \alpha_n\} u_{j-1}^{(i)} \tag{A40e}$$

$$(s_6)_j = -\frac{1}{2}\{(p_2)^n_{j-\frac{1}{2}} + \alpha_n\} u_{j-1}^{(i)} \tag{A40f}$$

$$(s_7)_j = \frac{1}{2} \tag{A40g}$$

$$(s_8)_j = \frac{1}{2} \tag{A40h}$$

$$(s_9)_j = 0 \tag{A40i}$$

$$(s_{10})_j = 0 \tag{A40j}$$

Again the coefficients of energy equation are

$$(t_1)_j = \frac{1}{P_r} h_j^{-1} + \frac{1}{2}\{(p_1)^i_{j-1/2} + \alpha_n\} f_j^i - \frac{\alpha_n}{2} f^{n-1}_{j-1/2} \quad \text{(A41a)}$$

$$(t_2)_j = \frac{1}{P_r}(-h_j^{-1}) + \frac{1}{2}\{(p_1)^i_{j-1/2} + \alpha_n\} f_{j-1}^i - \frac{\alpha_n}{2} f^{n-1}_{j-1/2} \quad \text{(A41b)}$$

$$(t_3)_j = \frac{1}{2}\{(p_1)^n_{j-1/2} + \alpha_n\} p_j^i + \frac{\alpha_n}{2} p^n_{j-1/2} \quad \text{(A41c)}$$

$$(t_4)_j = \frac{1}{2}\{(p_1)^n_{j-1/2} + \alpha_n\} p_{j-1}^i - \frac{\alpha_n}{2} p^{n-1}_{j-1/2} \quad \text{(A41d)}$$

$$(t_5)_j = -\frac{\alpha_n}{2} g_j^i - \frac{1}{2} g^{n-1}_{j-1/2} \quad \text{(A41e)}$$

$$(t_6)_j = -\frac{\alpha_n}{2} g_{j-1}^i - \frac{1}{2} g^{n-1}_{j-1/2} \quad \text{(A41f)}$$

$$(t_7)_j = \frac{1}{2}\{(p_5)^i_{j-1/2} - \alpha_n[\frac{1}{2}u_j^i + \frac{1}{2}u^{n-1}_{j-1/2}] \quad \text{(A41g)}$$

$$(t_8)_j = -\frac{1}{2}\{(p_5)^i_{j-1/2}\} - \alpha_n[\frac{1}{2}u_j^i + \frac{1}{2}u^{n-1}_{j-1/2}] \quad \text{(A41h)}$$

$$(t_9)_j = \frac{1}{2}\left\{(p_7)^i_{j-1/2}\right\} - \alpha_n\left[\frac{1}{2}g_j^i + \frac{1}{2}g^{n-1}_{j-1/2}\right] \quad \text{(A41i)}$$

$$(t_{10})_j = -\frac{1}{2}\{(p_7)^i_{j-1/2}\} - \alpha_n[\frac{1}{2}g_j^i + \frac{1}{2}g^{n-1}_{j-1/2}] \quad \text{(A41j)}$$

$$(t_{11})_j = 0 \quad \text{(A41k)}$$

$$(t_{12})_j = 0 \quad \text{(A41l)}$$

Again the coefficients of concentration equation are

$$(l_1)_j = \frac{1}{S_c} h_j^{-1} + \frac{1}{2}\{(p_1)^i_{j-1/2} + \alpha_n\} f_j^i - \frac{\alpha_n}{2} f^{n-1}_{j-1/2} \tag{A42a}$$

$$(l_2)_j = \frac{1}{S_c}(-h_j^{-1}) + \frac{1}{2}\{(p_1)^i_{j-1/2} + \alpha_n\} f^i_{j-1} - \frac{\alpha_n}{2} f^{n-1}_{j-1/2} \tag{A42b}$$

$$(l_3)_j = \frac{1}{2}\{(p_1)^n_{j-1/2} + \alpha_n\} q^i_j + \frac{\alpha_n}{2} q^n_{j-1/2} \tag{A42c}$$

$$(l_4)_j = \frac{1}{2}\{(p_1)^n_{j-1/2} + \alpha_n\} q^i_{j-1} - \frac{\alpha_n}{2} q^{n-1}_{j-1/2} \tag{A42d}$$

$$(l_5)_j = -\frac{\alpha_n}{2} w^i_j - \frac{1}{2} w^{n-1}_{j-1/2} \tag{A42e}$$

$$(l_6)_j = -\frac{\alpha_n}{2} w^i_{j-1} - \frac{1}{2} w^{n-1}_{j-1/2} \tag{A42f}$$

$$(l_7)_j = \frac{1}{2}\{(p_5)^i_{j-1/2} - \alpha_n[\frac{1}{2}u^i_j + \frac{1}{2}u^{n-1}_{j-1/2}] \tag{A42g}$$

$$(l_8)_j = \frac{1}{2}\{(p_5)^i_{j-1/2} - \alpha_n[\frac{1}{2}u^i_j + \frac{1}{2}u^{n-1}_{j-1/2}] \tag{A42h}$$

$$(l_9)_j = 0 \tag{A42i}$$

$$(l_{10})_j = 0 \tag{A42j}$$

The boundary condition (A12) becomes

$$\partial f_0 = 0\,,\ \partial u_0 = 0\,,\ \partial\theta_0 = 1\,,\ \partial\phi_0 = 1$$
$$\partial u_j = 0,\ \ \partial\theta_j = 0\,,\ \partial\phi_j = 0 \tag{A43}$$

which just express the requirement for the boundary conditions to remain during the iteration process. Now the system of linear Equations (A40), (A41) and (A42) together with the boundary conditions (A43) can be written in matrix or vector form, where the coefficient matrix has a block tri-diagonal structure. The whole procedure, namely reduction to first order followed by central difference approximations, Newton's quasi-linearization method and the block Thomas algorithm, is well known as the Keller- box method.

References

Ahmad, N. and Zaidi, H. N., "Magnetic effect on oberback convection through vertical stratum". 2nd BSME-ASME International Conference on Thermal Engineering, Vol.1,pp. 157-168, (2004).

Ali, M. M, "Numerical Study of Radiation on Natural Convection Flow on a Sphere with Heat Generation", M.Phil Thesis, Department of Mathematics, Bangladesh University of Engineering and Technology (BUET), Dhaka, Bangladesh, (2007).

Cebeci T.and Bradshaw P., "Physical and Computational Aspects of Convective Heat Transfer", Springer, New York (1984)

Chang, C. L., "Numerical simulation of micropolar fluid flow along a flat plate with wall conduction and buoyancy effects", Journal of Applied Physics D, Vol.39, pp. 1132–1140, (2006).

Elbashbeshy, E. M. A., "Free convection flow with variable viscosity and thermal diffusivity along a vertical plate in the presence of magnetic field", International. Journal of. Engineering Science, Vol. 38, pp. 207-213, (2000).

Fairbanks, D. F. and Wick, C. R., "Diffusion and chemical reaction in an isothermal laminar flow along a soluble flat plate", Ind. Eng. Chem. Res., Vol.42, pp. 471–475, (1950).

Gebhart, B. and Pera, L., "The nature of vertical natural convection flows resulting from the combined buooyancy effects of thermal and mass diffusion", International. Journal of. Engineering Science, Vol. 14, No.12 pp. 2025-2050, (1971).

Hosain, M. A. and Takhar, H. S., "Radiation Effect on Mixed Convection along a Vertical Plate with Uniform Surface Temperature", Heat and Mass Transfer, Vol. 31, pp. 243-248, (2001).

Hossain, M .A., Das, S. K. and Pop, I., 'Heat transfer response of MHD free convection flow along a vertical plate to surface temperature oscillation', International.Journal of. Non- Linear Mechanics, Vol. 33, No. 3, pp. 41-553, (1998).

Hossain, M. A. and Rees, D. A. S., "Combined heat and mass transfer in natural convection flow from a vertical wavy surface", Acta Mechanica, Vol.136, pp. 133–141, (1999).

Hossain, M. A., Alim, M. A. and Rees, D. A. S., "The Effect of Radiation on Free Convection Flow from a Porous Vertical Plate", International Journal of Heat and Mass Transfer, Vol. 42, pp. 81-91, (1999).

Hossain, M. A., Khanafer, K. and Vafai, K. “The Effect of Radiation on Free Convection Flow with Variable Viscosity from a Porous Vertical Plate”, International Journal of Thermal science, Vol. 40, pp. 115-124, (1999).

Hossain, M.A. and Ahmad, M. , “MHD forced and free convection boundary layer flow near the leading edge”, International. Journal of. Heat and Mass Transfer, Vol.33, No. 3, pp. 571-575, (1990).

Hossain, M.A., Alam, K.C.A. and Rees, D.A.S., “MHD forced and free convection boundary layer flow along a vertical porous plate”, Applied Mechanics and Engineering, Vol.2, No. 1, pp. 33-51, (1997).

Hye, M. A. Molla, M. and Khan, M. A. H., “Conjugate Effects of Heat and Mass Transfer on Natural Convection Flow Across an Isothermal Horizontal Circular Cylinder with Chemical Reaction”, International Journal of Heat and Mass Transfer, Vol. 12, No.2, pp.191-201, (2007).

Karvinen, R., “Some new results for conjugate heat transfer in a flat plate”, International Journal of Heat and Mass Transfer, Vol.21, pp. 1261–1264, (1978).

Keller H.B., ‘Numerical methods in boundary layer theory, Annual Rev. Fluid Mechanics’, Vol. 10, pp. 417-433, (1978).

Kimura, S. ,Okajima, A. and Kiwata, T. “Conjugate natural convection from a vertical heated slab”, International Journal of Heat and Mass Transfer, Vol. 41, pp. 3203-3211, (1998).

Lin, H. T. and Yu, W. S., “Free Convection on Horizontal Plate with Blowing and Suction”, Transactions on ASME Journal of Heat Transfer, Vol.110, pp. 793-796, (1988).

Luikov, A. K., “Conjugate convective heat transfer problems”, International Journal of Heat and Mass Transfer, Vol.16, pp. 257–265, (1974).

Mamun, A. A., Chowdhury, Z. R., Azim, M. A. and. Maleque, M. A., “Conjugate Heat Transfer for a Vertical Flat Plate with Heat Generation Effect”, International Journal of Heat and Mass Transfer, Vol. 13, No.2, pp. 213-223, (2008).

Mendez, F. and Trevino, C., “The conjugate conduction-natural convection heat transfer along a thin vertical plate with non-uniform internal heat generation, International Journal of Heat and Mass Transfer, Vol. 43, pp. 2739–2748, (2000).

Mendez, F. and Trevino, C., “The conjugate conduction-natural convection heat transfer along a thin vertical plate with non-uniform internal heat generation”, International Journal of Heat and Mass Transfer, Vol. 43, pp. 2739-2748, (2000).

Merkin, J. H. and Pop, I., “Conjugate Free Convection on a Vertical Surface”, International Journal of Heat and Mass Transfer, Vol. 39, No. 7, pp. 1527-1534, (1982).

Miyamoto, M., Sumikawa, J., Akiyoshi, T. and Nakamura, T., "Effects of Axial Heat Conduction in a Vertical Flat Plate on Free Convection Heat Transfer", International Journal of Heat and Mass Transfer, Vol. 23, pp. 1545-1553, (1980).

Molla, M. M., Hossain, M. A. and Yao, L. S., "Natural Convection Flow along a Vertical Wavy Surface with Uniform Surface Temperature in Presence of Heat Generation/Absorption", International Journal of Thermal Science, Vol. 43, pp. 157–163, (2004).

Merkin, J.H. and Mahmood, T., "On the free convection boundary layer on a vertical plate with prescribed surface heat flux", Journal of Engineering Mathematics, Vol. 24, pp.95-107, (1990).

Merkin, J.H. and Pop, I., "Conjugate free convection on a vertical surface", International Journal of Heat and Mass Transfer, Vol. 39, pp. 1527–1534, (1982).

Nazar, R., Amin, N. and Pop, I., " Free convection boundary layer flow on a horizontal circular cylinder with constant heat flux in a micropolar fluid", International Comm. Heat and Mass Transfer, Vol. 7, No.2, pp. 409–431, (2002a).

Nazar, R., Amin, N., Grosan, T. and Pop, I., " Free convection boundary layer on an isothermal sphere in a micropolar fluid", International Comm. Heat and Mass Transfer, Vol. 29, No.3, pp. 377–386, (2002b).

Pozzi, A. and Lupo, M. "The coupling of conduction with laminar natural convection along a flat plate", International Journal of Heat and Mass Transfer, Vol. 31, No.8, pp. 1807-1814, (1988).

Pozzi, A. and Lupo, M., "The coupling of conduction with laminar natural convection along a flat plate", International Journal of Heat and Mass Transfer, Vol. 31, pp. 1807–1814, (1988).

Sparrow, E. M. and Chyu, M. K., "Conjugated forced convection-conduction analysis of heat transfer in a plate fin", International Journal of Heat and Mass Transfer, Vol.104, pp. 204–206, (1982).

Taher, M. A. and Molla, M.M., "Natural convection boundary layer flow on a sphere in presence of heat generation", The 5th International conference on Mechanical Engineering and 10th annual paper meet, Dhaka, pp.223-228, (2005).

Vynnycky, M. and Kimura, S., "Conjugate free convection due to heated vertical plate", International Journal of Heat and Mass Transfer, Vol. 38, No.5, pp. 1067–1080, (1982).

Vynnycky, M., Kimura, S., Kanev, K. and Pop, I., "Forced convection heat transfer from a flat plate: the conjugated problem", International Journal of Heat and Mass Transfer, Vol.41, pp. 45–59, (1998).

Yu, W-S. and Lin, H-T., “Conjugate Problems of conduction and free convection on vertical and horizontal flate plate”, International Journal of Heat and Mass Transfer., Vol. 36, No.5, pp. 1303-1313, (1982).

Yao, L.S., “Natural convection along a vertical wavy surface”, ASME Journal of Heat Transfer., Vol.105, pp. 465-468, (1983).